UNIVERSITY OF CALIFORNIA, SAN DIEGO

Manipulation of Cellular DNA Repair by Early Adenovirus Proteins

A dissertation submitted in partial satisfaction of the

requirements for the degree Doctor of Philosophy

in

Biology

by

Nicole Ise Orazio

Committee in charge:

Professor Matthew D. Weitzman, Chair
Professor Michael David
Professor Tony Hunter
Professor Amy Pasquinelli
Professor Aleem Siddiqui
Professor Jean Wang

2010

The Dissertation of Nicole Ise Orazio is approved, and it is acceptable in quality and form for publication on microfilm and electronically:

Chair

University of California, San Diego

2010

DEDICATION

I dedicate this to my parents who have always supported me, believed in me and made me believe that I can accomplish anything…as long as I work hard at the things I need help with and remember to put a lilt in my voice.

TABLE OF CONTENTS

LIST OF FIGURES

Chapter 1

Chapter 2

Chapter 3

Appendix

LIST OF TABLES

Chapter 4

ACKNOWLEDGEMENTS

I thank Matthew Weitzman for allowing me to work on my graduate degree under his guidance and for teaching me how to think about science and accomplish my goals. I also am grateful for all the members of the Weitzman lab for providing a wonderful atmosphere full of support and innovation especially Seema, Caroline, Rachel and Mira, I couldn't have done it without your guidance.

I thank the members of my graduate committee: Michael David, Tony Hunter, Amy Pasquinelli, Aleem Siddiqui, Jean Wang and Matt Weitzman for their guidance, support and scientific discussions.

Chapters 2 and 3 were co-authored in part, and I am grateful to all of my co-authors on the following publications:

Carson CT*, Orazio NI*, Lee DV*, Suh J, Bekker-Jensen S, Araujo FD, Lakdawala SS, Lilley CE, Bartek J, Lukas J, Weitzman MD. Mislocalization of the MRN complex prevents ATR signaling during adenovirus infection. EMBO Journal, 2009, Mar 18; 28(6): 652-62.

Orazio NI, Naeger, C, Karlseder J, Weitzman MD., Adenovirus targets the Blooms Syndrome Helicase for degradation during infection. *Submitted to J. Virology*

I am grateful to Zhongsheng You who was an inspiration to me and provided me with invaluable advice, support (and reagents) during my graduate career.

I am thankful to everyone in San Diego past and present who helped me through this time, especially Sam Serey and Aaron Parker who kept me up when things were down, and made the Verma lab, “my lab away from lab”.

VITA

2010	Ph.D., Biology University of California, San Diego
2003-2009	Graduate Student and Teaching Assistant, University of California, San Diego
2003	B.S., Microbiology University of California, Santa Barbara
2002-2004	Undergraduate Researcher, Department of Biology University of California, Santa Barbara

PUBLICATIONS

You Z, Orazio NI, Lamache BJ, Hunter T, Weitzman MD. *In preparation*

Orazio NI, Naeger C, Karlseder J, Weitzman MD., Adenovirus targets the Bloom Syndrome Helicase for degradation during infection. *Submitted to J. Virology*

Larmarche BJ, Orazio NI, Weitzman MD., The MRN complex in double-strand break repair and telomere maintenance. Review. FEBS lett, 2010 Sep 10;584(17):3682-95

Carson CT*, Orazio NI*, Lee DV*, Suh J, Bekker-Jensen S, Araujo FD, Lakdawala SS, Lilley CE, Bartek J, Lukas J, Weitzman MD. Mislocalization of the MRN complex prevents ATR signaling during adenovirus infection. EMBO Journal, 2009, Mar 18; 28(6): 652-62.

Sanchez V, Mahr JA, Orazio NI, Spector DH., Nuclear export of the human cytomegalovirus tegument protein pp65 requires cyclin-dependent kinase activity and the Crm1 exporter. J Virol. 2007 Nov;81(21):11730-6.

Fleisig HB*, Orazio NI*, Liang H, Tyler AF, Adams HP, Weitzman MD, Nagarajan L., Adenoviral E1B55K oncoprotein sequesters candidate leukemia suppressor sequence-specific single-stranded DNA-binding protein 2 into aggresomes. Oncogene. 2007 Jul 19;26(33):4797-805.

*Denotes equal contribution to publication

ABSTRACT OF THE DISSERTATION

Manipulation of Cellular DNA Repair by Early Adenovirus Proteins

By

Nicole Ise Orazio

Doctor of Philosophy in Biology

University of California, San Diego 2010

Matthew D. Weitzman, Chair

After induction of DNA double strand breaks (DSBs) the cellular DNA damage response (DDR) functions to inhibit the cell cycle, allowing for repair of the damage. Adenovirus is a double strand DNA virus that replicates in the host cell nucleus and expresses early proteins to inactivate the DNA damage response in order to prevent the recognition of its viral genome as a cellular DSB. Adenovirus that is deleted for the E4 region cannot inactivate the DNA

damage response and consequently the viral genome is recognized as DNA damage and the cellular DNA repair machinery ligates the viral genome into end-to-end concatemers. Adenovirus expresses two proteins from the E4 region E4orf3 and E4orf6 that have been demonstrated to inhibit the DNA damage response. E4orf3 mislocalizes cellular proteins to prevent their accumulation at viral replication centers during infection. The E4orf6 protein interacts with the viral protein E1b55K to mediate degradation of cellular proteins in a proteasome-dependent manner. The research presented in this thesis demonstrates that E4orf3 and E4orf6/E1b55K target specific components of the DDR, and provides insight into the consequences of targeting these components for the virus and for cells. The Mre11-Nbs1-Rad50 (MRN) complex is the main sensor of DNA damage and functions to activate the DDR and promote repair of DSBs. We show that E4orf3 mislocalization of the MRN complex prevents a DNA damage response mediated by the Ataxia-Telangiectasia Mutated Rad3 related (ATR) protein. CtIP and BLM are proteins implicated to function in the DDR and in resection of DSBs. We identified the BLM helicase as a novel target of E1b55K/E4orf6 mediated degradation during infection. We also found that CtIP is required for concatemer formation *in vitro* and is inhibitory to adenovirus replication. Together, the data presented in this thesis demonstrate that adenovirus infection provides an ideal model system for study of DNA damage response and repair pathways. Our studies not only provide information on the function

of cellular proteins during infection, but also can yield insights into broader functions for these cellular proteins in a non-viral context.

Chapter 1. Introduction

Introduction

Maintaining the integrity of genomic DNA is a constant battle for cells. Ultraviolet irradiation, replication stress, ionizing radiation and radiometric chemicals can all cause DNA damage (Bartek and Lukas, 2007). Damage that creates double-strand DNA breaks (DSB) is particularly harmful to cells, since faulty repair of DSBs can lead to deletions or translocations that could cause cancer. The cellular DNA damage response (DDR) is an ordered pathway that functions to arrest the cell cycle after DNA damage to allow for repair of the DSB (Reinhardt and Yaffe, 2009). More specifically, immediately after induction of a DSB, the DDR is initiated by recruitment of damage "sensor" proteins. The sensors activate signaling kinases that initiate a phosphorylation cascade resulting in further recruitment of repair proteins and cell cycle arrest (Harper and Elledge, 2007). If the break cannot be repaired or the extent of damage is too great, the DNA damage response can signal to induce cellular senescence or apoptosis. The downstream responses of the DDR cannot occur without the initial damage sensors, which underscores the importance of the damage sensors for a robust DDR.

The Mre11-Rad50-Nbs1 complex

The Mre11-Rad50-Nbs1 (MRN) complex is thought to be the initial sensor of DSBs (Lisby et al., 2004; Mirzoeva and Petrini, 2001). The MRN

complex is recruited to sites of DSBs where it activates the DDR and also processes broken DNA ends to promote repair (Buis et al., 2008; Lukas et al., 2004; Maser et al., 1997; Mirzoeva and Petrini, 2001; Usui et al., 2001). Hypomorphic mutations in Mre11 and Nbs1 cause the human genetic diseases Ataxia-Telangiectasia Like Disorder (A-TLD) and Nijmegen Breakage Syndrome (NBS), respectively (Carney et al., 1998; Stewart et al., 1999). The immunological deficiency and cancer predisposition in patients with these diseases suggests that the MRN complex plays a role in genome stability. *S. cerevisiae* mutants in the homologous MR(Xrs2) complex are hypersensitive to DNA damage and/or defective in meiotic recombination, suggesting that these proteins are also involved in DNA repair (Ajimura et al., 1993; Cox and Parry, 1968; Suslova and Zakharov, 1974). Knockout mice lacking individual MRN complex members are embryonic lethal (Luo et al., 1999; Xiao and Weaver, 1997; Zhu et al., 2001). Each of the MRN complex proteins promotes stability of the complex, and contributes to functions in damage signaling as well as DNA repair.

Mre11 has DNA binding activity and also exhibits DNA endonuclease and exonuclease activity with 3' to 5' directionality (D'Amours and Jackson, 2002; Paull and Gellert, 1998a; Paull and Gellert, 1999b; Trujillo et al., 1998). *In vitro,* Mre11 forms stable dimers that promote DNA binding and bridge together the two ends of a DSB. Rad50 also forms a dimer *in vitro* creating a flexible hinge domain (Anderson et al., 2001; Williams et al., 2008). *In vivo,*

each of the Mre11 proteins binds a single Rad50 protein forming an $Mre11_2Rad50_2$ heterotetrameric complex that promotes the nuclease activity of Mre11 (Anderson et al., 2001). The nuclease activities of Mre11 are required for repair of DSBs but not for activation of DNA damage signaling responses (Buis et al., 2008; Williams et al., 2008). Nbs1 has a nuclear localization signal (NLS) required for MR nuclear localization (Desai-Mehta et al., 2001; You et al., 2005), and also functions to communicate with the ATM damage signaling kinase (Falck et al., 2005; You et al., 2005). The N-terminus of Nbs1 has one forkhead associated (FHA) domain and two BRCA C-terminal (BRCT) domains that form the protein core. These domains are required for various protein-protein and phospho-protein interactions (e.g., phosphorylated Mdc1 and CtIP)(Cerosaletti and Concannon, 2003; Durocher et al., 1999; Durocher et al., 2000; Lloyd et al., 2009; Williams et al., 2009a). The C-terminus of Nbs1 is a flexible tail that maintains Nbs1 interaction with the $Mre11_2Rad50_2$ complex and ATM and activates the damage signaling pathways (Falck et al., 2005; Williams et al., 2009a; You et al., 2005). Rad50 has Walker Domain A and B nucleotide binding motifs and a zinc coordinating CXXC motif that tethers distal DNA ends for repair (Bhaskara et al., 2007; Hopfner et al., 2002). Rad50 also has an ATPase domain that functions in partial unwinding of the DNA ends and promotes Mre11 nuclease activity (Hopfner et al., 2000). Together the functional domains of the MRN complex coordinate the activation of DNA damage signaling pathways and DSB repair.

MRN complex function in the DNA damage response

The DNA damage signaling kinases Ataxia-Telangiectasia mutated (ATM) and Ataxia-Telangiectasia Mutated-Rad3 Related (ATR) are the main signaling kinases activated after DNA damage (**Fig. 1-1**). ATM and ATR are members of the family of phosphatidylinositol-3-kinase-like kinases (PIKKs), which also includes the DNA-dependent protein kinase catalytic subunit (DNA-PKcs) that is involved in DNA repair. Individuals with A-TLD and NBS are phenotypically similar to patients with Ataxia-Telangiectasia (ATM deleted) (Carney et al., 1998; Stewart et al., 1999; Varon et al., 1998), and Seckel syndrome (ATR hypomorphic) (O'Driscoll et al., 2003). The similarity of disease phenotypes suggests that the MRN complex and these kinases function in similar pathways. However, unlike MRN, ATM can be knocked out in mouse models resulting in viable but underweight mice that are predisposed to cancer (Barlow et al., 1996; Xu et al., 1996; Xu and Baltimore, 1996). ATR knockout mice are embryonic lethal (Brown and Baltimore, 2000; de Klein et al., 2000), which suggests a more important and expansive role for ATR in genome maintenance (as reviewed by (O'Driscoll, 2009)). ATM and ATR activation both lead to cell cycle arrest mediated through the phosphorylation of the Chk1 and Chk2 kinases (Reinhardt and Yaffe, 2009). ATM and ATR also marks the sites of damage for further recruitment of proteins by

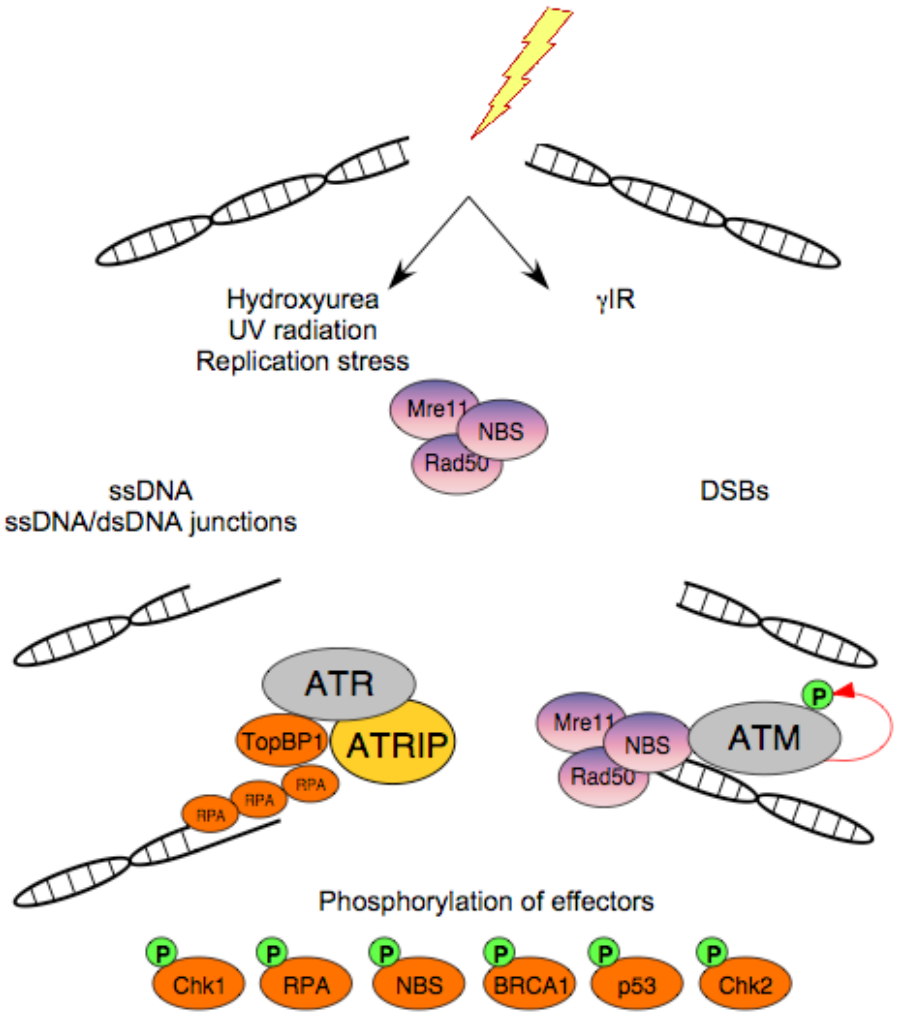

Figure 1-1. Activation of the DNA damage response. After DNA damage creates a DSB the Mre11-Rad50-Nbs1 complex is immediately recruited to sites of damage. Damage that causes replication stress, such as that created by UV radiation or hydroxyurea creates ssDNA that activates ATR. DSBs that occur by ionizing radiation result in clean breaks and activate ATM and can then be processed to ssDNA leading to activation of ATR. RPA bound ssDNA recruits ATR-ATRIP to the ssDNA. TopBP1 interaction with ATR is required for the full kinase activation. ATM is recruited to sites of damage and activation occurs by interaction with the C-terminus of Nbs1 leading to ATM autophosphorylation and conversion into the active kinase. Activation of the ATM and ATR kinases leads to phosphorylation of effectors which function to arrest the cell cycle and recruit proteins to repair the break.

phosphorylation of the histone variant H2AX (Dickey et al., 2009; Rogakou et al., 1998). Although ATM and ATR are both activated after DNA damage, their activation occurs by direct interactions with unique proteins and in response to different types of DNA damage (**Fig. 1-1**).

In the absence of damage, ATM resides in the nucleus in inactive dimers (Bakkenist and Kastan, 2003). After the induction of DSBs ATM autophosphorylates at S1981 and dissociates into monomers whereby it becomes an active kinase and proceeds to phosphorylate its downstream substrates (**Fig. 1-1**)(Bakkenist and Kastan, 2003). Contrary to this, in mice the equivalent phosphorylation site on ATM, S1987 is not required for activation of ATM after γIR suggesting that human and murine ATM is activated differently (Pellegrini et al., 2006). MRN is essential for full ATM activation, as ATM autophosphorylation and phosphorylation of its downstream substrates is decreased in cells deficient for members of the MRN complex (Carson et al., 2003; Uziel et al., 2003). There are two steps of ATM activation: the initial recruitment to DNA breaks, and the autophosphorylation leading to a kinase active ATM. The MRN complex is required for ATM recruitment to and physical tethering with damaged DNA ends (Falck et al., 2005; You et al., 2005). However, initial recruitment of ATM to sites of damage can bypass the need for MRN if there is a high concentration of free DNA ends (Dupré et al., 2006). The presence of short oligonucleotides has also been shown to activate ATM in an MRN dependent

manner, even in the absence of cellular DNA damage (Jazayeri et al., 2008). The conversion of ATM into the active kinase is DNA independent, but requires direct binding of ATM to the C-terminus of Nbs1 (Falck et al., 2005; You et al., 2005). Once the ATM kinase is activated it can then phosphorylate its downstream targets (of which there are hundreds) including Nbs1, Chk2 and 53BP1 (Bakkenist and Kastan, 2003; Matsuoka et al., 2007; Matsuoka et al., 1998; Matsuoka et al., 2000). Activation of ATM is rapid, robust, and highly amplified, stressing the importance of immediate cell cycle arrest after exposure to DSBs.

ATR signaling is primarily a response to damage caused by replication stress, and this damage is characterized by stretches of ssDNA and ssDNA/dsDNA junctions. Activation of ATR can be induced in cells by ultraviolet (UV) irradiation to create damage and treatment with hydroxyurea (HU) or aphidicolin that arrests DNA replication (**Fig. 1-1**)(as reviewed by (Shechter et al., 2004; Zou, 2007). In the absence of damage, ATR resides in a stable complex with its interacting partner ATRIP (Cortez et al., 2001). The association of ATR with ATRIP is sufficient for recruitment to sites of damage, and is promoted by the binding of ATR-ATRIP to Replication Protein-A (RPA) bound ssDNA (Namiki and Zou, 2006; Zou and Elledge, 2003). However, full kinase activation of ATR requires interaction of the ATR-ATRIP complex with TopBP1 (Cortez et al., 2001; Falck et al., 2005; Kumagai et al., 2006; Mordes et al., 2008; Zou and Elledge, 2003). ATR activation can be detected by the

phosphorylation of its known targets including Chk1 and RPA (Cortez et al., 2001; Falck et al., 2005; Kumagai et al., 2006; Liu et al., 2000; Mordes et al., 2008; Olson et al., 2007a; Zou and Elledge, 2003). Although there is no evidence for direct activation of ATR by the MRN complex, ATR activation and phosphorylation of its targets is abrogated in cells deficient for MRN (Manthey et al., 2007; Olson et al., 2007a; Stiff et al., 2005). The proteins required for activation of ATR signaling are well characterized; however, the role of MRN in ATR activation still needs to be elucidated.

ATM and ATR are activated after specific types of DNA damage; however, they functionally overlap to induce cell cycle arrest and to recruit proteins to sites of damage. ATM and ATR can also activate each other, resulting in dual kinase activation after damage. After IR induced DSBs, ATR is activated in an Nbs1 and ATM dependent manner (Jazayeri et al., 2006). ATM activates ATR by phosphorylating TopBP1, which enhances the ability of TopBP1 to activate ATR (Yoo et al., 2009). Conversely, after replication stress the active ATR kinase activity also leads to ATM activation by phosphorylating ATM at S1981, which is also the site of ATM autophosphorylation (Stiff et al., 2006). It is interesting that although ATM and ATR can individually arrest the cell cycle they have mechanisms to activate each other. The secondary activation of either kinase could result in an extended response during extensive damage allowing more time for repair. The dual activation of these kinases to enact similar downstream

consequences highlights the importance of the DDR to activate cell cycle checkpoints for maintaining genome stability.

The MRN complex in double strand DNA break repair

Repair of DSBs occurs by two main mechanisms: non-homologous end joining (NHEJ) and homologous recombination (HR). NHEJ is thought to be the more error-prone mechanism of repair and generally does not require regions of homology to repair the break. HR is thought to be the more error proof mechanism of repair and requires large regions of homology on a sister chromatid to repair the break. The relative contribution of these mechanisms is cell cycle regulated. HR is more prevalent in S and G_2 when a sister chromatid is present to use as a template for repair, while NHEJ is more prevalent in G_1 (**Fig. 1-2**)(Branzei and Foiani, 2008). Analysis of proteins required for NHEJ or HR reveals that many of the main players are not cell cycle regulated. However, the availability of certain processing proteins, whose levels are regulated by cell cycle, may determine which repair mechanism is used.

HR dependent DSB repair requires the processing of dsDNA ends to create extended 3' ssDNA tails for correct pairing with a homologous sequence. Specifically, an initial resection step is required to trim the 5' ends of the DSB, followed by secondary resection creating extended 3' ssDNA tails that become coated with RPA (Mimitou and Symington, 2009b). Rad51

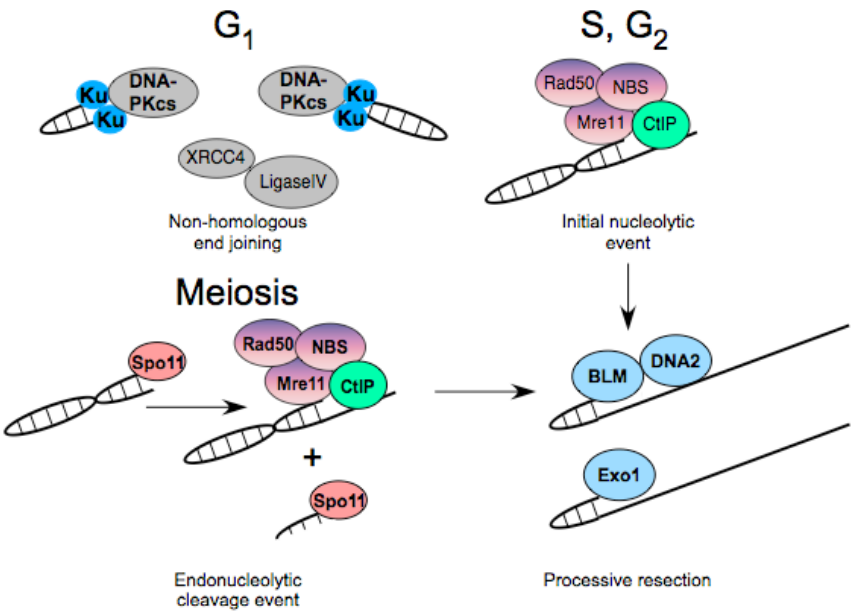

Figure 1-2. DSB repair throughout the cell cycle. During G_1, DSB repair occurs primarily by non-homologous end joining (NHEJ). Proteins involved are the Ku70/80 proteins that bind the ends of DNA and recruit DNA-PKcs as well as DNA Ligase IV (Ligase IV), XRCC4 and XLF that repair the break by ligation of the ends. In S and G_2, repair occurs by homologous recombination. The MRN complex and CtIP are suggested to promote an initial nucleolytic event, and processive resection is promoted by the Exo1 nuclease or the BLM helicase and DNA2 nuclease. During meiosis, the proteins required are similar to those required during repair by mitotic HR. The MRN complex and CtIP are suggested to mediate an endonucleolytic cleavage event based on the homology of these proteins to MR(X) and Sae2 that promote removal of Spo11 from the 5' DNA ends prior to the processive resection.

protein filaments then displace RPA and function to find homologous DNA sequences in a sister chromatid (in mitosis) or a homologous chromosome (in meiosis), and recombination and repair occurs through a double Holliday junction (Mimitou and Symington, 2009b). Although DSBs are generally detrimental to genome stability, during meiosis I, DSBs are created deliberately by Spo11 to promote correct pairing and segregation of homologous chromosomes (Sasaki et al., 2010). Spo11 creates DSBs through an endonucleolytic mechanism whereby it becomes covalently attached to the 5' ends of the DNA (Keeney et al., 1997; Keeney and Kleckner, 1995; McKee and Kleckner, 1997). Therefore, HR repair during meiosis I requires removal of Spo11 prior to initial resection. Interestingly, in yeast, the removal of Spo11 and the initial processing of DSBs seem to be dependent on the same proteins. The proteins that mediate the initial DNA processing steps in HR are currently coming to light.

The MRN complex was initially proposed to be involved in HR due to deficiencies in both DSB repair and meiotic recombination in *S. cerevisiae* deleted for MR(X) complex members (**Fig. 1-2**) (Ajimura et al., 1993; Alani et al., 1990; Cao et al., 1990). However, the MRN complex cannot initiate HR alone, as Mre11 does not exhibit the 5'-3' exonuclease or dsDNA endonuclease activities required to create the requisite 3' overhangs for HR to proceed (D'Amours and Jackson, 2002; Paull and Gellert, 1998a; Paull and Gellert, 1999b; Trujillo et al., 1998; Williams et al., 2008). In addition to MRN,

S. cerevisiae deleted for Sae2 are also defective in Spo11 removal (Neale et al., 2005). Further studies have shown that Sae2 promotes MR(X) endonuclease activity *in vitro* and Sae2 may also exhibit nuclease activity itself (Lengsfeld et al., 2007). It has been reported that functional homologs of Sae2 include the *S. pombe* protein Ctp1, and the metazoan protein CtIP (Limbo et al., 2007; Sartori et al., 2007; Takeda et al., 2007). Although there is weak sequence homology in the C-terminus of CtIP with the yeast proteins, all interact with the MRN complex and are regulated similarly by CDK phosphorylation (Huertas et al., 2008; Limbo et al., 2007; Sartori et al., 2007). MRN and CtIP are proposed to promote HR by creating the short 3' ssDNA overhangs (**Fig. 1-2**); however, no biochemical studies have shown that these proteins enzymatically function in 5-3' resection (You and Bailis, 2010). After the initial resection step, processive resection creates extensive 3' ssDNA that can be bound by RPA. Proteins recently implicated in the extensive resection step include the nucleases DNA2 and Exo1 and the Sgs1 helicase (*S. cerevisiae*) (**Fig. 1-2**)(Budd and Campbell, 2009; Manfrini et al., 2010; Mimitou and Symington, 2008; Zhu et al., 2008a). The mammalian homolog of Sgs1 is suggested to be the BLM helicase, which has also been implicated in processive resection for repair by HR (Gravel et al., 2008; Johnson et al., 2000; Kusano et al., 1999; Neff et al., 1999; Nimonkar et al., 2008; Stewart et al., 1997; Watt et al., 1996; Wu et al., 2000). Future studies to understand the

properties of these nucleases and helicases, and how they are regulated will provide us with a greater understanding of how repair by HR is initiated.

Repair by NHEJ occurs predominately during the G_1 phase of the cell cycle and requires minimal processing of the DSB. In the simplest form, the Ku70/Ku80 complex binds the ends of the DNA and then recruit and bind the catalytic subunit DNA-PKcs, forming the DNA-PK holoenzyme complex. The DNA-PK holoenzyme then recruits DNA Ligase IV-XRCC4-XLF, which mediates ligation of the ends (**Fig. 1-2**). DNA-PKcs activation involves autophosphorylation and phosphorylation of substrates including RPA and WRN; however, DNA-PKcs activation alone has not been shown to affect the cell cycle (Chan et al., 2002). A second form of end joining is independent of DNA Ligase IV, and is referred to as non-classical NHEJ, micro-homology mediated end joining (MMEJ) or alternative-NHEJ; in these forms of repair, a small region of homology (4-6 nucleotides) is created and used for repair (Lieber, 2008). The MRN complex has been implicated in steps of both classical- and alternative-NHEJ (Deng et al., 2009; Dinkelmann et al., 2009; Rass et al., 2009; Xie et al., 2009).

The most important factor regulating the choice of repair by HR and NHEJ seems to be cell cycle regulation (Branzei and Foiani, 2008). Although the MRN complex is recruited to sites of DSBs at all stages of the cell cycle, repair by NHEJ is preferred in G_1. As described above, CtIP functions in resection during S and G_2 phases (Chen et al., 2008; Huertas et al., 2008;

Nakamura et al., 2010; Williams et al., 2009b; You et al., 2009; Yun and Hiom, 2009). Since Ku has a low affinity for ssDNA (Dynan and Yoo, 1998), CtIP involvement in resection could also promote HR by decreasing the availability of dsDNA ends for Ku binding. Supporting a role for CtIP in repair pathway choice, studies have shown that the removal of CtIP not only decreases repair frequency by HR but also increases repair by MMEJ (Nakamura et al., 2010; Yun and Hiom, 2009). Determining how cell cycle regulation affects different types of repair is important for understanding how deviations in these pathways can lead to mutations and affect genome stability.

Viruses and DNA damage

The DDR is an ordered pathway that quickly responds to cellular DNA breaks, beginning with the localization of the MRN complex to sites of damage (Lukas et al., 2003; Mirzoeva and Petrini, 2001; Paull et al., 2000). The MRN complex not only recognizes cellular DNA damage, but can also recognize the presence of exogenous DNA that is presented to cells in the form of virus infection (Lilley et al., 2007). Viruses are obligate intracellular parasites that take advantage of various host pathways to replicate their own genetic material. DNA viruses that replicate in the host cell nucleus are exposing their viral DNA genome to the damage repair machinery. Recognition of viral genomes by DDR proteins is demonstrated by the localization of DDR proteins at sites of viral replication by immunofluorescence analysis. DDR proteins reported to be at sites of viral replication in wildtype and mutant viruses

include the MRN complex, NHEJ machinery and ATM and ATR kinases (Carson et al., 2009; Kudoh et al., 2005, Lilley et al., 2007; Kudoh et al., 2009; Luo et al., 2007; Stracker et al., 2002; Taylor and Knipe, 2004; Wilkinson and Weller, 2004; Zhao et al., 2008). While DNA viruses are the most widely studied viruses that affect the DDR, RNA viruses with DNA intermediates such as retroviruses also influence/abrogate DNA repair machinery (Skalka and Katz, 2005). Viruses respond to the DDR in multiple ways: they can hijack the DDR to benefit their lifecycle or inactivate the DDR to prevent inhibition of their lifecycle. However, it is emerging that most DNA viruses inactivate specific parts of DDR pathways, but allow recruitment of other pathways that are beneficial or inconsequential to the virus lifecycle (Lilley et al., 2007). In the case of Adenovirus the activation of the DDR is detrimental to the virus, and the virus has evolved mechanisms to inhibit the earliest steps of the response (Blackford et al., 2010; Carson et al., 2009; Carson et al., 2003; Evans and Hearing, 2003; Evans and Hearing, 2005; Mathew and Bridge, 2007; Mathew and Bridge, 2008; Stracker et al., 2002).

Adenovirus introduction

Adenoviruses infect a wide variety of vertebrates and include 5 clades organized by sequence homology and the host organism from which the virus was originally isolated (Berk, 2007). There are over 50 serotypes of human adenovirus that cause mild disease phenotypes including conjunctivitis, gastrointestinitis and respiratory infections. However, in immunocompromised

patients adenovirus infection can be fatal, causing pneumonia and encephalitis (Berk, 2007). The human adenoviruses are divided into various subgroups (A-F) based on sequence homology, hemagglutination ability and oncogenicity, with Group C adenoviruses being the best-studied (Berk, 2007). During infection, adenovirus expresses viral proteins that hijack cellular processes to create a cellular environment that is beneficial to the lifecycle of the virus. Studying the alteration of the cellular host pathways by adenovirus has provided insights into basic cellular processes including splicing (Bachenheimer and Darnell, 1975; Berget et al., 1977; Berk and Sharp, 1978; Chow and Broker, 1978), oncogenic transformation (Graham et al., 1974), and DNA damage response (Carson et al., 2003; Stracker et al., 2002). Therefore, beyond basic virus biology, adenovirus can also be used as a model system to study cellular pathways.

The adenovirus genome is linear dsDNA with inverted terminal repeats (ITRs) at either end of the genome with the 5' terminal nucleotide covalently bound to a virally encoded terminal protein (TP) (Rekosh et al., 1977). The TP is bound to the genome by a phosphodiester linkage from a serine residue in the TP to the terminal deoxycytidine residue of the viral DNA (Desiderio and Kelly, 1981). The pre-Terminal Protein (pTP) is the precursor to the TP; pTP is used to prime replication but is cleaved by the viral protease creating the mature TP during packaging (Weber, 1995). Replication of adenovirus is

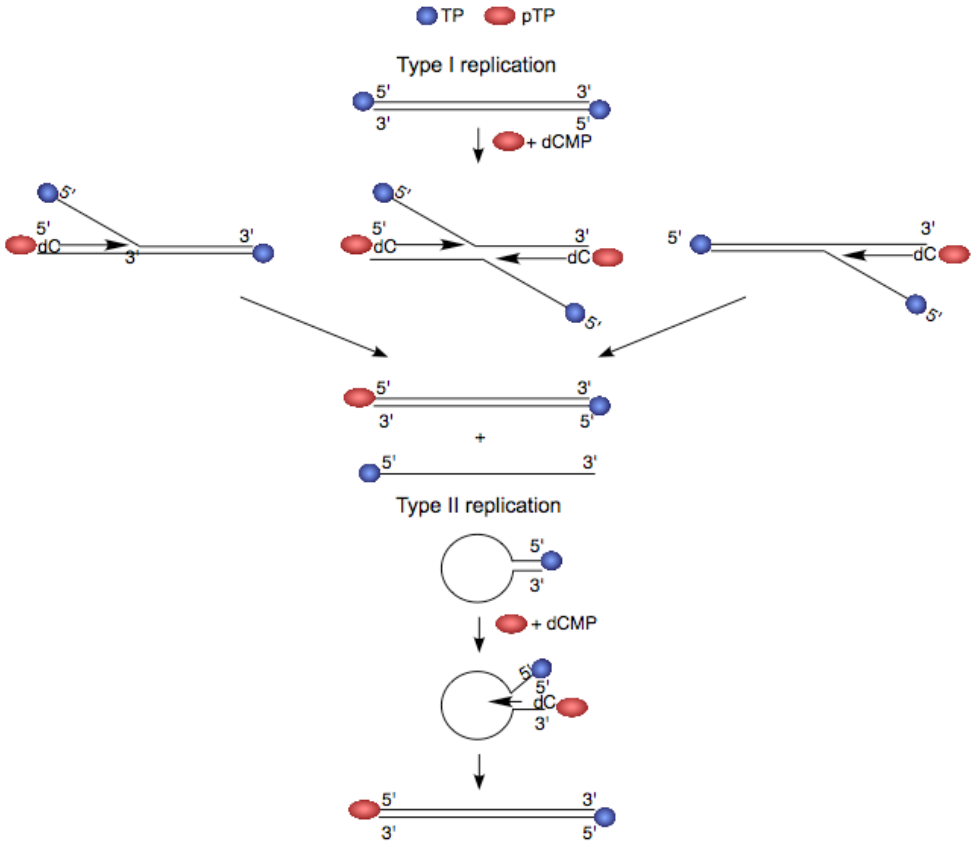

Figure 1-3. Adenovirus replication. The adenovirus input genome is represented by the presence of the mature TP represented in blue. The pTP required for initiation of replication is represented in red. Type 1 replication begins with pTP and AdPol melting the ends of the duplex, and then displacing the 5' strand to synthesize the new strand along the 3' stand. Intermediates of type 1 replication are shown in the second row. Replication forks can potentially occur from both sides of the input genome, resulting in dual replication forks converging towards the center of the genome. Type 1 products include a duplex consisting of the template strand and the newly synthesized DNA, and a displaced ssDNA strand. Type 2 replication occurs when the ITRs of the displaced strand anneal together, creating a ssDNA loop with dsDNA ends. The pTP-AdPol complex can then recognize this "panhandle" structure and addition of dCMP can lead to the melting of the annealed ITRs and replication can occur along the 3' strand. Adapted from (Berk, 2007; Lechner and Kelly, 1977)

carried out by the adenovirus encoded DNA polymerase (AdPol), which uses pTP for initiation of replication in a protein primed mechanism (**Fig. 1-3**). Adenovirus replication occurs in the nucleus and also requires the virus-encoded DNA binding protein (DBP). Immunofluorescence staining against DBP serves as a marker for sites of viral replication and reveals replication centers as discrete compartments in the nucleus (**Fig. 1-4B**)(Pombo et al., 1994). Adenovirus replication occurs by 2 mechanisms: Type 1 replication and Type 2 replication (**Fig. 1-3**)(Lechner and Kelly, 1977). The same mechanisms of initiation are used for both types of replication, as the interaction between the pTP and AdPol is required for the complex to target the replication origin (Chen et al., 1990). To initiate replication, the pTP-AdPol melts the end of the DNA duplex to access the first nucleotide of the 3' strand (de Jong et al., 2003). The pTP is then covalently bound to the first nucleotide of the adenovirus genome, priming DNA synthesis by AdPol. In Type 1 replication, synthesis occurs along the 3' strand while simultaneously displacing the 5' strand. Intermediates of Type 1 replication include dsDNA with 5' flaps of ssDNA (**Fig. 1-3**)(Lechner and Kelly, 1977). It is also possible that replication simultaneously starts on both ends of the viral genome leading to dual replication forks converging towards each other (**Fig. 1-3**). In Type 2 replication, the ITRs from the displaced strand anneal together forming a ssDNA loop with dsDNA at the ends (Lechner and Kelly, 1977). The annealed dsDNA ITRs are then recognized by the pTP-AdPol complex and can be

replicated without the need for strand displacement. The wide variety of adenovirus replication intermediates subject the host machinery to secondary DNA structures resembling meiotic recombination intermediates, 3' tailed duplexes, bubble structures and DNA displacement loops (**Fig. 1-3**)(Chu and Hickson, 2009). The recognition of these intermediates by the host cell, and how the virus prevents or alters the recognition of its genome, could provide new insight into the functions of the cellular proteins in the context of replication and DNA damage.

Adenovirus has 5 early transcription regions that each encode multiple proteins that function to create an environment for optimal replication of the virus: E1a, E1b, E2, E3, and E4. Adenovirus also has 3 delayed early transcription regions (IX, IVa2 and E2 late) and one late region that encodes structural proteins required for virus capsid formation (Berk, 2007). The function of E1a is to activate viral promoters and to prime the cell for adenovirus replication by pushing the cell into S-phase (Berk, 2005). The E2 region encodes proteins that are required for viral replication including AdPol, pTP, and the viral ssDNA binding protein DBP. The E3 proteins encode genes required for immune evasion (as reviewed by Burgert and Blusch, 2000). The E1b region functions in preventing apoptosis by inactivating p53, and specifically E1b55K promotes infection through interactions with the E4orf6 protein from the E4 region (Berk, 2005). Finally, the E4 region

encodes proteins that overcome host pathways that can act as intrinsic barriers to the viral lifecycle.

During infection with wildtype Adenovirus serotype 5 (Ad5), the proteins encoded in the E4 region abrogate cellular proteins by two known mechanisms. The E4orf3 protein mislocalizes proteins into nuclear track-like structures and cytoplasmic aggresomes (Araujo et al., 2005; Evans and Hearing, 2003; Stracker et al., 2002) and the E1b55K and E4orf6 proteins form a ubiquitin ligase complex with cellular proteins Cullin-5, Elongins B and C and Rbx1 to degrade cellular proteins in a proteasome dependent manner (Boivin et al., 1999; Harada et al., 2002; Querido et al., 2001a). Proteins reported to be mislocalized by E4orf3 include the MRN complex, proteins associated with PML bodies and Tif1α (Carvalho et al., 1995; Doucas et al., 1996; Evans and Hearing, 2003; Stracker et al., 2002; Yondola and Hearing, 2007). The E1b55K/E4orf6 ubiquitin ligase complex targets the MRN complex, as well as Integrin α3, p53, and DNA Ligase IV for degradation (Baker et al., 2007; Carson et al., 2003; Cathomen and Weitzman, 2000; Dallaire et al., 2009; Querido et al., 2001a; Schwartz et al., 2008; Stracker et al., 2005; Wienzek et al., 2000). The E1b55K/E4orf6 complex and E4orf3 promote productive virus infection by targeting cellular proteins, and while new targets are still being identified, their mutual targeting of the MRN complex suggests that MRN functions as an intrinsic barrier to adenovirus infection.

Figure 1-4. MRN is inhibitory to adenovirus infection. (A) During infection with an E4-deleted virus (*dl*1004), the MRN complex abrogates infection by inhibiting viral replication, activating the ATM and ATR damage signaling pathways, promoting concatemerization of the genome, and inhibiting synthesis of structural proteins from the major late promoter. (B) Localization of MRN complex during infection. U2OS cells were uninfected (Mock) or infected with Ad5 or *dl*1004. Cells were fixed and immunofluorescence staining was performed for DBP (viral replication centers) and Nbs1. In the mock cells Nbs1 is diffusely nuclear. Cells are shown during progressive infection from early (left) to late (right). Early during Ad5 infection the free pool of Nbs1 is seen located in small foci that represent PML bodies (left panel), after expression of E4orf3, Nbs1 is detected in E4orf3 tracks (middle panel), late during infection the majority of Nbs1 is degraded (right panel). During *dl*1004 infection, Nbs1 localizes to PML bodies (left panel), and then localizes at viral centers (middle and right panels). DAPI staining represents the nucleus (Blue).

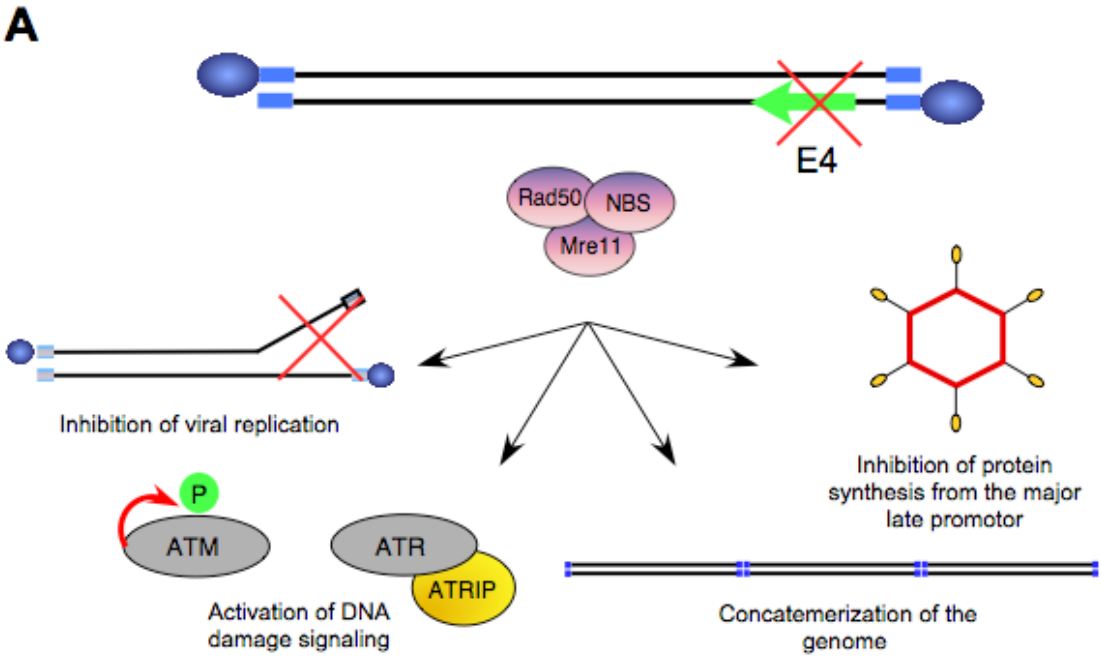
A
E4
Rad50
NBS
Mre11
Inhibition of viral replication
Inhibition of protein synthesis from the major late promotor
P
ATM
ATR
ATRIP
Activation of DNA damage signaling
Concatemerization of the genome

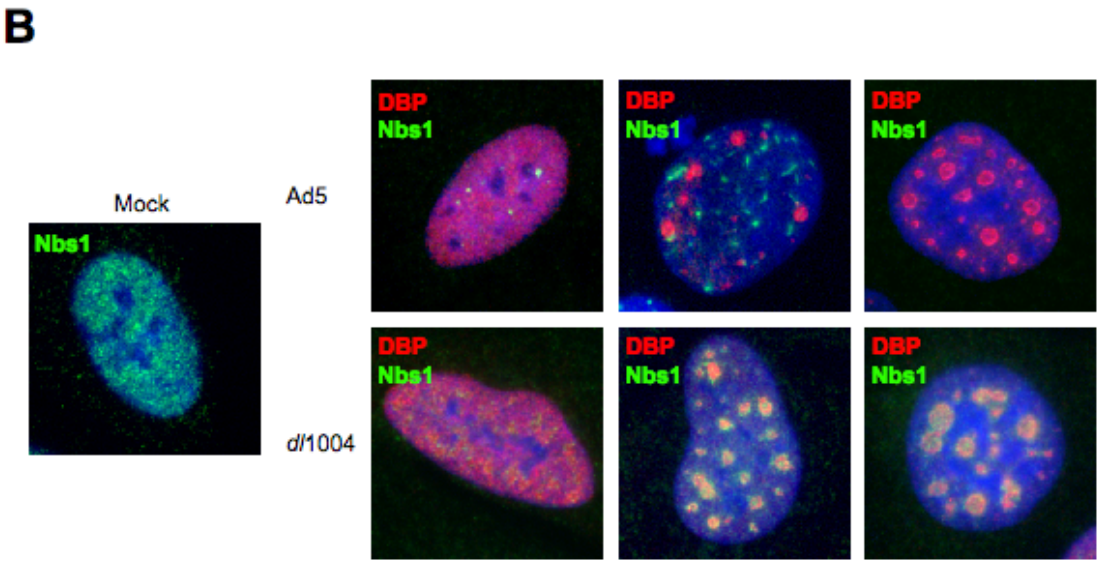
B
Mock
Ad5
dl1004
Nbs1
DBP
Nbs1

Adenovirus activation of the DNA damage response and DNA repair

During infection with an adenovirus that is deleted for the E4-region (*dl*1004), virus infection is severely debilitated (Bridge and Ketner, 1989; Halbert et al., 1985; Weiden and Ginsberg, 1994). The defects include a decrease in viral DNA replication, virus production, and synthesis of the structural late proteins that form the virus capsid (Bridge and Ketner, 1989; Halbert et al., 1985). During *dl*1004 infection, the viral genomes are also ligated into end-to-end concatemers that are too large to be packaged into virus capsids (Weiden and Ginsberg, 1994). The NHEJ proteins DNA-PKcs and DNA Ligase IV are both required for concatemer formation to ligate the genome ends (Boyer et al., 1999; Stracker et al., 2002). The MRN complex is required to promote concatemer formation, inhibit viral replication and suppress late protein synthesis (**Fig. 1-4A**)(Mathew and Bridge, 2008; Stracker et al., 2002, Lakdawala, 2008). During infection with Ad5, the MRN complex is mislocalized and then degraded by the E4 proteins (**Fig. 1-4B**)(Stracker et al., 2002). However, during *dl*1004 infection, the MRN complex localizes to sites of viral replication (**Fig. 1-4B**)(Stracker et al., 2002). The localization of the MRN complex at sites of *dl*1004 replication centers correlates with robust activation of the ATM and ATR signaling pathways (**Fig. 1-4A**). During infection with wildtype Ad5, E1b55K/E4orf6 prevents the activation of these kinases via degradation of the MRN complex (Carson et al., 2003). As described previously, the MRN complex plays separable roles in

damage repair and activation of the DDR, and studies are determining how the two functions of the MRN complex influence its inhibition of various stages of the viral lifecycle.

Inhibition of the MRN complex is required for adenovirus to replicate efficiently, promote synthesis of late proteins and to prevent the ligation of its genome into concatemers (Halbert et al., 1985; Mathew and Bridge, 2008; Stracker et al., 2002, Lakdawala, 2008, Bridge, 1989; Weiden and Ginsberg, 1994). The domains of the MRN complex that are required for each of these functions are starting to elucidate a mechanism for MRN mediated inhibition of adenovirus. The C-terminus of Nbs1 is required to inhibit viral replication during *dl*1004 infection (Lakdawala et al., 2008). However, the requirement of the C-terminus of Nbs1 is unrelated to its activation of ATM signaling pathways (Falck et al., 2005; You et al., 2005), as inhibition of ATM and ATR signaling kinases did not inhibit viral replication although it did inhibit concatemer formation (Lakdawala et al., 2008). It has also been demonstrated that the ability of MRN to inhibit replication and late protein synthesis is not a direct consequence of concatemer formation (Evans and Hearing, 2003; Lakdawala et al., 2008). Mre11 nuclease activity is required for concatemer formation (Stracker et al., 2002); however, biochemical characterization of Mre11 nuclease activities (Paull and Gellert, 1998a; Paull and Gellert, 1999b; Trujillo et al., 1998), do not suggest that Mre11 can function alone in TP removal. Therefore, removal of the TP and inhibition of

replication may require the processing function of the MRN complex in concert with another processing protein such as CtIP. However, promotion of concatemer formation may require both the DNA processing and the DDR functions of MRN. Determining how MRN inhibits adenovirus will provide insight into the separate functions of the complex members and potentially expand the known roles for MRN in damage responses and end processing.

The work presented in this thesis focuses on recognition of the viral genome by cellular repair proteins, and the consequences of this recognition for both the virus and the cell. The aim of the second chapter is to continue previous studies on MRN-mediated activation of damage signaling pathways. Specifically, it elucidates how E4orf3 inhibits ATR damage signaling but not ATM signaling during viral infection. The results in chapter 2 implicate a requirement for MRN activation of ATR kinase activity in a step downstream of recruitment of ATR/ATRIP/RPA/TopBP1 to sites of viral replication. The third and fourth chapters focus on the roles of DSB processing proteins CtIP and BLM during adenovirus infection. CtIP and BLM were found to inhibit adenovirus infection or be degraded during adenovirus infection, respectively, and our studies may have implications for these proteins in basic cellular processes beyond the context of adenovirus infection. The role of CtIP in inhibition of adenoviral replication, suggests that it plays a role in TP removal, which could correlate with a role for CtIP in Spo11 removal during meiosis. The degradation of BLM during adenovirus infection suggests BLM also plays

an inhibitory function and future studies to determine how BLM is affecting Ad may provide insight into the function of BLM in cells.

Chapter 2. Mislocalization of the MRN complex prevents ATR signaling during Adenovirus infection

Background

Work from our lab has demonstrated that the cellular DNA repair machinery presents an obstacle to productive adenovirus infection (Stracker et al., 2002). Infection with *di*1004 results in formation of virus genome concatemers by a cellular DNA repair pathway (Boyer et al., 1999; Stracker et al., 2002). The MRN complex is required for concatemer formation and more specifically Mre11 nuclease activity is also required for concatemer formation (Stracker et al., 2002). Ad5 has evolved two ways to prevent concatemers by targeting the MRN complex (Stracker et al., 2002). The viral E1b55K and E4orf6 proteins induce proteasome-mediated degradation of MRN proteins (Carson et al., 2003; Stracker et al., 2002), while expression of the Ad5 E4orf3 protein mislocalizes MRN proteins into intranuclear track-like structures and cytoplasmic aggregates (Araujo et al., 2005; Evans and Hearing, 2005; Stracker et al., 2002; Stracker et al., 2005).

Coincident with concatemer formation, infection with *di*1004 also elicits a cellular DNA damage response (Carson et al., 2003; Stracker et al., 2002). The ATM and ATR kinase signaling pathways are activated, as detected by auto-phosphorylation of ATM and phosphorylation of many known ATM and ATR substrates (**Fig. 1-1**) (Carson et al., 2003). The response is also

characterized by recruitment of the MRN complex and other DNA damage response proteins to viral replication centers (**Fig. 1-4**). In contrast, this cellular DNA damage response is not observed during infection with wild-type Ad5 that expresses E4 proteins (Carson et al., 2003). Our previous work demonstrated that the degradation of the MRN complex by E1b55K/E4orf6 prevented both an ATM and ATR DNA damage response (Carson et al., 2003). However, we had not previously examined the effect of E4orf3 expression independently of E1b55K/E4orf6 on the ATM and ATR damage responses.

Adenovirus infection provides a novel system in which to analyze the mechanism and consequences of ATR signaling. In this chapter we examine the effect of E4orf3-mediated MRN redistribution on ATM and ATR signaling. We show that activation of ATR signaling during viral infection is dependent on the MRN complex and is independent of ATM. The MRN complex is not required for accumulation of RPA, ATRIP, ATR and TopBP1 at viral replication centers. We examine MRN dynamics in living cells and demonstrate that E4orf3-induced immobilization prevents MRN from responding to the virus and other types of DNA. The results presented in this chapter demonstrate a novel role for MRN in activation of ATR signaling, independent of ATM and downstream of recruitment of RPA/ATR/ATRIP/TopBP1.

Results

The MRN complex is required for robust ATR signaling

We previously demonstrated phosphorylation of ATM and ATR kinase substrates in response to *dl*1004 infection (Carson et al., 2003). Some sites were modified by either ATM or ATR (e.g. Chk2-T68 and Nbs1-S343), whereas others were ATR specific (e.g. Chk1-S345 and RPA32). We demonstrated that MRN is required for ATM activation (Carson et al., 2003), but the requirement for MRN in ATR signaling during virus infection has not been clarified. To investigate the role of MRN specifically in ATR-dependent signaling responses to virus, we examined phosphorylation events during infections of cells with hypomorphic mutations in Mre11 and Nbs1. Infections were performed in mutant and complemented versions of the A-TLD1 cell line, that expresses mutant Mre11 (Carson et al., 2003), and the NBS-ILB1 cell line that harbors an Nbs1 mutation (Cerosaletti et al., 2000). Lysates from cells infected with *dl*1004 were analyzed by immunoblotting with a phospho-specific antibody to Chk1-S345, and with an antibody to RPA32 (**Fig. 2-1**). Phosphorylation of Chk1 and RPA32 was detected in cell lines complemented with wild-type cDNAs. In contrast, infection with *di*1004 in the A-TLD1 (**Fig. 2-1A**) and NBS (**Fig. 2-1B**) mutant lines produced significantly reduced signaling. Wild-type Ad infection did not generate these phosphorylation events due to degradation of MRN proteins. These data demonstrate that the MRN complex is required for robust ATR signaling in response to Ad infection.

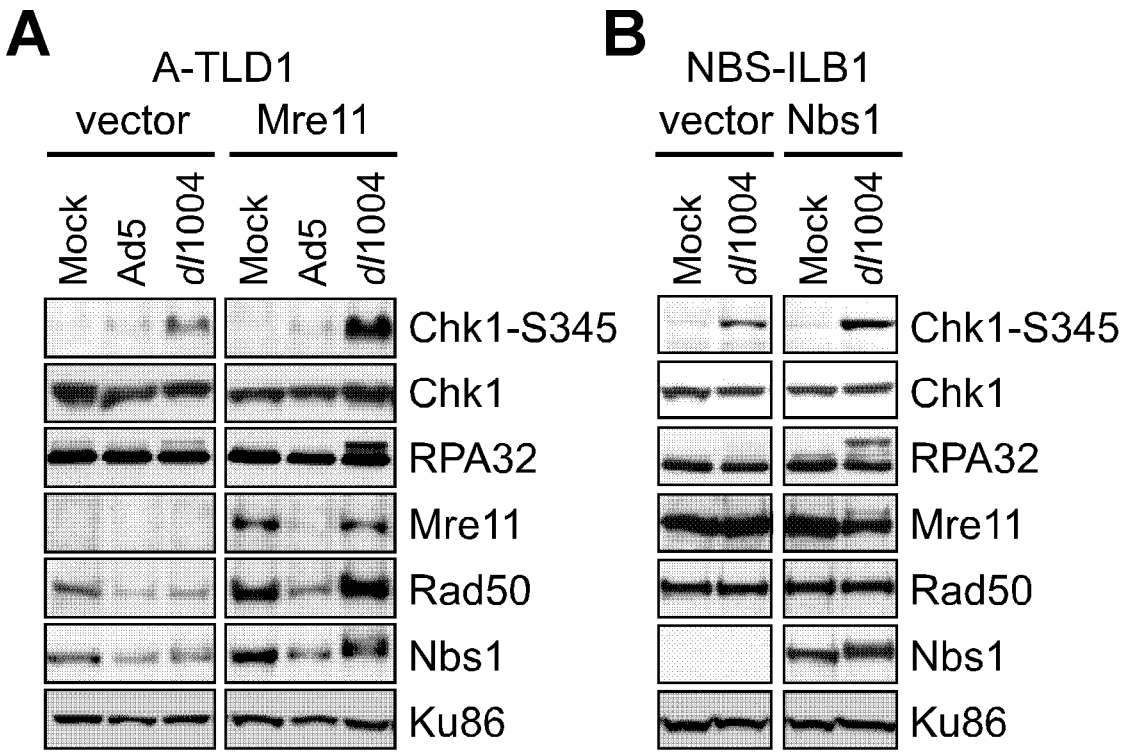

Figure 2-1. The Mre11 and Nbs1 proteins are required for robust ATR signaling in response to mutant Ad infection. (A) Infections were performed in a transformed cell line deficient for Mre11 (A-TLD1) that was transduced with an empty retrovirus vector (vector) or in a vector expressing the wild-type Mre11 cDNA (Mre11). Cells were uninfected (mock) or infected with Ad5 or *dl*1004. Immunoblotting of lysates prepared at 30 hpi were assayed for western by using antibodies for total protein or phospho-specific sites as indicated in the figure. Ku86 served as a loading control. (**B**) Infections were performed in the transformed NBS cell lines (NBS-ILB1) transduced with an empty retrovirus vector (vector) or a vector expressing the wild-type Nbs1 cDNA.

The presence of Ad5-E4orf3 reduces ATR signaling but not ATM

Since the Ad5 E4orf3 protein affects MRN complex localization, we investigated whether E4orf3 alters ATM and ATR signaling during infection. Because the viral E1b55K and E4orf6 proteins downregulate damage signaling via degradation of the MRN complex (Carson et al., 2003), we tested a mutant that is deleted of E4orf6 and E1b55K but retains E4orf3 (*dl*1017), and compared it to wild-type Ad5 and *dl*1004 (**Fig. 2-2A**). The *dl*1004 virus induced phosphorylation of ATR substrates Chk1 and RPA32, as detected by a shift in the mobility of RPA32 and by recognition with phospho-specific antibodies (Chk1-S345 and RPA32-S4,8)(**Fig. 2-2B**). These phosphorylation events were greatly reduced during infection with *dl*1017 that expresses E4orf3, indicating that ATR signaling is reduced in the presence of Ad5-E4orf3. We also examined the effect of E4orf3 on ATM signaling. In contrast to ATR, ATM signaling was intact during infection with *dl*1017, as evidenced by ATM auto-phosphorylation on S1981 (**Fig. 2-2B**). Together these data suggest that MRN mislocalization by E4orf3 is not sufficient to prevent ATM activation, indicating that ATM and ATR signaling pathways can be independently regulated during Ad infection.

To determine the interdependence of ATR and ATM, we examined signaling in cells with kinase mutations. Cells derived from a Seckel syndrome patient with mutation in *ATR* (O'Driscoll et al., 2003) and from an A-T patient with mutation in *ATM* were infected with viruses that express E4orf3 (Ad5 or

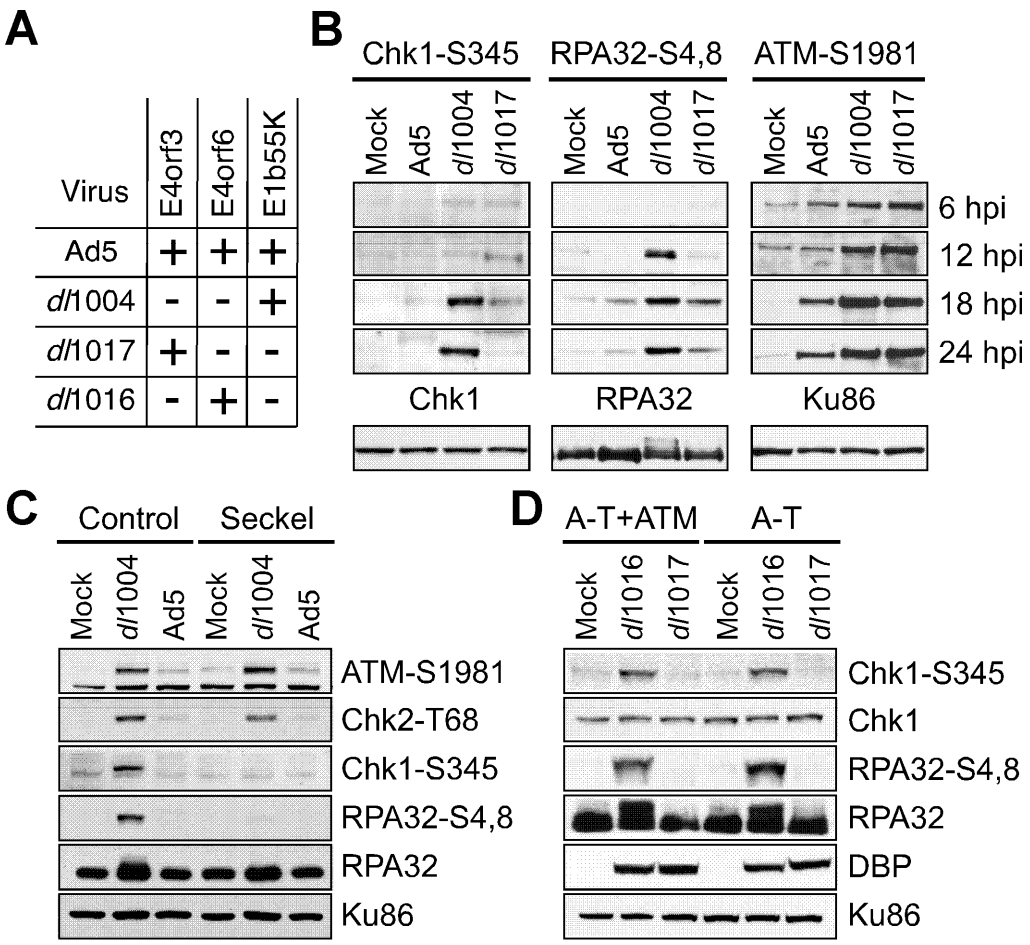

Figure 2-2. Phosphorylation of ATR substrates is reduced in the presence of Ad5-E4orf3, and is independent of ATM. (A) Genotypes of mutant viruses used for infection. (**B)** HeLa cells were Mock infected or infected with indicated viruses. Cells were harvested at 6, 12, 18 and 24 hpi and prepared for analysis by immunoblotting using the indicated antibodies to assay total protein or phosphorylation of phospho-specific residues. (**C**) Immunoblots of infections in control cells (48BR) or Seckel cells with mutants ATR (GM18366). (**D)** Immunoblots of infections in A-T cells with mutant ATM (AT221JE-T) or a complemented line (A-T + ATM). DBP was a marker of virus infection and Ku86 served as a loading control.

*dl*1017) and those that lack E4orf3 (*dl*1004 or *dl*1016). Phosphorylation of Chk1-S345 and RPA32-S4,8 was abolished in the Seckel cells (**Fig. 2-2B**). ATM activation and signaling were intact in Seckel cells, as detected by auto-phosphorylation on S1981 (**Fig. 2-2C**). Infections of A-T cells or a matched complemented line with the double mutant virus *dl*1016 (ΔE1b55K/ΔE4orf3) induced ATR signaling (**Fig. 2-2D**). However, signaling to Chk1 and RPA32 was abrogated in the presence of E4orf3 (*dl*1017). These results demonstrate that ATR activation in response to Ad infection, and its inhibition by E4orf3, are independent of ATM.

Accumulation of ATR at viral replication centers is independent of MRN

Viral replication centers can be detected by staining with antibodies to the viral DNA binding protein (DBP) that coats ssDNA accumulated at viral replication sites (Pombo et al., 1994). The cellular RPA32 protein also accumulates at these sites (Stracker et al., 2005) with both wild-type and mutant viruses (**Fig. 2-3A**). The E4orf3 protein is excluded from viral replication centers and appears in intranuclear tracks and cytoplasmic aggregates (Araujo et al., 2005; Evans and Hearing, 2005), with both wild-type Ad5 or the *dl*1017 mutant (**Fig. 2-3A**). The Ad5-E4orf3 protein is sufficient to redistribute the MRN complex, as detected by staining for Nbs1 (**Fig. 2-3A**). In contrast, infection with *dl*1004 leads to accumulation of MRN at viral centers. We therefore investigated whether MRN mislocalization by E4orf3 correlates with inhibition of ATR signaling (**Fig. 2-3B**). Phosphorylation of RPA32 at viral

Figure 2-3. Signaling by ATR at viral replication centers. (A) E4orf3 sequesters Nbs1 into tracks away from viral replication centers. HeLa cells were mock infected or infected with indicated viruses. Cells were fixed 16 hpi and immunofluorescence was performed. Staining shows that Nbs1 but not RPA32 is excluded from viral replication centers in the presence of E4orf3. (**B)** Colocalization of the MRN complex with RPA 32 at replication centers correlates with RPA32 phosphorylation. Immunofluorescence with a phospho-specfic antibody to RPA32-S4,8 shows colocalization with viral replication centers stained with an antibody to DBP only in the absence of E4orf3. (**C**) Accumulation of RPA32, ATR and ATRIP at viral centers is independent of E4. (**D**) TopBP1 accumulated at viral centers independently of E4. (**E)** Activation is observed for ATM, but not ATR, in Seckel cells.

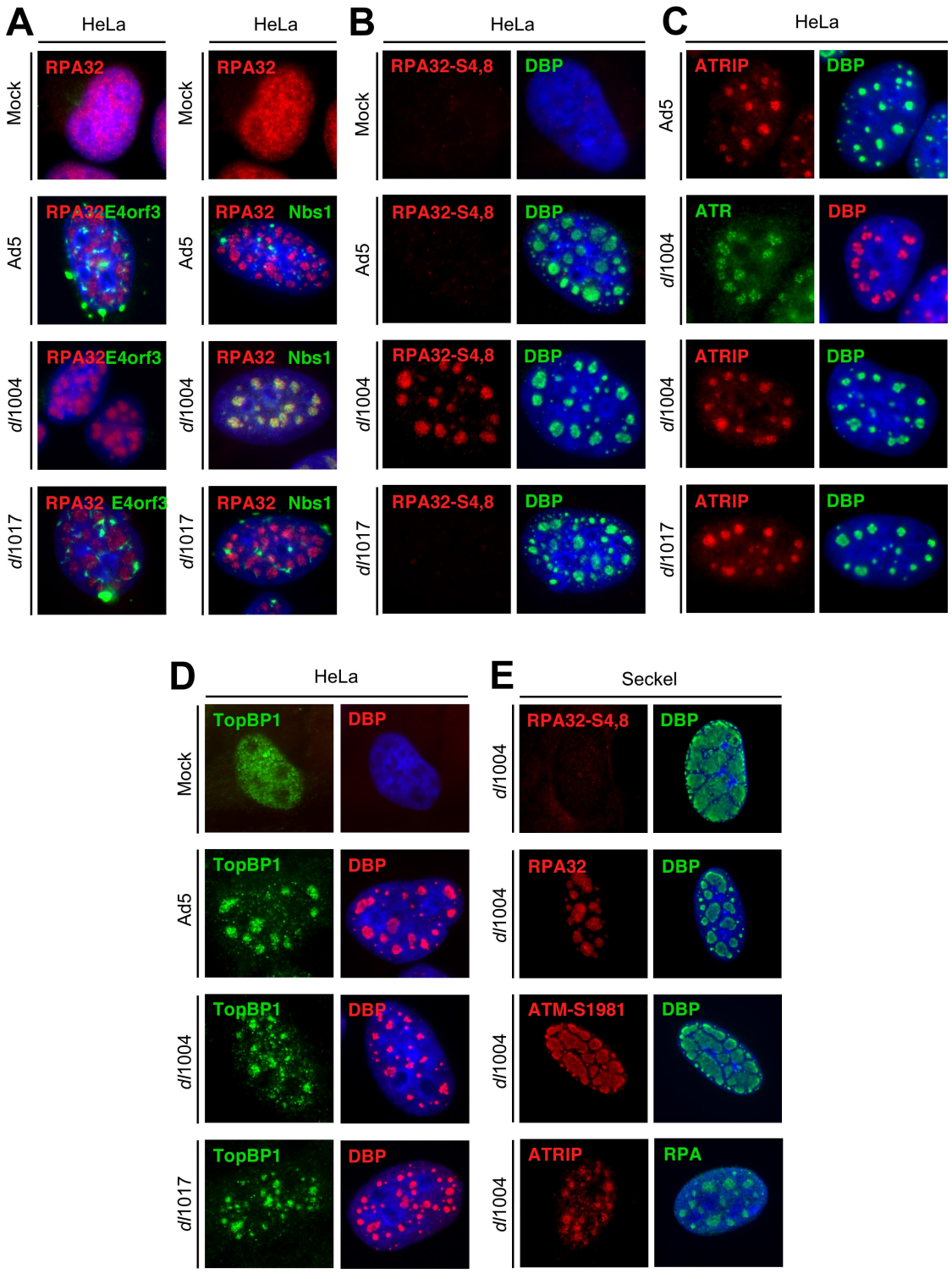
A
HeLa
HeLa
Mock
RPA32
Mock
RPA32
Ad5
RPA32E4orf3
Ad5
RPA32 Nbs1
dl1004
RPA32E4orf3
dl1004
RPA32 Nbs1
dl1017
RPA32 E4orf3
dl1017
RPA32 Nbs1
B
HeLa
Mock
RPA32-S4,8
DBP
Ad5
RPA32-S4,8
DBP
dl1004
RPA32-S4,8
DBP
dl1017
RPA32-S4,8
DBP
C
HeLa
Ad5
ATRIP
DBP
dl1004
ATR
DBP
dl1004
ATRIP
DBP
dl1017
ATRIP
DBP
D
HeLa
Mock
TopBP1
DBP
Ad5
TopBP1
DBP
dl1004
TopBP1
DBP
dl1017
TopBP1
DBP
E
Seckel
dl1004
RPA32-S4,8
DBP
dl1004
RPA32
DBP
dl1004
ATM-S1981
DBP
dl1004
ATRIP
RPA

centers, as detected by staining with the RPA32-S4,8 antibody, was only observed when the MRN complex was associated with viral replication centers. When the virus expressed E4orf3, RPA32 phosphorylation was not detected. This shows that E4orf3 mislocalization of the MRN complex prevents its accumulation at viral replication centers, and that this correlates with the absence of ATR signaling to RPA32.

We also investigated whether E4orf3 affects localization of other proteins involved in ATR signaling. We observed that ATR, RPA and ATRIP accumulated at viral replication centers with all viruses tested, irrespective of E4orf3 expression (**Fig. 2-3C**). These data suggest that E4orf3 does not abrogate ATR signaling by mislocalizing ATR, RPA32 or ATRIP. It also demonstrates that the presence of ATR at viral centers is not sufficient to initiate or maintain the DNA damage signaling during infection. The TopBP1 protein is a regulator of ATR that stimulates kinase activity through an interaction with ATRIP (Kumagai et al., 2006; Mordes et al., 2008). We examined localization of TopBP1 during infection and found it localized in viral DBP centers with wild-type and *dl*1004 (**Fig. 2-3D**). Immunofluorescence of infected Seckel cells confirmed that phosphorylation of RPA32-S4,8 was not observed in the absence of functional ATR, although RPA32 and ATRIP accumulated at viral centers (**Fig. 2-3E**). ATM activation was detectable in Seckel cells as revealed by staining for ATM-S1981, and is therefore independent of ATR in response to Ad infection (**Fig. 2-3E**).

Mre11 nuclease activity is not required for ATR activation at sites of viral replication

ATR activation occurs though its interaction with ATRIP and is mediated by additional interactions with TopBP1 and RPA bound ssDNA (Kumagai et al., 2006; Lee et al., 2007; Mordes et al., 2008; Zou, 2007; Zou and Elledge, 2003). We hypothesized that the nuclease domain of Mre11 could create excess ssDNA that would be bound by RPA thus triggering the ATR activation induced during viral infection. To determine if Mre11 nuclease activity was required for ATR activation we analyzed the presence of RPA32-S4,8 at sites of viral replication in A-TLD1 cells, which are hypomorphic for Mre11 (**Fig. 2-4A**). We did not detect phosphorylation of RPA32-S4,8 at viral centers in A-TLD1 cells, further demonstrating that MRN association at viral centers is required for ATR activation. However, ATR signaling was detected when infections were performed in A-TLD1 cells transduced with retroviruses that express either wild-type Mre11 or the nuclease-defective Mre11-3 mutant (**Fig. 2-4A**). This demonstrated that the nuclease defective mutant of Mre11 was sufficient to complement A-TLD1 cells for activation of ATR, suggesting the nuclease activity of Mre11 is not required for Ad induced ATR activation. To confirm this result we also used a chemical inhibitor of Mre11 (mirin), which has been shown to inhibit Mre11 nuclease activity in *X. Laevis* extracts

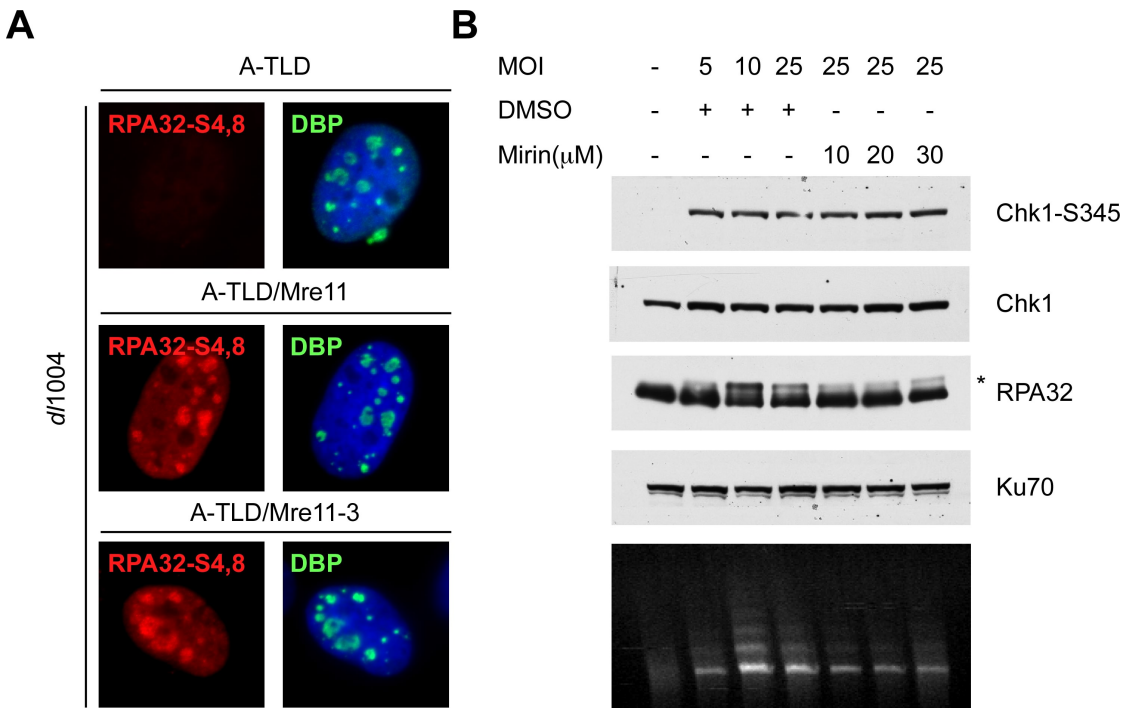

Figure 2-4. Mre11 nuclease activity is not required for ATR signaling during *dl*1004 infection. (A) A-TLD cells were complemented with either wild-type Mre11 (A-TLD/Mre11) or nuclease defective Mre11 A-TLD/Mre11-3) and immunofluorescence was performed to determine presence of phosphorylated RPA (RPA-S4,8) and DBP to show viral replication compartments. DAPI was used to stain nuclei. **(B**) Inhibiting Mre11 nuclease activity with mirin prevents concatemers but not ATR signaling during infection with *dl*1004. Mirin was added to infected cells in varying concentrations and cells were also infected with varying MOIs. Samples were harvested and split for analysis by both immunoblotting (Top 4 panels) and PFGE analysis (Lower panel). In our PFGE analysis cells infected with an MOI of 5 displayed levels of viral DNA comparable to that of mirin treated cells infected with an MOI of 25. Concatemer formation is inhibited with 10mM mirin however there is still ATR signaling demonstrated by western blotting with a phospho-specific antibody to Chk1-S345 and an antibody to RPA32 to evaluate the hyperphosphorylation shift. Chk1 and Ku70 were used as loading controls.

(Dupré et al., 2008). Our previous work demonstrated that Mre11 nuclease activity is required for formation of viral genome concatemers during *dl*1004 infection (Stracker et al., 2002). To determine an effective concentration of mirin, we titrated mirin into our infected cells and found that prevention of viral genome concatemers occurred at concentrations of 10μM mirin (**Fig. 2-4B**, Lower panel, Lane 4,5). While mirin addition to cells inhibited concatemer formation, it also inhibited overall accumulation of viral DNA (**Fig. 2-4B**, Lower panel, lanes 5-7). To compensate for the replication defect of the virus, we titrated the MOI of *dl*1004 to an amount that was comparable to the amount of DNA in the mirin treated cells. We found that untreated cells infected with an MOI of 5 (**Fig. 2-4B** Lower panel, Lane 2) had comparable amounts of DNA as 10μM mirin treated cells that were infected with an MOI of 25 (**Fig. 2-4B**, Lower panel, Lane 5). When we evaluated the level of ATR activation in the cells with comparable amounts of DNA (Lane 2 and 5), we saw no difference in the level of ATR activation (Chk1-S345 and RPA hyper-phosphorylation shift) (**Fig. 2-4B**). These experiments suggest that although MRN nuclease activity is required for concatemer formation, is not required for ATR signaling during *dl*1004 infection.

Mislocalization of the MRN complex by Ad5-E4orf3 is required for disruption of ATR signaling

Although E4orf3 proteins from all serotypes tested form nuclear tracks, rearrange the promyelocytic leukemia protein PML and redistribute

components of the PML bodies, only Ad5-E4orf3 mislocalizes the MRN complex (Stracker et al., 2005). Sequence analysis for the highly conserved E4orf3 proteins revealed residues specific to the subgroup C viruses (Ad1, Ad2 and Ad5) that uniquely mislocalize MRN. Based on these alignments, we converted isoleucine at position 104 of Ad5 E4orf3 to arginine, which is present in all other serotypes (**Fig. 2-5A**). The Ad5 E4orf3-I104R mutant retained the ability to form nuclear tracks and disrupt PML, but was defective for redistribution of the MRN complex (**Fig. 2-5B**). This identified a region of E4orf3 involved in targeting the MRN complex and provided a separation-of-function mutant. We next wanted to determine if converting the Ad4 arginine at 105 to isoleucine would exhibit a gain-of-function phenotype and confer the ability to mislocalize the MRN complex. We constructed an Ad4 E4orf3-R105I mutant and transfected this construct into HeLa cells in parallel with the wild-type Ad4-E4orf3. We found that while both the wild-type Ad4-E4orf3 and the R105I mutant were able to mislocalize PML (and form track structures), the R105I mutant did not mislocalize the MRN complex (**Fig. 2-5C**). We examined other mutants including a double mutant of R105I and R130L, the triple mutant RDR113-115DNL and the quadruple mutant RDR113-115DNL/R105I but none of these mutants mislocalized MRN (Data not shown). These experiments suggest that while Ad5-I104 is required for mislocalization of MRN, the converse mutation of Ad4-R105I is not sufficient to mislocalize the MRN complex.

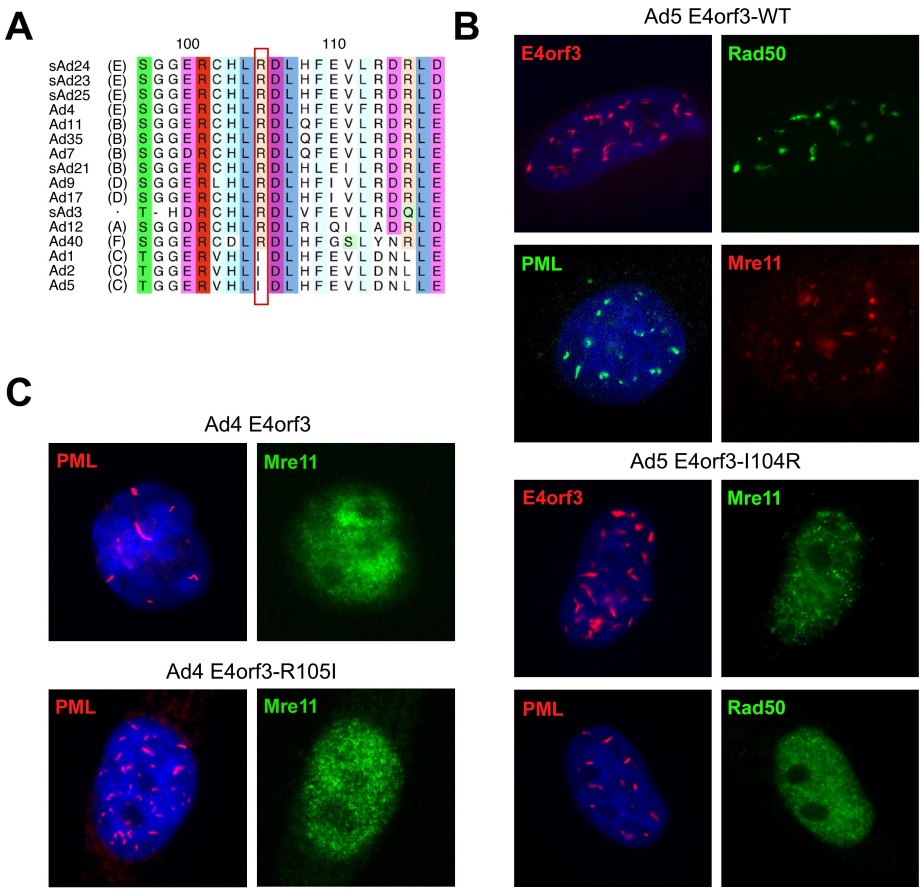

Figure 2-5 Identification of a region in Ad5-E4orf3 important for targeting the MRN complex. (**A**) Sequence alignment of E4orf3 proteins. E4orf3 sequences from different human (subgroup noted in brackets) and simian adenoviruses were aligned using the CLUSTAL algorithm. Conserved residues are shown boxed, with CLUSTAL color scheme reflecting amino acids of similar chemical nature. The I104 residue is highlighted, demonstrating that this site differs between subgroup C and all other sequenced E4orf3 genes. (**B**) The Ad5 E4orf3-I104R mutant does not redistribute the MRN complex. Plasmids for wild-type and mutant E4orf3 were transfected into HeLa cells. Immunofluorescence shows that the E4orf3 mutant protein still forms tracks and disrupts PML structures, but is unable to redistribute members of the MRN complex. Representative images are shown and nuclei are located by co-staining cellular DNA with DAPI. (**C)** The Ad2-R105I mutant is not sufficient to allow mislocalization of the MRN complex. Plasmids expressing wild-type Ad4 E4orf3 and Ad4 E4orf3-R105I were transfected into HeLa cells. Immunofluorescence shows that the Ad4 E4orf3 and Ad2-R105I E4orf3 proteins do not mislocalize Mre11 displayed by its diffusely nuclear localization, although they retain the ability to form tracks and mislocalize PML.

We next examined the ability of Ad5-E4orf3, Ad12-E4orf3, and E4orf3-I104R proteins to prevent ATR signaling during infection with *dl*1004 (**Fig. 2-6**). Cells were transfected with E4orf3 expression vectors, and then infected with *dl*1004. Immunoblotting revealed abrogated ATR signaling in the presence of Ad5-E4orf3 (reduced Chk1-S345 and RPA32-S4,8 phosphorylation and RPA32 mobility shift) although ATM auto-phosphorylation was not significantly altered (**Fig. 2-6A**). In contrast, the Ad12-E4orf3 and E4orf3-I104R proteins, that failed to mislocalize the MRN complex, did not inhibit ATR signaling (**Fig. 2-6A** and **B**). Cells from the same experiment were also examined by immunofluorescence for RPA32-S4,8 phosphorylation, as a marker of ATR signaling (**Fig. 2-6C**). We observed that Ad5-E4orf3, but not Ad12-E4orf3 or E4orf3-I104R, prevented RPA phosphorylation at viral replication centers. Cotransfection of a plasmid expressing GFP served as a marker for transfected cells. Control staining demonstrated that viral DBP centers were formed in all cells, and that expression of E4orf3 proteins resulted in PML disruption (data not shown). Together these data support the hypothesis that mislocalization of the MRN complex by E4orf3 leads to abrogation of ATR signaling.

Figure 2-6. E4orf3 proteins that mislocalize the MRN complex abrogate ATR signaling in response to virus infection. HeLa cells were transfected with an empty plasmid (vector) or with vectors expressing E4orf3 proteins. After 24 h cells were either mock infected, infected with the E1b55K/E4orf6 mutant (*dl*1017) (positive control), or infected with *dl*1004. (**A** and **B**) Lysates from cells at 24 hpi were immunoblotted with antibodies to Chk1-S345, RPA32-S4,8, ATM-1981 and RPA32. (**C**) Cells were fixed at 18 hpi and immunofluorescence was performed with an antibody to RPA32-S4,8. Images are shown merged with DAPI staining. A plasmid expressing GFP was co-transfected with that for E4orf3 at a ratio of 1:10 and GFP staining is shown in the lower left insert panel as a positive control for transfection. (**D**) HeLa cells were transfected with vectors as in (B), cells were infected with *dl*1004 and harvested after 48 hpi, cells were prepared for PFGE analysis and DNA was visualized with Syber Green staining.

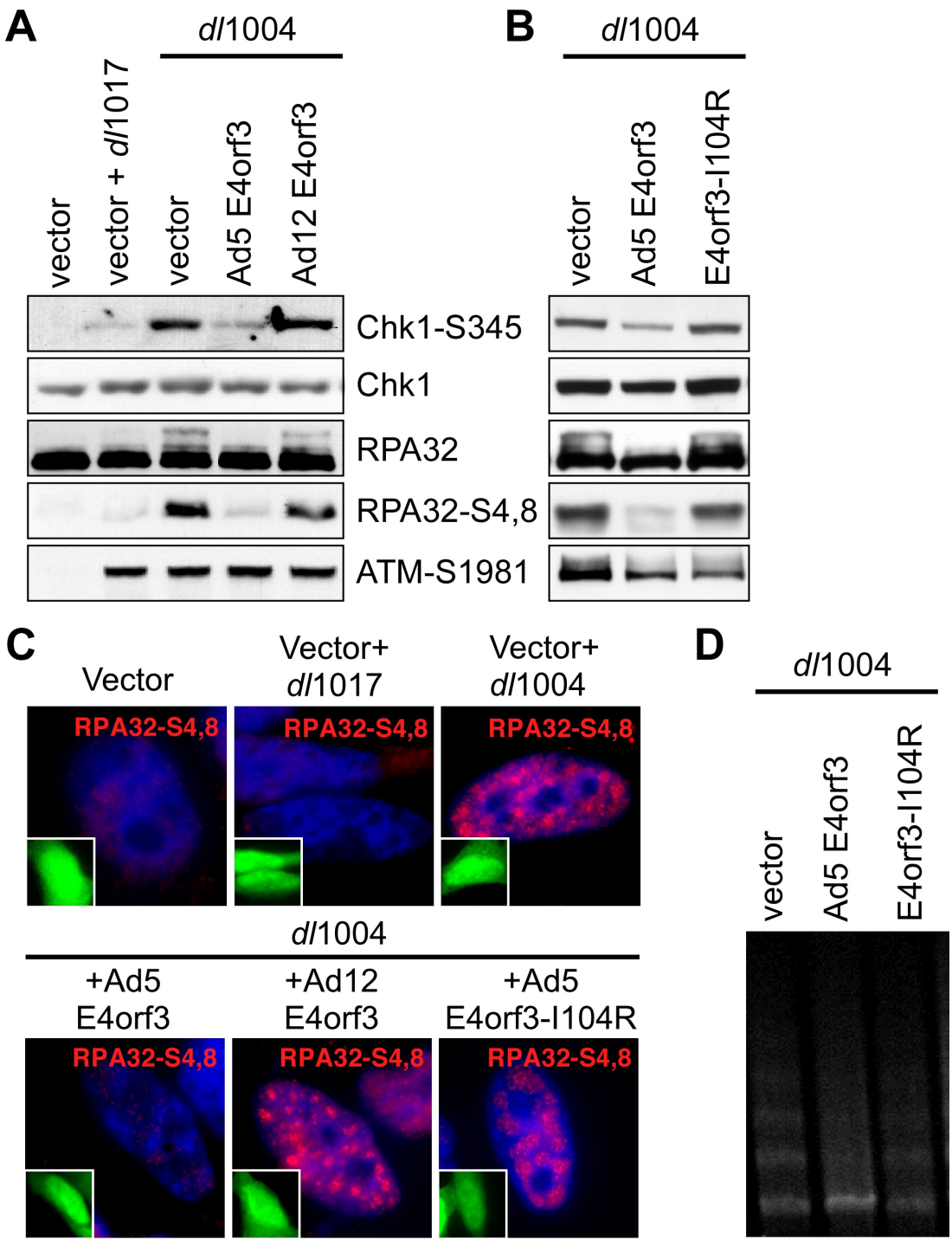
A
dl1004
vector
vector + dl1017
vector
Ad5 E4orf3
Ad12 E4orf3
Chk1-S345
Chk1
RPA32
RPA32-S4,8
ATM-S1981
B
dl1004
vector
Ad5 E4orf3
E4orf3-I104R
C
Vector
Vector+ dl1017
Vector+ dl1004
RPA32-S4,8
dl1004
+Ad5 E4orf3
+Ad12 E4orf3
+Ad5 E4orf3-I104R
D
dl1004
vector
Ad5 E4orf3
E4orf3-I104R

Mislocalization of the MRN complex by E4orf3 correlates with E4orf3 inhibition of Ad genome concatemers

Cells infected with *dl*1004 ligate the viral genome into end-to-end concatemers (Weiden and Ginsberg, 1994). The expression of E4orf3 is sufficient to prevent concatemer formation (Stracker et al., 2002). To confirm that E4orf3 prevention of concatemers was due to mislocalization of the MRN complex but not related to its mislocalization of PML, we transfected HeLa cells with either empty plasmid (vector), or a construct expressing Ad5-E4orf3, Ad5-E4orf3 I104R and subsequently infected the cells with *dl*1004 and analyzed the DNA by PFGE (**Fig. 2-6D**). In the lane transfected with the wild-type Ad5 E4orf3, the viral DNA runs as a single band representing linear genome monomers. In contrast, in the samples that expressed either the empty vector or the I104R mutant concatemers are formed (**Fig. 2-6D**). This confirms our previous hypothesis that concatemer formation is prevented by E4orf3 due to its ability to mislocalize the MRN complex and not PML.

The MRN complex is immobilized by Ad5-E4orf3

We previously reported that Ad5-E4orf3 expression alters MRN complex solubility (Araujo et al., 2005). To examine the effect of E4orf3 on protein dynamics in live cells we utilized fluorescently-tagged fusion proteins of Mre11 and Nbs1. We expressed Mre11-YFP and Nbs1-YFP by cell transfection either in the presence of E4orf3 alone or in virus infected cells (**Fig. 2-7**). The fusion proteins were distributed diffusely in the nucleoplasm in

Figure 2-7. E4orf3 abrogates MRN function by immobilizing the MRN complex. (**A**) HeLa cells were transfected with Nbs1-YFP or Mre11-YFP alone or together with Ad5-E4orf3 plasmid vector. After 24 h cells were infected with *dl*1004 or *dl*1017. Cells were fixed 18 hpi, and immunofluorescence was performed with a Rad50 antibody. Images shown are merged with DAPI staining. (**B**, **C**, and **D**) FRAP analysis of Nbs1 and Mre11 in cells expressing E4orf3 by infection or transfection. The unbleached portion of the cell served to normalize the overall fluorescence decay during the repeated image collection. Arrows above indicate the time of bleaching. (**B**) Stable U2OS cells expressing Nbs1-2GFP were untreated, transfected with E4orf3 or treated with 10gy gamma-irradiation. (**C**) HeLa cells were transfected with Nbs1-YFP and then mock treated or infected with *dl*1004 and *dl*1017. Cells were analyzed by FRAP at 18 hpi. (**D**) HeLa cells transfected with Mre11-YFP together with either empty vector, or vectors expressing Ad5-E4orf3 and E4orf3-I104R were analyzed by FRAP.

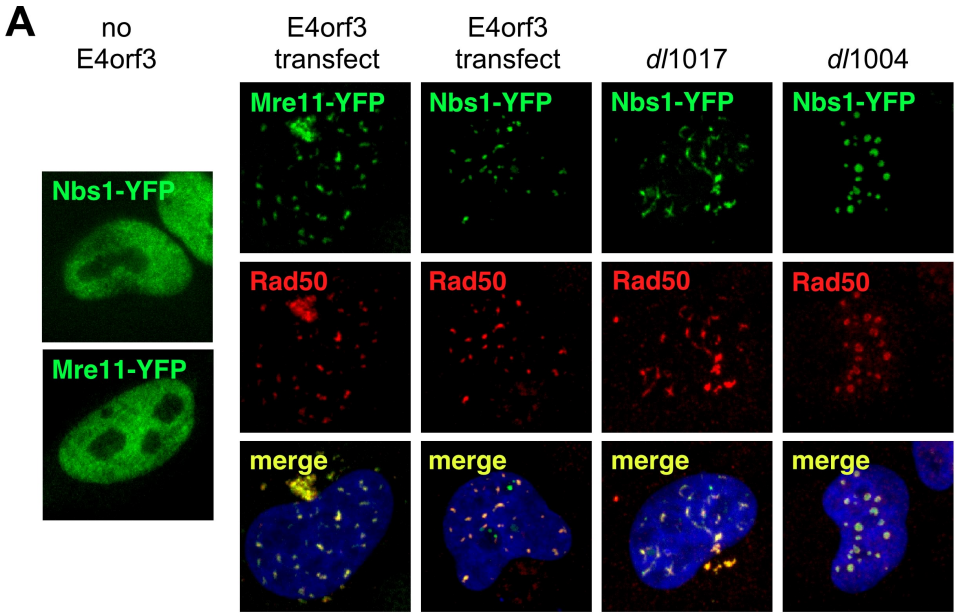
A
no E4orf3
E4orf3 transfect
E4orf3 transfect
dl1017
dl1004
Nbs1-YFP
Mre11-YFP
Mre11-YFP
Nbs1-YFP
Nbs1-YFP
Nbs1-YFP
Rad50
Rad50
Rad50
Rad50
merge
merge
merge
merge

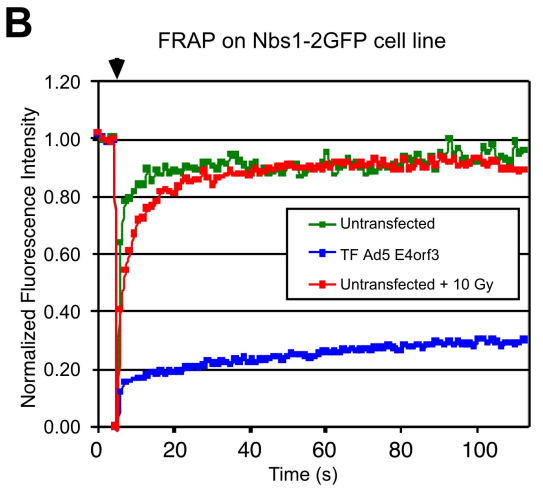
B
FRAP on Nbs1-2GFP cell line
Normalized Fluorescence Intensity
Time (s)
Untransfected
TF Ad5 E4orf3
Untransfected + 10 Gy

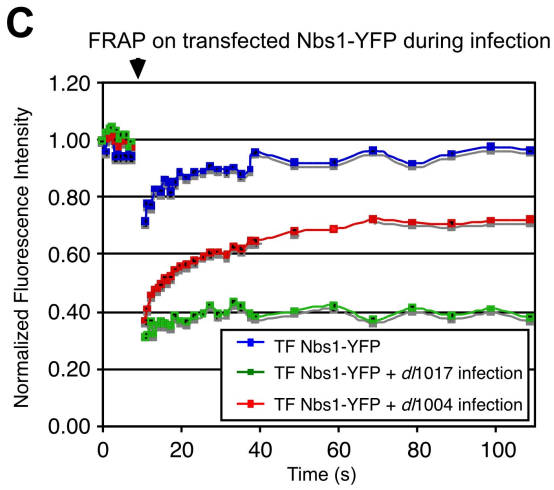
C
FRAP on transfected Nbs1-YFP during infection
Normalized Fluorescence Intensity
Time (s)
TF Nbs1-YFP
TF Nbs1-YFP + dl1017 infection
TF Nbs1-YFP + dl1004 infection

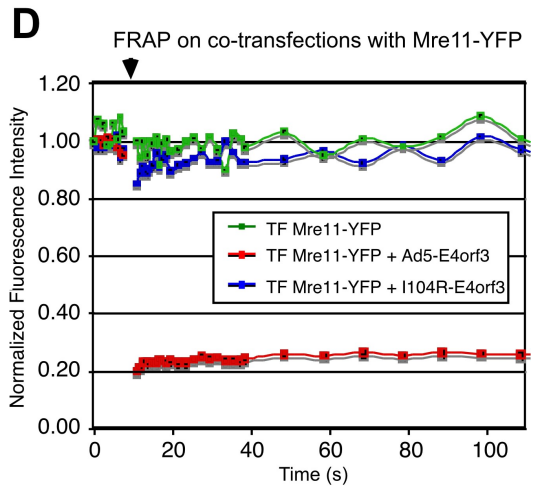
D
FRAP on co-transfections with Mre11-YFP
Normalized Fluorescence Intensity
Time (s)
TF Mre11-YFP
TF Mre11-YFP + Ad5-E4orf3
TF Mre11-YFP + I104R-E4orf3

untreated cells (**Fig. 2-7A**) as previously reported (Lukas et al., 2003). In the presence of E4orf3, provided by virus infection or plasmid transfection, the fusion proteins localized into track-like structures and accumulated in cytoplasmic aggregates (**Fig. 2-7A**). Both Mre11-YFP and Nbs1-YFP fusion proteins colocalized with endogenous Rad50 protein. Similar results were obtained using a stable cell line expressing Nbs1-2GFP (Lukas et al., 2003) (data not shown). These results demonstrate that the fusion proteins are correctly incorporated into E4orf3-induced structures. During infection with *dl*1004, Nbs1-YFP formed foci at viral replication centers (**Fig. 2-7A**), as previously reported for endogenous MRN (Stracker et al., 2002).

We then examined the dynamics of MRN in E4orf3 tracks using Fluorescence Recovery After Photobleaching (FRAP) to determine the rate at which a bleached area is repopulated with new fluorescent protein. As previously reported, we observed that the Mre11 and Nbs1 proteins are highly mobile in the absence of E4orf3 (**Fig. 2-7B** and **D**). FRAP analysis of Nbs1 foci at viral replication centers during infection with *dl*1004 demonstrated that the signal recovered with kinetics slower than that of an undamaged area (**Fig. 2-7C**). The increased residence time at virus centers resembles that observed for recruitment of the MRN complex at DSBs (Lukas et al., 2003). In contrast, the kinetics of fluorescence recovery was much more significantly affected by the presence of E4orf3, where the fluorescence signal did not recover after photo-bleaching of MRN in tracks induced by E4orf3 during transfection (**Fig.**

2-7B) or infection (**Fig. 2-7C**). We also compared MRN mobility in the presence of wild-type and I104R mutant E4orf3 proteins (**Fig. 2-7D**). While wild-type Ad5-E4orf3 expression led to immobilization of Mre11-YFP, the I104R mutant barely affected Mre11 dynamics. This supports our observations from fixed images that show I104R does not alter Mre11 localization. Together, these data demonstrate that MRN in tracks induced by Ad5-E4orf3 represent immobilized proteins.

E4orf3 prevents ATR-dependent signaling in response to non-viral damage

In order to assess the impact of MRN immobilization on the ability of cells to respond to DNA damage, we generated spatially restricted DSBs through laser micro-irradiation (Lukas et al., 2003). Local DNA damage was generated in subnuclear regions by a focused laser beam programmed to move once across individual cell nuclei. Previous studies using visualization with specific antibodies and fluorescently-tagged proteins have demonstrated that DNA damage proteins are redistributed to these DSBs (Lukas et al., 2003; Lukas et al., 2004). We examined recruitment of endogenous cellular repair proteins to laser-induced DSBs in cells expressing E4orf3. The sites of micro-irradiation can be visualized by recruitment of the mediator protein Mdc1 (Lukas et al., 2004), which is unaffected by E4orf3 (**Fig. 2-8A**). Cells expressing Ad5-E4orf3 localized Nbs1-GFP into the characteristic nuclear tracks, and displayed minimal accumulation of Nbs1 at micro-irradiation sites

Figure 2-8. E4orf3 prevents ATR dependent damage signaling induced by non-viral sources. (A) U2OS cells transfected with a plasmid vector expressing Ad5-E4orf3 were laser micro-irradiated. Cells were fixed and stained for endogenous Nbs1 and Mdc1. Arrows indicate cells with E4orf3-induced tracks of Nbs1. (**B**) Stable U2OS cell lines expressing Nbs1-2GFP were transfected with a plasmid expressing Ad5-E4orf3, together with prRFP-C1, which was used as a marker for transfected cells. Cells were laser micro-irradiated (as indicated by dashed line) and images show the recruitment of Nbs1 to sites of damage. (**C**) HeLa cells were mock infected, or infected with E1-deleted recombinant Ads expressing GFP (rAd-GFP) or E4orf3 (rAd-E4orf3). At 24 hpi the cells were mock treated or treated with 2 mM hydroxyurea (HU) for 2 h, and cells were harvested for immunoblotting. Cellular proteins were detected with antibodies to RPA32 and specific phosphorylated sites at RPA-S4,8 and Nbs1-S343. Ku86 served as a loading control.

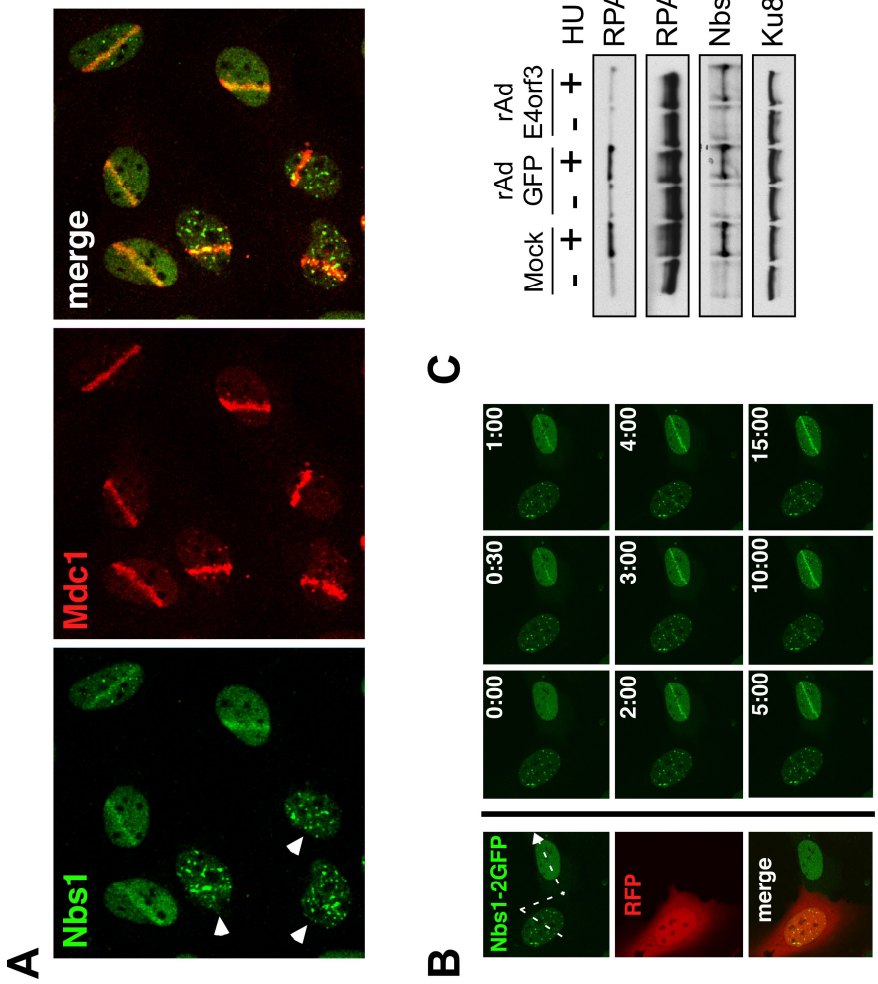
A
Nbs1
Mdc1
merge
B
Nbs1-2GFP
RFP
merge
0:00
0:30
1:00
2:00
3:00
4:00
5:00
10:00
15:00
C
Mock
rAd GFP
rAd E4orf3
HU
RPA32-S4,8
RPA32
Nbs1-S343
Ku86

compared to neighboring untransfected cells. This result shows that Nbs1 immobilization in E4orf3-induced tracks prevents its accumulation at DSBs.

To examine the effect of E4orf3 expression on kinetics of the DNA damage response, we combined laser micro-irradiation with live cell imaging (**Fig. 2-8B**). The Nbs1-2GFP cell line was cotransfected with the Ad5-E4orf3 expression vector and a plasmid expressing RFP to serve as a transfection marker. Generation of subnuclear restricted DSBs resulted in very rapid recruitment of Nbs1-2GFP. In contrast, there was barely detectable recruitment of Nbs1 in cells expressing Ad5-E4orf3, even at 15 min after treatment. These data indicate that the MRN complex immobilized in E4orf3-induced tracks is unable to respond efficiently to exogenous DNA damage. Since MRN has been demonstrated to be required for ATR signaling in response to HU treatment (Manthey et al., 2007), we used recombinant Ad vectors to express Ad5-E4orf3 or GFP in cells and then exposed them to HU (**Fig. 2-8C**). E4orf3 abrogated signaling as demonstrated by decreased hyper-phosphorylation of RPA32 and staining with phospho-specific antibodies to RPA32-S4,8, Nbs1-S343 and Chk1-S345. Together these data demonstrate that immobilization of MRN by E4orf3 prevents the ATR-mediated response to replication stress.

Discussion

The MRN complex plays a central role in the cellular DNA damage response to Ad infection. We previously demonstrated that during infection with E4-deleted Ad, MRN is required for concatemerization of the viral genome and activation of ATM signaling (Carson et al., 2003; Stracker et al., 2002). In this report we show that MRN also plays a role in ATR signaling in response to infection with *dl*1004. Substrates known to contribute to ATR kinase activation include ssDNA coated with RPA, and junctions of single and double-stranded DNA (Kumagai et al., 2006; MacDougall et al., 2007; Zou, 2007). Our data show that ssDNA at viral replication centers (Pombo et al., 1994) is sufficient for recruitment of ATR and ATRIP but that ATR signaling to Chk1 and RPA32 is only detected when the MRN complex also accumulated at viral centers. Although we have focused on MRN, we cannot exclude additional roles for other proteins implicated in ATR activation and checkpoint signaling, such as the 9-1-1 complex, the Rad17 complex, and Claspin (Zou, 2007). The cellular E1b55K-associated protein E1B-AP5 was recently implicated in ATR signaling during Ad infection (Blackford et al., 2008) but this factor localizes to wild-type Ad5 centers and therefore does not explain the induction of ATR signaling in the absence of E4.

MRN has recently been implicated in facilitating ATR activation and signaling in response to some types of damage. Processing of DSBs in an MRN-dependent manner results in formation of ssDNA and ATR activation

(Adams et al., 2006; Jazayeri et al., 2006; Myers and Cortez, 2006). MRN is involved in ATR-mediated phosphorylation events in response to replication stress, although signaling events may also be MRN-independent, depending on the substrate and dose of damaging agent (Olson et al., 2007a; Pichierri and Rosselli, 2004; Stiff et al., 2005; Zhong et al., 2005). During infection with *dl*1004, it is not clear which DNA structures serve as the trigger for ATR signaling, and there may be multiple ways that the MRN complex contributes to ATR activation. Although the nuclease activity of Mre11 is required for joining adenovirus genomes into concatemers (Stracker et al., 2002), we found that it was not required for ATR signaling. In contrast to DSBs caused by IR or replication stress, where the nuclease activity of Mre11 is required for resection (Buis et al., 2008), we found that Mre11 nuclease activity is not required for generation of ssDNA and recruitment of RPA/ATR/ATRIP at viral centers. However, signaling may be triggered by further processing of the viral genome, for example by removal of the terminal protein from the 5' end of the genome by other nucleases to generate free DNA ends. MRN-dependent processing of DSBs has been suggested to generate small oligonucleotides that stimulate ATM activity (Jazayeri et al., 2008). It will be interesting to determine if these are generated during virus infection and whether they play a role in ATR activation. The MRN complex could have a direct role in stimulating ATR kinase activity, as has been shown *in vitro* for ATM (Lee and Paull, 2004). The MRN complex may also facilitate phosphorylation of

downstream substrates through recruitment or retention of proteins to viral centers, as has been proposed for stalled replication forks (Stiff et al., 2005). MRN associates with RPA at sites of DNA damage to mediate the intra-S-phase checkpoint (Olson et al., 2007a; Robison et al., 2004), and also interacts with ATR/ATRIP (Olson et al., 2007b). Either of these two interactions could contribute to ATR activation by MRN at viral centers. The ATM and ATR kinases may be coordinated and interdependent in response to some types of damage (Hurley et al., 2007). In response to IR, activation of ATR is ATM-dependent (Jazayeri et al., 2006; Myers and Cortez, 2006), whereas in response to HU and UV activation of ATM is ATR-dependent (Liu et al., 2005; Stiff et al., 2006). In the case of virus infection we have found that although both rely upon the MRN complex, ATM and ATR signaling are independent of each other. This may reflect the fact that during infection there are numerous substrates for kinase activation, including replication intermediates and double-strand ends. In addition to the viral genome, infection may also induce chromosomal damage to the host genome. Early Ad genes alter cell cycle progression, which could lead to collapse of replication forks, and also cause genomic instability and chromosomal aberrations (Caporossi and Bacchetti, 1990; Lavia et al., 2003). Therefore, although the phosphorylated ATR substrates predominantly accumulate at viral replication centers, it is possible that chromosomal damage also contributes to induction of ATR signaling during infection.

There is functional redundancy between the E4orf3 and E4orf6 products from Ad, and either is sufficient to promote viral replication, prevent concatemerization of the viral genome, and enable viral late protein production. Both E4 proteins target the MRN complex to prevent concatemer formation (Evans and Hearing, 2003; Stracker et al., 2002). Together with previous observations of MRN degradation by E1b55K/E4orf6 (Carson et al., 2003), our data show that both E4 proteins target MRN to prevent damage signaling. Inactivation of MRN is also likely to be responsible for the ability of E4 proteins to promote viral DNA replication. We and others have found that MRN inhibits replication of the *dl*1004 mutant virus, although the mechanism is unclear (Evans and Hearing, 2005; Lakdawala et al., 2008; Mathew and Bridge, 2007; Mathew and Bridge, 2008). Replication of cellular DNA is tightly regulated to ensure that the genome is replicated only once per cell cycle (Arias and Walter, 2007). MRN is recruited to cellular replication origins, and can inhibit firing of new origins of DNA replication upon damage (Olson et al., 2007b) and suppress rereplication (Lee et al., 2007; Wu et al., 2004). Mre11 has recently been suggested to bind the Ad genome (Mathew and Bridge, 2008), but it is unclear how this inhibits replication. Checkpoint signaling by ATM and ATR is not responsible for the defective replication of *dl*1004 (Lakdawala et al., 2008). The virus uses its own protein-priming mechanism and polymerase, which could be affected by MRN binding to the origin or its participation in removal of the terminal protein from the viral genome.

Our work links the E4orf3-induced redistribution of proteins associated with PML nuclear bodies to their role in sensing DNA damage (Everett, 2006). We show that relocalization of the MRN complex dramatically reduces its dynamics, essentially immobilizing the proteins in E4orf3-induced intranuclear tracks. Similar observations were made with FRAP analysis of other fluorescently tagged components of the PML bodies (unpublished observations). Experiments with laser micro-irradiation and live cell imaging demonstrated that recruitment of MRN to damage sites was severely abrogated in cells expressing Ad5 E4orf3. This correlated with decreased recruitment of RPA and ATR, as well as abrogated damage signaling, and was not seen with the I104R mutant (data not shown). Together these results show that immobilization by E4orf3 prevents the MRN damage sensor from responding to new damage sites. This supports the hypothesis that sequestering MRN (and other host factors) into E4orf3-induced tracks will prevent these proteins from sensing and accumulating at virus centers, and will thus thwart host antiviral responses. It has also been suggested that sequestration of MRN in cytoplasmic aggresomes by the adenoviral E1b55K inactivates the complex and protects the viral genome (Liu et al., 2005). Since the E4orf3 and E4orf6 proteins both block damage signaling and also promote production of late viral proteins, it will be interesting to determine whether these activities are linked. Understanding how viruses such as Ad manipulate

signaling pathways will provide insights into the regulation of DNA damage responses in mammalian cells.

Materials and methods

Cell lines. HeLa and 293 cells were purchased from the American Tissue Culture Collection. W162 cells for growth of E2-deleted viruses were from G. Ketner, A-T cells (AT221JET and complemented version) were from Y. Shiloh, and Seckel cells were from Coriell Institute (GM18366) and A D'Andrea (F02-98). Immortalized A-TLD1 and NBS (NBS-ILB1) and matched cells reconstituted with wild-type Mre11 and NBS1 were described (Carson et al., 2003; Cerosaletti et al., 2000). The retrovirus expression plasmid for the Mre11-3 mutant (HD129/130LV) was generated by site-directed mutagenesis and A-LD1 cells were transduced by the retrovirus as previously described (Carson et al, 2003). The U2OS derived stable cell line with Nbs1-2GFP has been described (Lukas et al., 2003). Cells were maintained as monolayers in either Dulbecco modified Eagle's medium (DMEM) or MEM plus Earle's salts (Seckel cells) supplemented with 10 or 20% fetal bovine serum (FBS), at 37°C in a humidified atmosphere containing 5% CO_2.

Plasmids and transfections. Expression vectors for Ad5-E4orf3 and Ad12-E4orf3 proteins were described (Stracker et al., 2005). Site-directed mutagenesis of E4orf3 was performed using QuikChange (Stratagene). Cells

were transfected with Lipofectamine 2000 (Invitrogen) according to manufacturer's protocol.

Viruses and infections. The mutant viruses *dl*1004 (ΔE4), *dl*1016 (ΔE4orf3/ΔE1b55K) and *dl*1017 (ΔE4orf6/ΔE1b55K) have been described (Bridge and Ketner, 1990), and were obtained from G. Ketner. Wild-type Ad5 and *dl*1017 were propagated in 293 cells. The *dl*1004 and *dl*1016 viruses were propagated on W162 cells (Weinberg and Ketner, 1983). All viruses were purified by two sequential rounds of ultra-centrifugation in cesium chloride gradients and stored in 40% glycerol at -20^{o}C. Infections were performed in DMEM supplemented with 2% FBS. After 2 h at 37°C additional serum was added to a total of 10%.

Antibodies. Primary antibodies were purchased from Novus Biologicals Inc. (Nbs1), Genetex (Mre11-12D7, Rad50-13B3), Cell Signaling (Chk1-S345), Rockland (ATM S1981-P), Santa Cruz (ATR, PML, Chk1, Ku86), Upstate Biotechnology (ATRIP), BD Bioscience (TopBP1) and Bethyl (RPA32-S4,8). The antibody to RPA32 was from T. Melendy, the monoclonal B6 antibody to DBP was from A. Levine, polyclonal rabbit antisera to DBP was from P. van der Vliet, and the E4orf3 antibody was from T. Dobner. Secondary antibodies were from Jackson Laboratories, Eurogentec and Invitrogen Molecular Probes.

Immunoblotting and immunofluorescence. Immunoblotting and immunofluorescence were performed as previously described (Carson et al.,

2003). Novex (Invitrogen) 3-8% gradient gels were used for the resolution of ATM. For immunofluorescence, cells grown on glass coverslips were infected at an MOI of 25-100 pfu/cell. After 16-24 h the cells were washed, fixed, stained and counter-stained with 4',6-diamidino-2-phenylindol (DAPI). Immunoreactivity was visualized using a Nikon microscope in conjunction with a CCD camera (Cooke Sensicam) or a Leica confocal microscope.

FRAP analysis. FRAP analysis was performed in the Nbs1-2GFP U2OS cells as previously reported (Lukas et al., 2003). Further details are provided in Supplemental Material. Image collection and FRAP data were processed on a Leica confocal microscope.

Acknowledgements

I am grateful to Christian Carson for his contributions to this project and for making the initial discovery that E4orf3 prevented ATR signaling. He was responsible for Figures 2-1, and parts of Figure 2. I would like to thank Darwin Lee and Felipe Araujo who were responsible for parts of Figure 2-2. I would also like to thank J. Bartek, J. Lukas, and S. Bekker-Jensen for their expertise; they are responsible for Figures 2-7A and 2-7B. I would also like to thank the other authors on this paper for their discussions, reagents and contributions.

Some material from this chapter is reprinted in part as it appears in: Carson CT*, Orazio NI*, Lee DV*, Suh J, Bekker-Jensen, S, Araujo FD, Lakdawala SS, Lilley CE, Bartek J, Lukas J, Weitzman MD. Mislocalization of the MRN complex prevents ATR signaling during adenovirus infection. EMBO J (2009) vol. 28 (6) pp. 652-62

The dissertation author was one of the primary researchers and authors of this paper.

* Denotes equal contribution to publication

Chapter 3. Adenovirus targets the BLM helicase for degradation

Background

Cellular proteins involved in DNA end processing and repair are inhibited by adenovirus in order to prevent the detection of the adenovirus genome as DNA breaks that need to be “repaired” (Baker et al., 2007; Stracker et al., 2002). As mentioned in chapter 1, Ad5 expresses proteins in the E4 region that counteract these mechanisms by inhibiting the DNA damage sensing and repair machinery. The E4 region inhibits repair machinery by two mechanisms: mislocalization/immobilization and degradation of these proteins (Araujo et al., 2005; Boyer et al., 1999; Carson et al., 2009; Stracker et al., 2002). Degradation occurs through the viral E1b55K/E4orf6 proteins that interact with cellular proteins Cullin-5, Elongins B and C and Rbx1 to form a ubiquitin ligase complex that degrades cellular proteins (Boivin et al., 1999; Harada et al., 2002; Querido et al., 2001a).

During infection, the E1b55K/E4orf6 ubiquitin ligase complex promotes accumulation of late viral mRNAs (Bridge and Ketner, 1989), viral replication (Bridge et al., 1993; Weinberg and Ketner, 1986) and prevents ligation of the viral genome into concatemers (Baker et al., 2007; Stracker et al., 2002; Weiden and Ginsberg, 1994). E1b55K provides the substrate specificity, and E4orf6 interacts with the cellular machinery and provides the nuclear localization signal (NLS) for the complex (Dobbelstein et al., 1997; Goodrum et

al., 1996; Konig et al., 1999; Liu et al., 2005; Orlando and Ornelles, 1999). In the absence of E4orf6, E1b55K localizes to the aggresome, a cytoplasmic, juxtanuclear aggregate at the microtubule-organizing center (Araujo et al., 2005; Liu et al., 2005). Some E1b55K interacting proteins also localize to the aggresome, although they are not all targets of E1b55K and E4orf6 mediated degradation (Araujo et al., 2005; Fleisig et al., 2007; Liu et al., 2005). Known cellular targets of the E1b55K/E4orf6 ubiquitin ligase complex are p53 (Cathomen and Weitzman, 2000; Grand et al., 1994; Harada et al., 2002; Moore et al., 1996; Querido et al., 2001a; Querido et al., 2001b; Roth et al., 1998; Steegenga et al., 1998), DNA ligase IV (Baker et al., 2007), integrin α3 (Dallaire et al., 2009), and the MRN complex (Carson et al., 2003; Stracker et al., 2002). It has recently been shown that the cellular transcriptional regulator Daxx is also degraded by E1b55K in a proteasome dependent manner during infection, but does not require E4orf6 (Schreiner et al., 2010)

The MRN complex promotes DSB processing, and recently other proteins including the RecQ helicases have also been implicated in end processing (Gravel et al., 2008; Nimonkar et al., 2008). The degradation of the MRN complex by E1b55K/E4orf6 led us to question whether other proteins implicated in genome processing were also affected during infection. Cellular DNA structures including 3' tailed duplexes, bubble structures, G quadruplexes, DNA displacement loops and double Holliday junctions need to be resolved in order for cells to replicate efficiently (Chu and Hickson, 2009).

The RecQ helicases are a family of enzymes that play a role in unwinding and resolving a variety of DNA structures and are named for their homology to the *E. coli* RecQ helicase (Chu and Hickson, 2009). RecQ helicases are composed of three main domains, the Helicase domain, the RecQ carboxy-terminal domain (RQC), and the Helicase and RNase D C-terminal (HDRC) domain. All RecQ helicases must contain the Helicase domain, but not all members have the RQC or HDRC domains (Chu and Hickson, 2009). There are 5 members of the human family of RecQ helicases: RecQ1, WRN, BLM, RecQ4 and RecQ5. Hypomorphic mutations in WRN, BLM, and RecQ4 are known to cause recessive genetic diseases: Werner syndrome, Bloom syndrome and Rothmund-Thomson syndrome, respectively. The RecQ diseases display similar phenotypes including genome instability, premature aging and predisposition to cancer, although the exact manifestation of these phenotypes may vary (Bohr, 2008).

Most unicellular organisms have only one RecQ helicase, for example the budding yeast *S. cerevisiae* has the Sgs1 helicase (Chu and Hickson, 2009). Recently, it has been demonstrated that Sgs1 is involved in processive 5'-3' resection of DNA that is required for repair by homologous recombination (HR). Sgs1 mediated resection, requires Sgs1 helicase activity and collaboration with the nucleases DNA2 and/or Exo1 and is also mediated by yeast RPA (Budd and Campbell, 2009; Cejka et al., 2010; Mimitou and Symington, 2008; Niu et al., 2010; Zhu et al., 2008b). The mammalian BLM

helicase has the most functional homology with Sgs1 (Johnson et al., 2000; Kusano et al., 1999; Neff et al., 1999; Stewart et al., 1997; Watt et al., 1996; Wu et al., 2000) and is similarly implicated in processive resection of DSBs with Exo1 and DNA2 (Gravel et al., 2008; Nimonkar et al., 2008). BLM is located throughout the nucleus, and is also located at ND10 or PML bodies and in the nucleolus (Ishov et al., 1999; Neff et al., 1999; Yankiwski et al., 2000; Zhong et al., 1999). BLM is reported to be a member of the BRCA1 Associated genome Surveillance Complex (BASC) of proteins that interact with the BRCA1 tumor suppressor protein (Wang et al., 2000). Consistent with its association with the BASC complex, after treatment with chemical and physical agents causing genotoxic stress, BLM re-localizes to sites of damage (Davalos and Campisi, 2003; Rao et al., 2005; Sengupta et al., 2004). BLM is post-translationally modified both by phosphorylation and SUMOylation (Ababou et al., 2000; Beamish et al., 2002; Davies et al., 2004; Dutertre et al., 2000; Eladad et al., 2005; Franchitto and Pichierri, 2002). SUMOylation of BLM is required for its localization to PML bodies and regulates its ability to localize to sites of DNA damage (Eladad et al., 2005; Ouyang et al., 2009). Phosphorylation of BLM occurs after genotoxic stress and is mediated by the ATM and ATR kinases (Ababou et al., 2000; Beamish et al., 2002; Davies et al., 2004). The function of BLM in the DDR and in processing of DNA ends at sites of breaks led us to question if BLM would have an effect on adenovirus infection.

In this chapter we show that the BLM helicase is the only member of the human RecQ helicase family that is targeted for proteasome-mediated degradation during adenovirus infection. We demonstrate that the known adenovirus ubiquitin ligase complex containing viral proteins E1b55K and E4orf6 mediates the degradation of BLM. Our experiments demonstrate that BLM localizes to discrete foci around sites of viral replication prior to degradation during infection with wild-type virus and also during infection with viruses unable to degrade BLM. These discrete BLM foci are adjacent to sites of active viral replication. However, although BLM is believed to function as a DNA end processing protein (Gravel et al., 2008; Nimonkar et al., 2008), depleting BLM does not rescue the *dl*1004 virus phenotypes of defective viral replication or concatemerization of the viral genome. The results presented in this chapter demonstrate that BLM is a new degradation target of the adenovirus E1b55K/E4orf6 ubiquitin ligase complex, and adds helicases to ligases, nucleases, cell surface proteins and transcription factors as a new class of protein targeted by adenovirus during infection.

Results

Levels of BLM are decreased during infection with Ad5 virus.

RecQ helicases are a family of helicases involved in maintaining genome integrity (Bohr, 2008). Since proteins involved in DNA end processing and repair are inactivated by adenovirus infection, we investigated

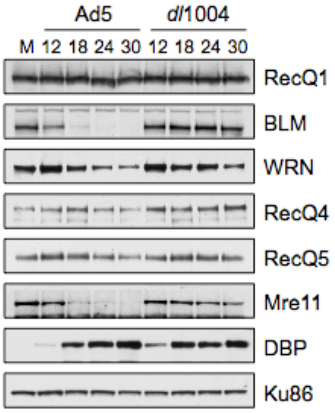

Figure 3-1. The levels of the RecQ helicases over a time course of adenovirus infection. Protein lysates were separated by SDS-PAGE and transferred to membranes and immunoblotting was performed with the indicated antibodies. Ku86 served as a loading control. DBP served as an infection control. Mre11 served as a control to demonstrate the degradation properties of Ad5 versus *dl*1004.

if human RecQ helicases were also inactivated. We infected HeLa cells with wild-type Ad5 or *dl*1004 virus, which is deleted for the E4-region, and harvested the cells at regular intervals 12-30 hours post infection (hpi). We examined the levels of the RecQ proteins by separation on SDS-PAGE gel and immunoblotting with antibodies specific to the each of the RecQ Helicases (**Fig. 3-1**). Infection with Ad5 or *dl*1004 did not alter the protein levels of RecQ1, RecQ4 or RecQ5 throughout the time course examined. Levels of WRN were slightly decreased over time in cells infected with Ad5 or *dl*1004; however, the decrease in WRN is not specific to Ad5 infection and is not rescued by proteasome inhibitors (**Appendix Fig. 6**). Levels of the BLM helicase remained stable throughout *dl*1004 infection; however, during infection with wild-type Ad5 the levels of BLM were not detectable by 18 hpi (**Fig. 3-1**). The decrease in BLM mimicked the pattern of Mre11 protein levels during infection (**Fig. 3-1**). Mre11 is a known degradation target of adenovirus and localizes to sites of viral replication during infection with *dl*1004 (Lakdawala et al., 2008; Stracker et al., 2002). We predicted that BLM, which is associated with MRN in the BASC complex (Wang et al., 2000), might localize similarly during infection.

Cellular repair and replication proteins are often localized to viral replication centers during adenovirus infection (Carson et al., 2009; Stracker et al., 2002). To analyze further the decrease in BLM protein levels during infection, we examined the localization of BLM in cells infected with Ad5 or

Figure 3-2. Localization of BLM at sites of viral replication early during the infection process. (A) HeLa cells were pre-extracted fixed and immunofluorescence was performed with BLM antibody (green) and DBP (red). DAPI staining indicated the location of the nuclei in all merged images. Cells representative of those seen in Mock infected cells, Ad5 infected cells (early stage DBP centers in the left panel and late stage DBP centers in the right) and *dl*1004 infected cells are shown. In (B), 100 DBP stained cells were counted at each time indicated and cells with BLM staining were scored as positive. The percentage of BLM positive cells is represented in green and percent without BLM staining are represented in red.

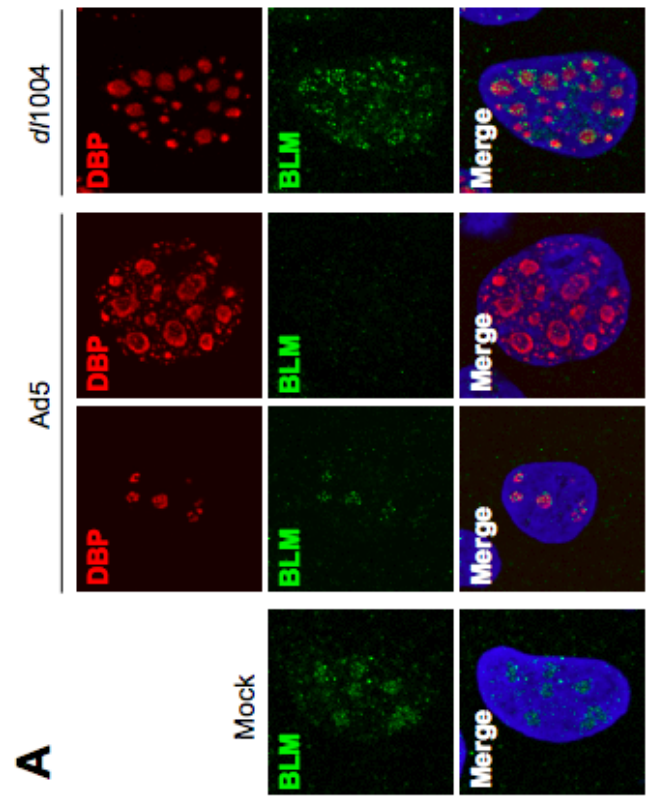
A
Mock
Ad5
d/1004
DBP
BLM
Merge
B
Centers with BLM
Centers without BLM
Infected cells with BLM at replication centers (%)
0
10
20
30
40
50
60
70
80
90
100
12
16
18
30
Hours post-infection

*dl*1004 virus (**Fig. 3-2A**). Infected cells can be identified by positive immunofluorescence staining to the virally encoded ssDNA binding protein (DBP) (Pombo et al., 1994). The cells were pre-extracted prior to fixation to remove soluble protein. In mock-infected cells, the localization of BLM was similar to that reported in the literature: BLM localized throughout the nucleus, in foci reported to be ND10 or PML bodies and in the nucleolus (**Fig. 3-2A**) (Ishov et al., 1999; Neff et al., 1999; Yankiwski et al., 2000; Zhong et al., 1999). In HeLa cells that are at an early stage during Ad5 infection, as represented by small DBP centers (Pombo et al., 1994), BLM localized to 2-10 foci at and around the DBP centers (**Fig. 3-2A**). However, BLM staining was not detected in Ad5 infected cells with large ring shaped DBP centers representative of a later stage of infection (**Fig. 3-2A**)(Pombo et al., 1994). To quantify the decrease in BLM fluorescence, we calculated the percent of cells containing BLM foci at DBP centers fixed at regular intervals from 12-30 hpi. We counted 100 cells positive for DBP staining at each time point and scored cells that also had BLM staining. We found that at 12 hpi, 100% of cells were positive for BLM foci, but by 30 hpi only 8% of cells had BLM foci (**Fig. 3-2B**). In cells infected with *dl*1004, BLM localized at and around viral replication centers and immunofluorescence did not decrease over time (**Fig. 3-2A,** and data not shown). These experiments demonstrate that during infection, BLM localizes to foci at and around viral replication centers and the levels of BLM are decreased over time in an E4-dependent manner.

Figure 3-3. E4orf6 and E1b55K are required for proteasome-mediated degradation of BLM. In (A, B, C) lysates were analyzed by SDS-PAGE and immunoblotting with the indicated antibodies and either Ku70 or GAPDH served as loading controls. In (A) HeLa cells were infected with an MOI of 10-25 and cells were harvested at 24 hpi Levels of BLM degradation were compared to that of Ad5 infected cells. In (B) cells were infected with Ad5 (MOI of 10) or *dl*1004 (MOI of 25) at 12 hpi proteasome inhibitors were added to the cells (+ present, - absent) and cells were harvested at 24 hpi (C) Cells were infected with Ad5 (MOI of 10) and were super-infected with Ψ5, Ψ5-Cul5 or Ψ5-NTD-Cul5 (MOI 50) and harvested at 24 h after the primary infection. In these infections the Flag antibody demonstrates expression of the Cul5 or NTD-Cul5 from the Ψ5 viruses.

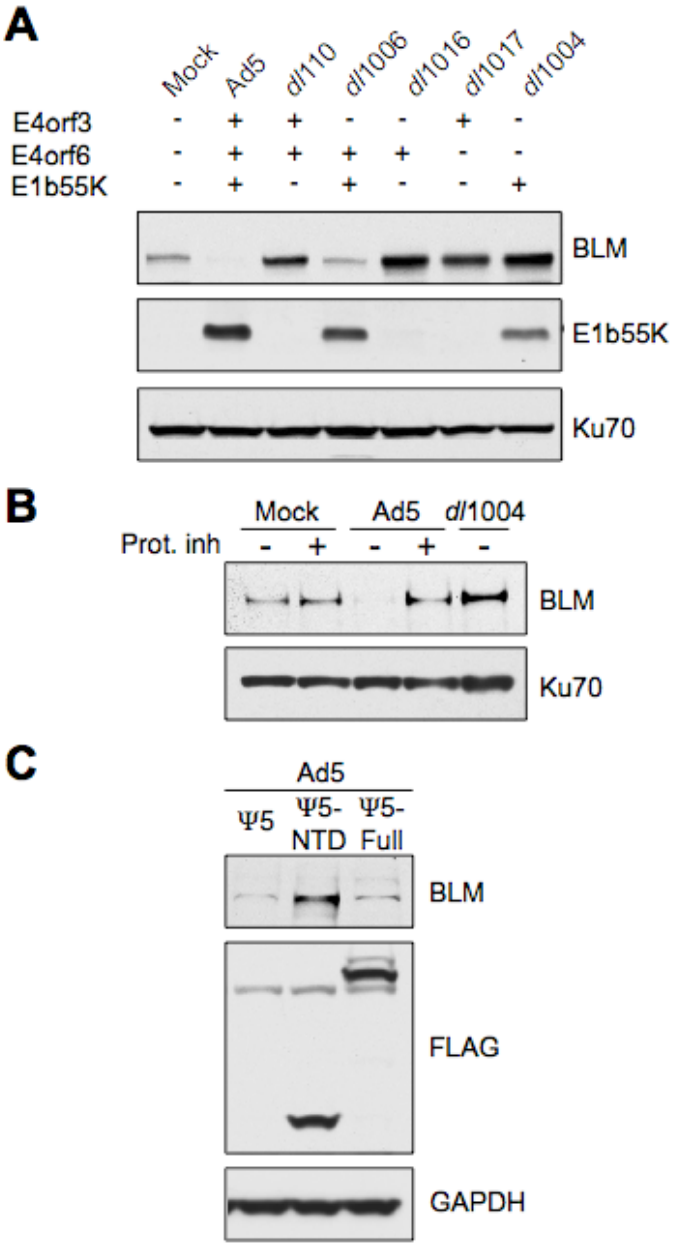
A
Mock
Ad5
dl110
dl1006
dl1016
dl1017
dl1004
E4orf3
E4orf6
E1b55K
BLM
E1b55K
Ku70
B
Mock
Ad5
dl1004
Prot. inh
BLM
Ku70
C
Ad5
Ψ5
Ψ5-NTD
Ψ5-Full
BLM
FLAG
GAPDH

E1b55K and E4orf6 are required for BLM degradation during infection.

To determine which viral proteins were required for degradation of BLM during infection, we infected HeLa cells with adenovirus deleted singularly or in combination for E1b55K, E4orf6 and E4orf3 (**Fig. 3-3A**). The levels of BLM degradation were compared to that during Ad5 infection. The only viruses competent for BLM degradation were wild-type Ad5 and *dl*1017, which contains E4orf3 but is deleted for E1b55K and E4orf6. The efficiency of degradation is slightly reduced in the *dl*1006 (ΔE4orf3) virus, perhaps due to the inability of the E4orf3 protein to disturb the PML bodies where a fraction of the BLM is sequestered (Ishov et al., 1999; Neff et al., 1999; Yankiwski et al., 2000; Zhong et al., 1999). In contrast, all viruses deleted for E1b55K, E4orf6 or both E1b55K and E4orf6 were completely defective in their ability to degrade BLM (**Fig. 3-3A**). We observed that the levels of BLM were also higher in the virus-infected cells that were unable to degrade BLM when compared to uninfected cells. BLM levels are cell cycle regulated, peaking in S phase (Dutertre et al., 2000); the higher level of BLM may be due to E1a expression which forces infected cells into S-phase thereby increasing levels of BLM (Berk, 2005). This experiment demonstrates that E1b55K and E4orf6 are both required for the degradation of BLM during infection.

BLM undergoes proteasome-mediated degradation by the viral E3 ubiquitin ligase complex containing Cullin-5.

The decrease in BLM protein levels during Ad5 infection mirrored that of the Mre11 protein, which along with p53, integrin α3 and DNA ligase IV are degraded in a proteasome-dependent manner during infection (Baker et al., 2007; Carson et al., 2003; Cathomen and Weitzman, 2000; Dallaire et al., 2009; Grand et al., 1994; Harada et al., 2002; Moore et al., 1996; Querido et al., 2001a; Querido et al., 2001b; Roth et al., 1998; Steegenga et al., 1998; Stracker et al., 2002). To identify if BLM was degraded in a proteasome-dependent manner, we infected HeLa cells with Ad5 (MOI of 10) or *dl*1004 (MOI of 25) and added the proteasome inhibitors MG132 and epoxomicin at 12 hpi. We harvested cells 24 hpi and analyzed the lysates by SDS-PAGE and immunoblotting (**Fig. 3-3B**). In the mock-infected cells, the presence of proteasome inhibitors did not affect the levels of BLM. In cells infected with Ad5, the levels of BLM were decreased as seen previously (**Fig. 3-1**). However, the addition of proteasome inhibitors to the Ad5 infected cells increased the levels of BLM to mock/*dl*1004 levels (**Fig. 3-3B**). The increase in BLM levels upon addition of proteasome inhibitors demonstrates that BLM is degraded in a proteasome-dependent manner during wild-type Ad5 infection.

The adenovirus E1b55K/E4orf6 ubiquitin ligase complex contains the cellular proteins Cullin-5 (Cul5), Rbx1 and elongins B and C (Boivin et al., 1999; Harada et al., 2002; Querido et al., 2001a). To determine if

E1b55K/E4orf6 were mediating the degradation of BLM using the same cellular proteins, we utilized a dominant-negative version of Cul5 (Woo and Berk, 2007). The N-terminal domain (NTD) of Cul5 interacts with Elongins B,C/E4orf6/E1b55K and allows for complex formation and substrate binding by E1b55K, but cannot interact with Rbx1 and the E2, preventing the ubiquitination and degradation of substrates (Woo and Berk, 2007). HeLa cells were infected with Ad5 and super-infected after 12 h with recombinant adenovirus expressing an empty vector (Ψ5), or expressing Flag-Cul5 (Ψ5-Cul5) or Flag-NTD-Cul5 (Ψ5-NTD-Cul5) and harvested 24 h after the initial infection (**Fig. 3-3C**). We assessed the levels of BLM by SDS-PAGE and western blot. Super-infection with the Ψ5 control virus or the Ψ5-Cul5 virus did not prevent degradation of BLM by wild-type Ad5. However, super-infection with the Ψ5-NTD-Cul5 prevented the degradation of BLM during Ad5 infection (**Fig. 3-3C**). These results show that during infection BLM undergoes proteasome-mediated degradation by the E1b55K/E4orf6 ubiquitin ligase complex containing Cul5.

E1b55K and E4orf6 are sufficient for the degradation of BLM.

To identify if E1b55K and E4orf6 were sufficient for the degradation of BLM in the absence of infection, we analyzed the expression of BLM in HEK293A cell lines transiently transfected with E4orf6. HEK293A cells are

Figure 3-4. E1b55K and E4orf6 are sufficient for degradation of BLM. (A) HEK293A cells were fixed (Left panel) or transfected with E4orf6 (Middle panel) or E4orf6:mRFP at a 9:1 ratio (Right panel) for 24 h prior to fixation as described in materials and methods. (B) Cells were either Mock transfected, or transfected with vectors expressing GFP or E4orf6, proteasome inhibitors were added at 8 h (+ present, - absent) and cells were harvested at 20 h after transfection. In (B,C) lysates were analyzed by SDS-PAGE and immunoblotting with the indicated antibodies. In these experiments, Ku70 served as a loading control and Mre11 served as a degradation control. (C) U2OS cells that stably express GFP or E1b55K were infected with rAd-E4orf6 (+ infected, - uninfected) with an MOI of 50 for 24 h.

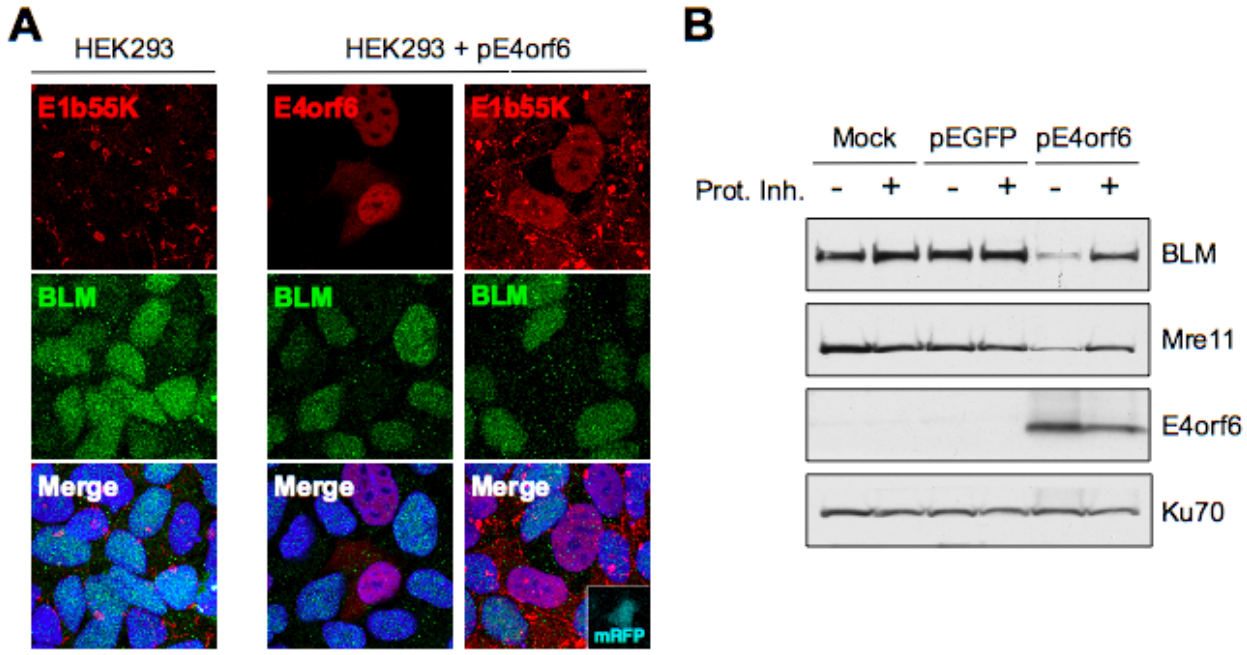
A
HEK293
HEK293 + pE4orf6
E1b56K
E4orf6
E1b55K
BLM
BLM
BLM
Merge
Merge
Merge
mRFP
B
Mock
pEGFP
pE4orf6
Prot. Inh. - + - + - +
BLM
Mre11
E4orf6
Ku70

transformed with a region of adenovirus expressing E1a and E1b (Graham et al., 1977). In HEK293A cells, E1b55K localizes to the aggresome, a juxtanuclear structure at the microtubule-organizing center (MTOC) (Araujo et al., 2005; Liu et al., 2005). Cellular proteins reported to interact with E1b55K often localize to the E1b55K aggresome in these cells including the MRN complex, p53 and SSBP2 (Araujo et al., 2005; Fleisig et al., 2007; Liu et al., 2005). In contrast to these studies, when we fixed HEK293A cells, and performed dual immunofluorescence with antibodies to E1b55K and BLM, we found that BLM does not localize to the aggresome in HEK293A cells and instead remains diffusely nuclear (**Fig. 3-4A**). In HEK293A cells, expression of E4orf6 leads to E4orf6 binding of E1b55K, which relocalizes E1b55K from the aggresome into the nucleus (Dobbelstein et al., 1997; Goodrum et al., 1996; Konig et al., 1999; Liu et al., 2005; Orlando and Ornelles, 1999). We expressed E4orf6 in HEK293A cells by transient transfection and analyzed the localization of BLM and E4orf6. We found that cells that exhibited BLM staining did not have E4orf6 staining and *vice versa* by dual immunofluorescence with E4orf6 and BLM antibodies (**Fig. 3-4A**). We confirmed that relocalization of E1b55K to the nucleus was causing BLM degradation by co-transfecting 90% E4orf6 with 10% mRFP, and staining for E1b55K and BLM. In these cells, mRFP (E4orf6 transfection marker) is shown in the merged image as cyan. BLM was only absent in the cells with positive staining for nuclear E1b55K demonstrating that E1b55K/E4orf6 is required for

BLM degradation (**Fig. 3-4A**). We examined degradation in HEK293A cells by immunoblotting and found that transfection of E4orf6, but not an empty vector or GFP expressing vector led to degradation of BLM (**Fig. 3-4B**). The addition of proteasome inhibitors to the E4orf6 transfected cells prevented the degradation of BLM (**Fig. 3-4B**). Together these results demonstrate that expression of E1b55K and E4orf6 is sufficient to induce proteasome-mediated degradation of BLM.

Degradation and localization of BLM during infection is separable from that of the MRN complex.

As members of the BASC super-complex, BLM and the MRN complex are reported to interact (Wang et al., 2000). To investigate if degradation of the MRN complex was leading to destabilization of BLM by disrupting the BASC complex, we assessed the levels of BLM in the absence of Mre11 and Nbs1 (**Fig. 3-5A**). To look at BLM degradation in the absence of Mre11, we utilized HeLa cells that stably expressed an shRNA against Mre11 (HeLa-shMre11) and NBS syndrome cells (NBS), which are hypomorphic for Nbs1 and complemented with a control vector or wildtype Nbs1 (Cerosaletti et al., 2000; Vo et al., 2005). The levels of BLM were slightly decreased in the cells that did not have detectable levels of Mre11 or Nbs1, suggesting that the steady state levels of BLM may partially be affected by loss of MRN (**Fig. 3-5A** and **B**). To determine if E1b55K/E4orf6 mediated degradation of BLM in the

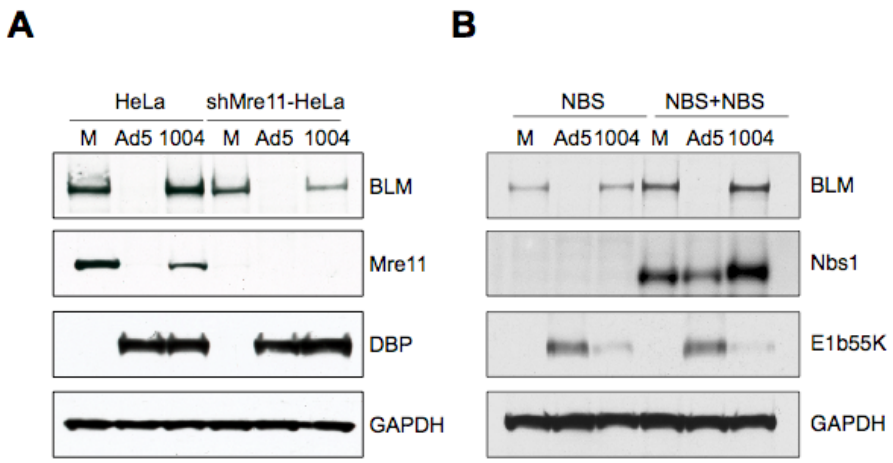

Figure 3-5. Degradation of BLM and MRN by E1b55K/E4orf6 are separable. (A) HeLa cells or HeLa cells that stably express shRNA targeting Mre11 (HeLa-shMre11) and (B) NBS hypomorphic cells that were complemented with an empty vector or wildtype Nbs1 were either Mock infected or infected with Ad5 (MOI 10) *dl*1004 (MOI 25) for 24 h. Cells were harvested and lysates were analyzed by SDS-PAGE and immunoblotting with the indicated antibodies. In (A, B) GAPDH served as a loading control, and Mre11 (A) and Nbs1 (B) demonstrated the efficiency of the shRNA.

Figure 3-6. Localization of BLM and MRN to viral centers is independent of one another. In (A) we demonstrate that localization of BLM to DBP centers is independent of Mre11. A-TLD cells or A-TLD cells expressing wild-type Mre11 (described in Materials and Methods) were infected with *dl*1004 (MOI 100) for 30 h, cells were pre-extracted, fixed and immunofluorescence was performed with antibodies to DBP to mark infection, Mre11 (left 2 panels) to demonstrate absence of Mre11. BLM staining for analysis is in the right 2 panels. In (B) Bloom Syndrome cells (BS) hypomorphic for BLM or IMR90 cells that express a wildtype BLM were infected with *dl*1004 for 48 h, cells were pre-extracted, fixed and immunofluorescence was performed as in (A)

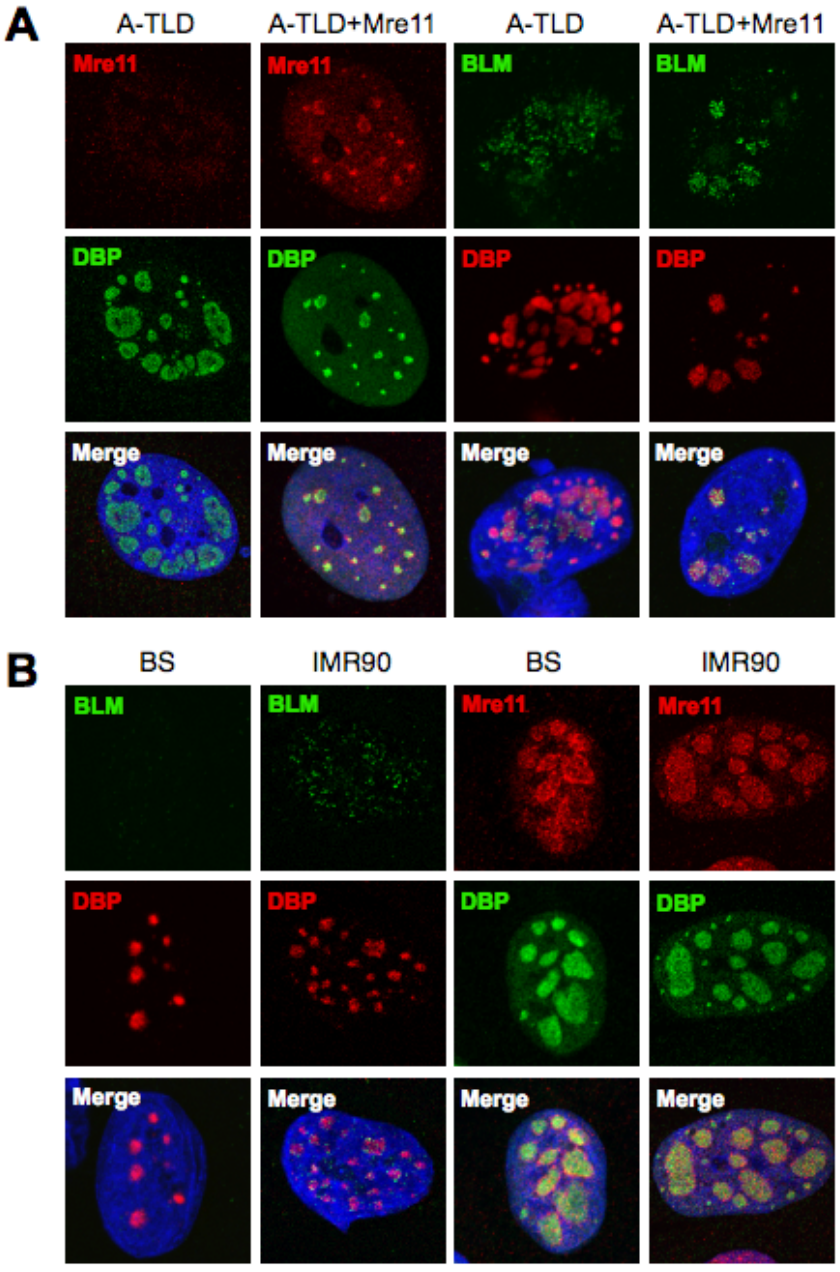
A
A-TLD
A-TLD+Mre11
A-TLD
A-TLD+Mre11
Mre11
Mre11
BLM
BLM
DBP
DBP
DBP
DBP
Merge
Merge
Merge
Merge
B
BS
IMR90
BS
IMR90
BLM
BLM
Mre11
Mre11
DBP
DBP
DBP
DBP
Merge
Merge
Merge
Merge

HeLa-shMre11 and NBS cells, we infected these cells with Ad5 or *dl*1004 virus for 24 h and assessed the levels of BLM by SDS-PAGE and immunoblotting BLM was still efficiently degraded by Ad5 infection in both the HeLa-shMre11 cells and the NBS hypomorphic cells (**Fig. 3-5A** and **B**). These results demonstrate that the degradation of BLM by E1b55K/E4orf6 is not a side effect of E1b55K/E4orf6 mediated degradation of the MRN complex.

Since the MRN complex is recruited to sites of viral replication during infection with *dl*1004, we also assessed whether the localization of BLM to sites of viral replication required the presence of a functional MRN complex (**Fig. 3-6A**). We infected cells hypomorphic for Mre11 (A-TLD) or A-TLD cells were transduced by a retrovirus encoding wild-type Mre11 (A-TLD+Mre11) (Carson et al., 2003) with *dl*1004 (**Fig. 3-6A**). Cells were pre-extracted and fixed 24 hpi and analyzed by immunofluorescence. In these cells, BLM still localized to foci at and around viral replication centers as shown by colocalization with DBP (**Fig. 3-6A**); however, the pattern of BLM foci was slightly more within the DBP centers in the presence of Mre11. BLM is reported to be required for localization of the MRN complex to the damage foci formed after treatment with hydroxyurea (HU)(Franchitto and Pichierri, 2002). To identify if BLM was required for MRN recruitment to viral centers, we utilized cells derived from Bloom syndrome patients that are hypomorphic for BLM (BS) or IMR90s that express a wildtype BLM. The BS cells and IMR90s were infected with *dl*1004

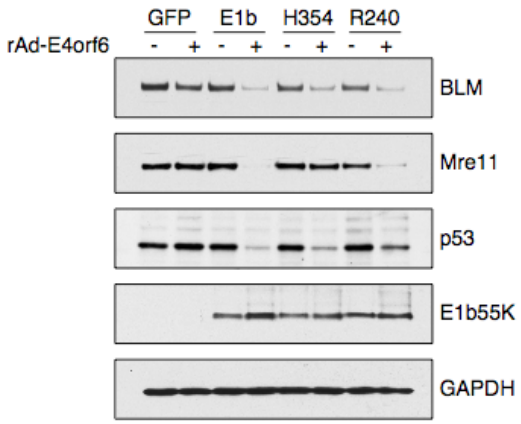

Figure 3-7. The region of E1b55K required for degradation of MRN or p53 is not required for degradation of BLM. U2OS cells that stably express GFP, wild-type E1b55K (E1b) or mutated E1b55K (H354 and R240) were infected with rAd-E4orf6 (MOI of 50) for 24 h. Cells were harvested and lysates were analyzed similar to (A). Mre11 served as a control to demonstrate the known H354 degradation defect and p53 served as a control to demonstrate the known R240 defect.

and analyzed by immunofluorescence. In the BS cells Mre11 localization at sites of viral centers was similar to that in IMR90s (**Fig. 3-6B**). Together, these results demonstrate that the degradation and localization of BLM seen during infection is separable from that of the MRN complex.

To identify if the region of E1b55K that is required for degradation of the MRN complex is also required for degradation of BLM, we utilized U2OS cell lines that stably express GFP, E1b55K or separation-of-function mutants of E1b55K (Carson et al., 2003; Schwartz et al., 2008). The H354 insertion mutant of E1b55K still retains its ability to degrade p53, but is dysfunctional in its ability to degrade the MRN complex (Schwartz et al., 2008). The R240A mutant of E1b55K is effective in degrading the MRN complex, but is unable to degrade p53 (Schwartz et al., 2008; Shen et al., 2001). U2OS-E1b, -R240A, -H354 and –GFP cell lines were infected with a recombinant adenovirus expressing E4orf6 (rAd-E4orf6). Cells were harvested at 24 hpi, and lysates were analyzed by SDS-PAGE and immunoblotting (**Fig. 3-7)**. As reported, the H354 insertion mutant was defective in its ability to degrade Mre11 and the R240A mutant did not degrade p53 efficiently (**Fig. 3-7)** (Schwartz et al., 2008; Shen et al., 2001). As expected, U2OS-GFP cells did not degrade BLM when infected with rAd-E4orf6, while the wild-type E1b55K expressing cells did degrade BLM (**Fig. 3-7)**. Interestingly, both mutant E1b55K cells lines; the H354 and R240 degraded BLM when infected with rAd-E4orf6 (**Fig. 3-7)**.

These experiments demonstrate that the region of E1b55K required for Mre11 and p53 degradation is different from the region required to degrade BLM.

BLM and E1b55K co-immunoprecipitate in the absence of Mre11.

E1b55K mediates substrate recognition for the E1b55K/E4orf6 ubiquitin ligase complex (Carson et al., 2003; Cathomen and Weitzman, 2000; Querido et al., 2001a; Querido et al., 2001b; Shen et al., 2001; Wienzek et al., 2000). To identify if BLM co-immunoprecipitated (co-IP'd) with E1b55K, we infected HeLa cells with recombinant adenovirus expressing GFP (rAd-GFP) or E1b55K (rAd-E1b55K) for 24 h. We made whole cell protein lysates, collected immunoprecipitates with the BLM antibody, and analyzed the co-IP by SDS-PAGE and immunoblotting. We found that E1b55K co-IP'd with BLM (**Fig. 3-8A**). To verify that E1b55K co-IP with BLM was independent of the known interaction between E1b55K and the MRN complex, we simultaneously preformed the same experiment in HeLa cell lines stably expressing shMre11 (Vo et al., 2005) and found that E1b55K could co-IP with BLM in the absence of Mre11 (**Fig. 3-8A**). We verified the co-IP results in HeLa cells transiently transfected with a vector expressing a TAP tagged E1b55K, and found that BLM co-purified with E1b55K but not a control TAP-RFP (**Fig. 3-8B**).

BLM localizes to sites of active viral replication.

Sites of active adenovirus DNA replication localize to small punctate foci around DBP centers and can be detected by incorporating BrdU in a short pulse during infection (Pombo et al., 1994). Prior to degradation, we observed

Figure 8. E1b55K co-immunoprecipitates with BLM. (A) HeLa cells or HeLa-shMre11 cells were infected with rAd-GFP or rAd-E1b55K at an MOI of 50 for 24 h, cells were harvested and lysed as described in materials and methods. Lysates were subjected to immunoprecipitation with the BLM antibody as described in materials and methods and approximately half of the total immunoprecipitate was loaded onto the gel and was compared with 5% of the input lysate. (B) HeLa cells were transfected with a vector expressing TAP-RFP (RFP) or TAP-E1b55K (E1B). TAP constructs were separated by affinity purification from the lysates, and approximately half of the purification was loaded onto the gel. Levels of purified complex were compared with 1% of the input lysate. CBP is used to demonstrate expression of the TAP constructs.

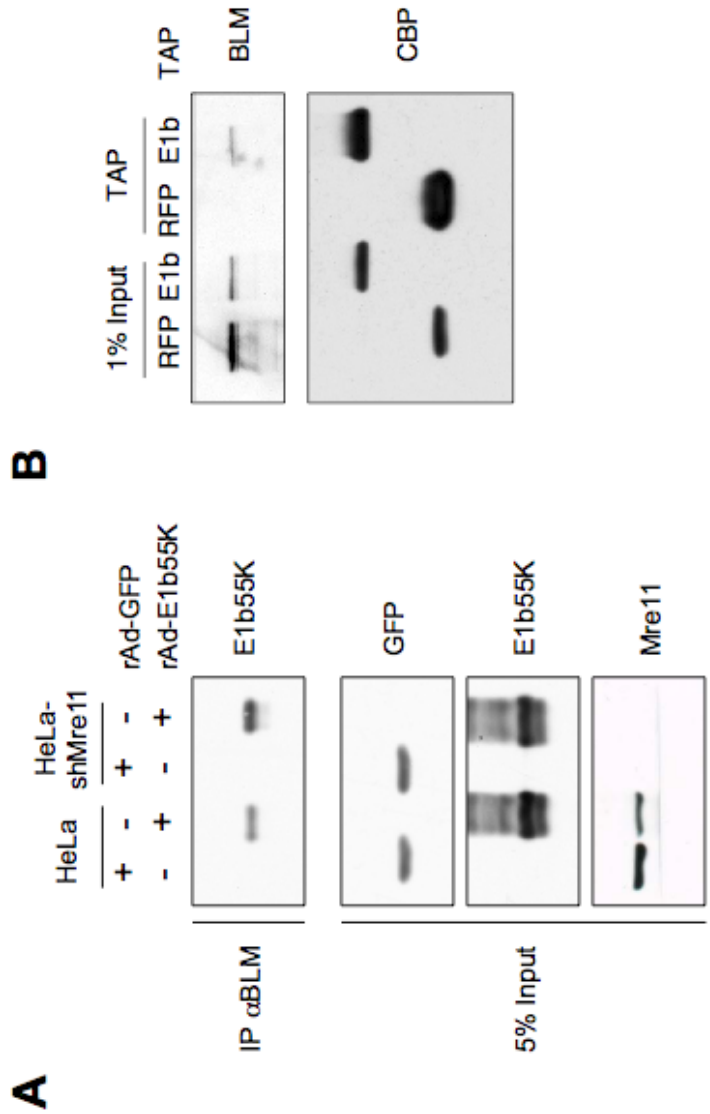
A
HeLa
HeLa-shMre11
rAd-GFP
rAd-E1b55K
E1b55K
IP αBLM
GFP
E1b55K
Mre11
5% Input
B
1% Input
TAP
RFP
E1b
RFP
E1b
TAP
BLM
CBP

that BLM localized to small foci at and around DBP centers during Ad5 infection (**Fig. 3-2A**). To examine if the BLM foci co-localized with active sites of viral replication, we transfected HeLa cells with a construct expressing an mRFP tagged DBP and then subsequently infected HeLa cells with Ad5 and harvested at 16 or 30 hpi (**Fig. 3-9A**). The infected cells were then pulsed with BrdU for 30 min, pre-extracted and fixed. We performed immunofluorescence using antibodies to BLM and BrdU. The BrdU antibody can only access incorporated BrdU if it is present in ssDNA, thus staining for BrdU will only appear at sites where the virus is actively replicating. We found that BLM foci localized adjacent to the BrdU foci formed at active sites of viral replication (**Fig. 3-9A**). The localization of BLM near sites of active viral replication suggested to us that BLM was perhaps being degraded to prevent recognition of the genome or a detrimental effect on viral replication.

Infection with *dl*1004 that is unable to degrade or mislocalize the MRN complex exhibits a defect in viral DNA replication compared to that of wild-type Ad5 (Bridge et al., 1993; Weinberg and Ketner, 1986). The *dl*1004 replication defect can be overcome by assessing replication in cells that are deficient for the MRN complex members (Lakdawala et al., 2008; Mathew and Bridge, 2008). To test whether BLM plays an active role in inhibiting adenovirus DNA replication similar to Mre11, we assessed if there was an increase in the replication of *dl*1004 virus in HeLa cells that were deficient for BLM (**Fig. 3-9B**). HeLa cells were retrovirally transformed to stably express shRNA against

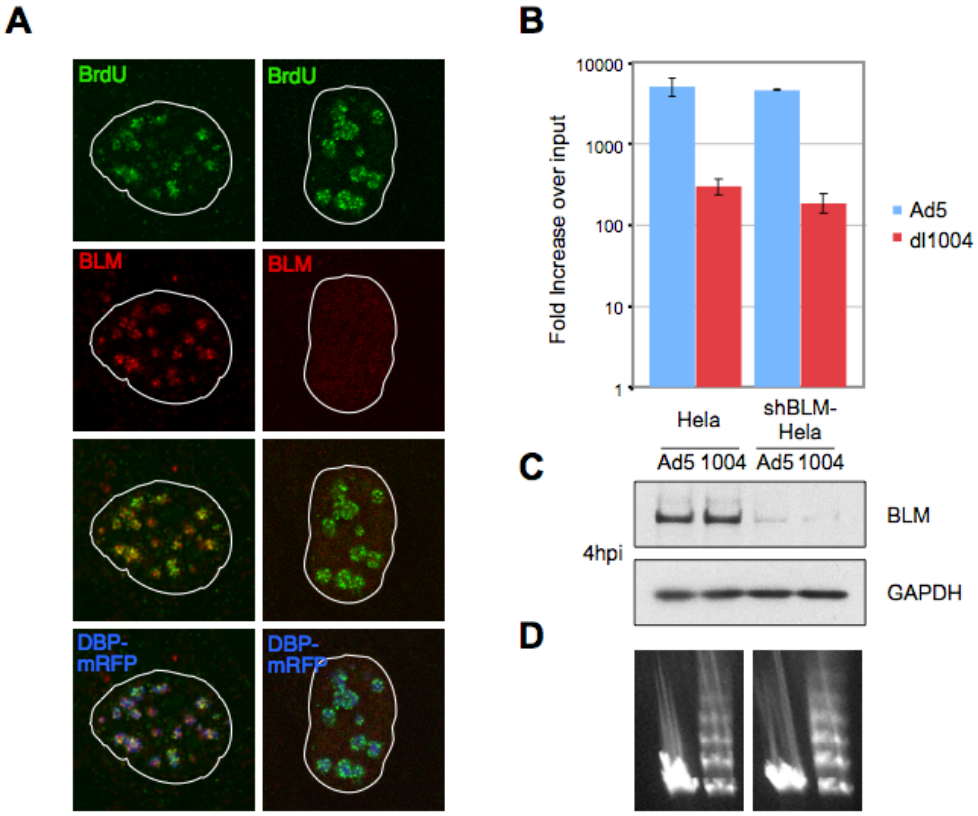

Figure 9. BLM localizes adjacent to active sites of viral replication but does not affect viral replication or concatemer formation. (A) HeLa cells were transfected with DBP-mRFP and were infected with Ad5 (MOI of 10) 8 h after transfection, at 16 h (left panel) or 30 h (right panel) post infection, cells were pulsed with BrdU for 30 min (as described in Materials and methods) and cells were pre-extracted and fixed and immunofluorescence was performed with the indicated antibodies. (B, C) HeLa cells or HeLa cells stably expressing shRNA to BLM (HeLa-shBLM) were infected with Ad5 (MOI 10) or *dl*1004 (MOI 3) in triplicate, cells were harvested at 4 and 30 hpi and 1/3 of the harvested samples were pooled for western analysis (B, C). (B) Quantitative PCR was used to quantify the amount of viral genomes and the data was analyzed as described in materials and methods. The fold change in total viral genomes over the input genomes was calculated and error bars represent the SEM of the triplicate samples. (D) HeLa cells or HeLa-shBLM cells were infected with Ad5 (MOI 25) or *dl*1004 (MOI of 50) for 48 h. Cells were harvested and prepared for analysis by Pulse Field Gel Electrophoresis as described in Materials and Methods. Formation of concatemers in the *dl*1004 infected HeLa-shBLM cells was compared to those formed in the HeLa cells.

BLM (HeLa-shBLM), and levels of BLM were not detected by western in HeLa-shBLM cells when compared to HeLa cells (**Appendix Fig. 1**). We infected HeLa cells or HeLa-shBLM cells with Ad5 or *dl*1004 and harvested the cells at 4 hpi to quantify the amount of internalized virus, which represents the "input" genomes. We harvested at 24 hpi to quantify the increase in viral genomes over input. The levels of BLM were not detectable in the shBLM cells at 4 hpi compared to the control cells (**Fig. 3-9C**). To quantify the change in replication, we extracted the DNA from the cells and quantified the amount of viral genomes present by using Quantitative PCR using internal primers to amplify a region within DBP as described previously (Lakdawala et al., 2008). We calculated the fold change over the input amount of DNA for each sample (**Fig. 3-9B**) Similar to our previous results (Lakdawala et al., 2008), we found that there was approximately a 10-fold defect in replication of *dl*1004 virus compared to that of Ad5 in HeLa cells. Similarly, when we calculated the fold change of *dl*1004 virus in the HeLa-shBLM cells, we found that there was still a 10-fold defect in *dl*1004 replication compared to that of wild-type Ad5 (**Fig. 3-9B**). This experiment demonstrates that knocking down BLM by shRNA does not by itself rescue the defect in viral DNA replication.

Since BLM is implicated in DNA end processing, we investigated if BLM contributed to end-processing events that result in viral genome concatemers in *dl*1004-infected cells. We infected HeLa or HeLa-shBLM cells with Ad5 or *dl*1004, harvested the cells at 48 hpi and analyzed the samples by Pulse Field

Gel Electrophoresis (PFGE). During Ad5 infection, the genome ran as a large single band on the gel in both HeLa and HeLa-shBLM cells (**Fig. 3-9D)**. The *dl*1004 virus genome runs as various species of genome concatemers as seen by the ladder of DNA in the *dl*1004 lanes, as seen previously. Concatemers of *dl*1004 were also present in the HeLa-shBLM cells (**Fig. 3-9D**). These results suggest that although BLM is implicated in end processing, it is not essential for concatemerization of adenovirus genomes.

Discussion

During infection, adenovirus targets cellular proteins for degradation. These proteins include the transcription factors p53 and Daxx (Cathomen and Weitzman, 2000; Grand et al., 1994; Harada et al., 2002; Moore et al., 1996; Querido et al., 2001a; Querido et al., 2001b; Roth et al., 1998; Steegenga et al., 1998), damage repair proteins including DNA Ligase IV and the MRN complex (Boyer et al., 1999; Carson et al., 2003; Stracker et al., 2002) and the cell surface protein Integrin α3 (Dallaire et al., 2009). We show here that the BLM helicase is also targeted for degradation by the adenovirus ubiquitin ligase complex. There are 5 human RecQ helicases with sequence and structural homology; therefore we found it surprising that BLM was the only member of the family that was targeted by E1b55K. Recently, we published findings that delved into the complexity of E1b55K protein-protein interactions by describing (mainly) two separation-of-function mutants of E1b55K: the

R240A point mutant and the H354 insertion mutant, which lost the ability of E1b55K to degrade p53 and MRN, respectively (Schwartz et al., 2008; Shen et al., 2001). However, both of these mutants still were able to degrade DNA Ligase IV (Schwartz et al., 2008). When we assessed the ability of the H354 and the R240 separation-of-function mutants to degrade BLM, we found that BLM was still degraded by these mutants. The ability of the separation-of-function mutants to degrade BLM demonstrates the complexity of protein-protein binding regions in E1b55K. Since there seems to be no obvious domain homology among E1b55K substrates, determining the binding sites of known substrates on E1b55K or a structure of the surface of E1b55K may give us insights into how it targets so many proteins. Recently, it has also been shown that E4orf6 from Adenovirus serotype 12 (Ad12) binds and degrades TopBP1 in conjunction with a Cullin2 containing complex in the absence of E1b55K (Blackford et al. 2010). Degradation of TopBP1 inhibits ATR activation by Ad12, similar to how abrogation of MRN inhibits ATM/ATR activation in Ad5 (Blackford et al., 2010; Carson et al., 2009; Carson et al., 2003). It will be interesting for future studies to determine if the degradation of BLM by Ad5 disturbs a pathway that is similarly abrogated either in the same manner or another manner across serotypes.

The presence of cellular damage and repair proteins at viral replication centers can be detrimental to Ad infection. In the absence of E4 proteins, the MRN complex is located throughout viral centers during infection (Stracker et

al., 2002). In contrast, we found that BLM localizes to DBP centers in small punctate foci prior to degradation in Ad5 infected cells and throughout infection in *dl*1004 infected cells. Interestingly, we found that these BLM foci were adjacent to sites of active viral replication foci. The localization suggests that the function of BLM leading to its targeting by E1b55K/E4orf6 may be related to the protection of the viral genome. However, it is also possible that BLM plays a beneficial role very early during infection and is then degraded to prevent a detrimental function later during infection.

Previously, it was shown that the MRN complex was required for concatemer formation and inhibition of replication during *dl*1004 infection (Lakdawala et al., 2008; Mathew and Bridge, 2008; Schwartz et al., 2008; Stracker et al., 2002). Our experiments to determine whether BLM is targeted during adenovirus infection were based on recent reports that BLM and its *S. cerevisiae* homolog Sgs1, function in DNA processing steps during HR (Budd and Campbell, 2009; Gravel et al., 2008; Mimitou and Symington, 2008; Nimonkar et al., 2008; Zhu et al., 2008b). However, there was no visible rescue of total viral replication or prevention of concatemer formation when *dl*1004 was infected in HeLa-shBLM cell lines. Although, BLM did not rescue *dl*1004 replication or prevent concatemer formation, we cannot rule out that there may be an effect lost in the sensitivity of our assay, such as slight delays in initiation or end joining that cannot be determined with our readout.

Our experiments tested the functions of BLM relating to its newly described role in DNA end processing; however, BLM has also been described to suppress hyper-recombination. In cells derived from patients with Bloom Syndrome (BS), there are high amounts of Sister chromatid exchanges (SCE)(Chaganti et al., 1974; German et al., 1965). The high amount of SCE and increase in micronuclei in BS cells is what originally suggested that BLM was involved in genome maintenance and functioned to suppress hyper-recombination (Chan et al., 2007; Rosin and German, 1985). During anaphase, BLM can be seen at bridges across the separating sister chromatids at both anaphase bridges at ultra fine bridges (UFB) during mitosis (Chan et al., 2007; Chu and Hickson, 2009). UFBs are thought to be late recombination intermediates or fully replicated chromosomes that need to be decatenated (Chu and Hickson, 2009). Cells deficient for BLM have increased numbers of UFBs and while BLM is present at the telomeric ends of DNA at the UFB, it is also associated with Fragile Site Loci (Chan et al., 2009; Naim and Rosselli, 2009). If BLM suppresses hyper-recombination, we propose that this could affect adenovirus negatively in two ways: the inappropriate resolution of Ad replication intermediates during replication or suppression of recombination between co-infected virus serotypes.

In our first hypothesis, the replication structures and intermediates formed during Adenovirus replication would be targets of BLM, which it tries to resolve thus complicating initiation and restart of replication. There are two

types of Adenovirus replication: Type 1 and Type 2 (**Fig. 1-3**) (Lechner and Kelly, 1977). Type 1 Adenovirus replication intermediates include dsDNA with a ssDNA flap and dual replication forks with two ssDNA flaps being displaced from the replicating genome (**Fig. 1-3**). The structure of Type 1 replication intermediates could potentially be identified as DNA structures that look like 3' tailed duplexes, a target of RecQ helicase resolution (Chu and Hickson, 2009). During Type 2 replication, the displaced strand forms a loop by annealing of the ITRs (**Fig. 1-3**), and has the potential to be recognized as a bubble structure or DNA displacement loop, which can be targeted by RecQ helicases for resolution (Chu and Hickson, 2009). In this model, the structure formed by the displaced strand protects the DNA strand from cellular exonucleases similar to the input/packaged genome. If BLM helicase acts to resolve these structures, viral replication intermediates may become exposed to cellular nucleases during infection, which might also lead to a decrease in the amount of template available for replication. However, If BLM functions to resolve replication intermediates, the decrease in viral replication could be negligible compared with the effects of the MRN complex, and may explain why we did not see a significant change when knocking down BLM in our replication assays.

The second hypothesis is that BLM suppression of hyper-recombination is evolutionarily detrimental for the fitness of adenovirus. Although end joining of viral genomes is detrimental because concatemerized genomes cannot be

packaged, internal recombination may be beneficial to the virus. Our cell based assays do not expose the importance of recombination to produce new serotypes, the *in vivo* co-infection of 2 adenovirus serotypes would result in production of mixed serotypes which could confer some evolutionary advantages to the virus. Therefore, degradation of BLM by E1b55K/E4orf6 to promote hyper-recombination would be beneficial to adenovirus evolution. Currently, the function of BLM that is detrimental to Ad infection remains elusive. Our experiments demonstrated that BLM is a newly found target of the E1b55K/E4orf6 ubiquitination ligase complex. BLM has emerging roles in DNA end processing and HR, in addition to its originally described function to suppress hyper-recombination. It will be interesting to determine how BLM is functioning during adenovirus infection and future studies may give us insights on the role of BLM in its cellular context beyond that during Ad infection.

Materials and Methods

Cells lines. HEK293A cells were purchased from Qbiogene. HeLa cells were purchased from the American Tissue Culture Collection. W162 cells for growth of E4 deleted viruses were from G. Ketner. Immortalized NBS (NBS-LXIN) and A-TLD1 cells and cells complimented with Nbs1 and Mre11, respectively were created and maintained as described previously (Carson et al., 2003). The U2OS cell lines expressing GFP, E1b55K or E1b55K mutants were created and maintained as described (Carson et al., 2003; Schwartz et

al., 2008). HeLa-shMre11 cells were a gift from C. Her and were described previously (Vo et al., 2005). HeLa cells expressing shRNA to BLM were created using the Phoenix retroviral system and shRNA sequences were from J. Karlseder and will be described elsewhere. Cells were maintained in Dulbecco's Modified Eagle's Medium supplemented with 10% Fetal Bovine Serum at 37ºC in a humidified atmosphere containing 5% CO2.

Viruses and infections. The mutant viruses *dl*1004 (ΔE4), *dl*1016 (ΔE4orf3/ΔE1b), *dl*1017 (ΔE4orf6/ΔE1b) *dl*110 (ΔE1b), and dl1006 (ΔE4orf3) have been described (Babiss and Ginsberg, 1984; Bridge and Ketner, 1990), and were obtained from G. Ketner. Wild type Ad5 and *dl*1017 were propagated in 293 cells. The *dl*1004 and *dl*1016 viruses were propagated on W162 cells (Weinberg and Ketner, 1983). The Ψ5, Ψ5-NTD-Cul5 and Ψ5-Cul5 have been described and were obtained from A. Berk and were propagated on 293 cells (Woo and Berk, 2007). The E1 deleted recombinant Adenovirus vectors rAd-E4orf6 and rAd-GFP were obtained from P. Branton. All viruses were purified by two sequential rounds of ultra-centrifugation in cesium chloride gradients and stored in 40% glycerol at -20^{o}C. Infections were performed in DMEM supplemented with 2% FBS. After 2 h at 37°C additional serum was added to a total of 10%.

Antibodies. Primary antibodies were purchased from Novus Biologicals Inc. (Nbs1), Genetex (Mre11-12D7 and Rad50-13B3), Santa Cruz (Ku70, Ku86, BLM, RecQL1) Invitrogen (GFP), Cell Signaling (RecQ4), BD Biosciences

(WRN), Calbiochem (p53), Research Diagnostics Inc (GAPDH), Sigma (Flag-M2, BrdU). The monoclonal B6 antibody against DBP and the monoclonal 2A6 antibody to E1b55K were from A. Levine. The polyclonal rabbit antisera to DBP was from P. Van der Vliet. The RecQ5 antibody was from P. Janscak. The anti-BLM antibody was created by C. Naeger and J. Karlseder and will be described elsewhere. Secondary antibodies were purchased from Invitrogen Molecular Probes and Jackson Labs.

Immunoblotting and Immunofluorescence. Immunoblotting and immunofluorescence were performed as previously described (Carson et al., 2003). Novex (Invitrogen) 3-8% or 4-12% gradient gels were used for resolution of proteins. For immunofluorescence, cells grown on glass cover slips were infected at an MOI of 10-100 pfu/cell. After 16-24 h the cells were washed, fixed, stained and counter-stained with 4',6-diamidino-2-phenylindol (DAPI). Where indicated, cells were pre-extracted prior to fixation by incubation on ice for 20 min with a solution of PBS with DTT, NaCl, HEPES Buffer pH 8 (Sigma), PBS, and $MgCL_2$. Where indicated cells were transfected using Lipofectamine 2000 (Invitrogen). BrdU incorporation was for 30 min at 37ºC. Addition of proteasome inhibitors was for 12 h at 37ºC. Immunoreactivity was visualized using a Leica confocal microscope.

Quantitative PCR analysis of DNA replication. Experiments were performed in triplicate and cells were harvested at 4 and 24 h post infection. 1/3 of the cells from triplicate sample were combined for western analysis to

demonstrate BLM knockdown. Total DNA was extracted from cells using DNeasy kit (Qiagen). qPCR was performed as previously described (Lakdawala et al., 2008). The results are presented as the mean and standard error of the mean from the triplicate experiments.

PFGE. Cells were infected with Ad5 (MOI of 25) or *dl*1004 (MOI of 50) for 48 h and viral DNA was analyzed for concatemer formation as previously described (Stracker et al., 2002; Weiden and Ginsberg, 1994). Cells were incorporated into agarose plugs that were loaded onto a 1.2% high gelling temperature agarose gel and subjected to pulsed-field gel electrophoresis (PFGE) for 16 h. DNA was visualized by staining with EtBr.

Acknowledgements

I am grateful to Colleen Naeger for reagents and helpful discussions, and I would also like to thank Jan Karlseder for providing me with reagents. I would also like to thank others who contributed reagents.

Some material from this chapter is in preparation for submission as: Orazio NI, Naeger, C, Karlseder, J, Weitzman MD. Adenovirus targets the BLM helicase for degradation during infection

The dissertation author was the primary researcher and author of this paper.

Chapter 4. Characterization of CtIP function during Adenovirus infection

Background

Adenovirus has a dsDNA genome with a virally encoded Terminal Protein (TP) covalently linked to the 5' end (Rekosh et al., 1977). Infection with adenovirus deleted for the E4 region (*dl*1004) activates the cellular DNA damage response and the viral genome is ligated into end-to-end concatemers (Boyer et al., 1999; Carson et al., 2003; Stracker et al., 2002; Weiden and Ginsberg, 1994). Concatemer formation requires the removal of the TP from the end of the genome and ligation of the genome ends. The MRN complex, DNA Ligase IV and DNA-PKcs are required for concatemer formation (Boyer et al., 1999; Schwartz et al., 2008; Stracker et al., 2002). Although the nuclease activity of Mre11 is required for concatemer formation (Stracker et al., 2002), the *in vitro* nuclease functions described for Mre11 do not include activities that could carry out TP removal (Paull and Gellert, 1998b; Paull and Gellert, 1999a; Trujillo et al., 1998). Combined, these observations suggest that there is an unknown protein (or proteins) required for TP removal and subsequent concatemer formation. During adenovirus infection, replication intermediates expose the cell to a range of structurally diverse DNA substrates (**Fig. 1-3**). In contrast, incoming virus genomes provide a unique DNA substrate that could be probed to reveal proteins required specifically to remove the TP from the dsDNA genome. In this chapter, we used an *in vitro*

system to uncover proteins required for concatemer formation without the complication of ongoing viral replication.

In order to study the function of cellular proteins essential to survival, protein levels can be knocked down by shRNA or be expressed in hypomorphic forms. However, in both of these scenarios some level of functional protein must be present to allow for cell survival. *Xenopus laevis* cell free extracts (*Xenopus* extracts) are useful for studying DNA damage repair pathways, and many pathways in *Xenopus* extracts are conserved in human cells (Garner and Costanzo, 2009). *Xenopus* extracts are advantageous because proteins essential to cell survival (e.g., Mre11) can be removed from the system by immunodepletion (Garner and Costanzo, 2009). In this chapter we demonstrate that the cellular protein CtIP is required for concatemer formation in *Xenopus* extracts and we characterize the role of CtIP function *in vitro* and during infection.

CtIP is a multifunctional protein implicated in the DNA damage response and transcriptional regulation (Chinnadurai, 2006). CtIP has multiple protein-protein interaction domains, as illustrated in **Figure 4-1**. It was identified as a protein that interacts with the CtBP transcriptional repressor (Schaeper et al., 1998). CtIP also interacts with Brca1 (Wong et al., 1998; Yu et al., 1998), Rb (Fusco et al., 1998; Meloni et al., 1999) and is reported to be a tumor suppressor itself (Chen et al., 2005). In mouse models, $CtIP^{-/-}$ homozygotes are embryonic lethal and the $CtIP^{+/-}$ heterozygotes, while viable,

Figure 4-1. Diagram of CtIP functional domains. Representation of published CtIP functional domains relevant to our studies. Protein-protein interaction domains include RB, BRCA1, CtBP and the MRN complex. The dimerization domain at the N-terminus (green) and the two CXXC Zn hook motifs are at either end of the protein. The sites of ATM phosphorylation after DNA damage are at S664 and S745. The DR damage recruitment motif is also indicated, including the point mutations that were found to prevent function of DR motif.

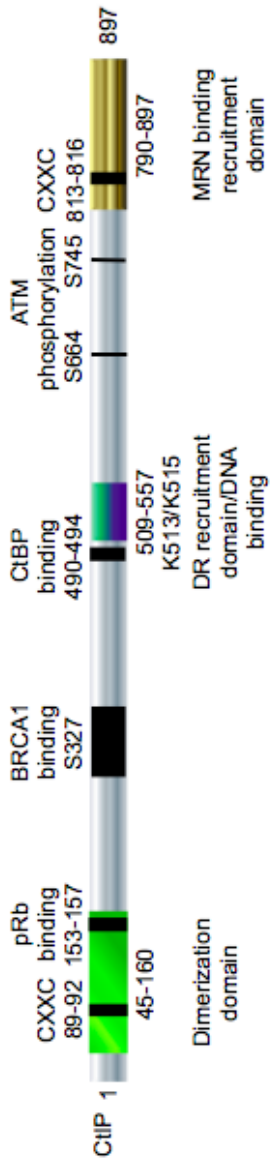
CtIP 1
CXXC 89-92
pRb binding 153-157
45-160
Dimerization domain
BRCA1 binding S327
CtBP binding 490-494
509-557
K513/K515
DR recruitment domain/DNA binding
ATM phosphorylation S664
S745
CXXC 813-816
790-897
MRN binding recruitment domain
897

exhibit a shorter life span due to lymphomas (Chen et al., 2005). The murine phenotypes characterize CtIP as an essential gene and *bona fide* tumor suppressor (Chen et al., 2005).

As mentioned in chapter 1, CtIP has also been implicated in the DNA end processing events required for repair of DSBs (Chinnadurai, 2006; Mimitou and Symington, 2009a). Speculation on the role of CtIP in processing events comes from the reports that CtIP is homologous to the *S. cerevisiae* protein Sae2 and the *S. pombe* protein Ctp1 (Limbo et al., 2007; Sartori et al., 2007). In *S. cerevisiae*, mutants deleted for Sae2 could not process meiotic breaks created by Spo11, and Sae2 was found to promote an endonucleolytic cleavage event. (Keeney and Kleckner, 1995; McKee and Kleckner, 1997; Neale et al., 2005). Sae2 promotes Mre11 nuclease activity to cleave hairpin structures, and is also suggested to have nuclease activity itself (Lengsfeld et al., 2007); however, which of these Sae2 functions contributes to Spo11 removal is not yet been determined. Ctp1 and CtIP also interact with the MRN(X) complex via Nbs1 FHA/BRCT domains (Chen et al., 2008; Lloyd et al., 2009; Sartori et al., 2007; Williams et al., 2009b; Yuan and Chen, 2009), and Sae2, Ctp1 and CtIP are all implicated in cell cycle dependent resection of DNA breaks (Farah et al., 2009; Huertas et al., 2008; Limbo et al., 2007; Terasawa et al., 2008).

Consistent with the implication that CtIP is required for resection of DBSs, it has been demonstrated that CtIP is recruited to sites of damage

(Sartori et al., 2007; You et al., 2009; Yuan and Chen, 2009). Multiple regions of CtIP have been suggested to be required for recruitment to sites of damage including the damage recruitment (DR) motif (You et al., 2009), the N-terminal dimerization domain (Yuan and Chen, 2009), and the C-terminal MRN binding domain (Sartori et al., 2007) (**Fig. 3-1**). CtIP recruitment in the damage response pathway is downstream of Nbs1 and ATM but upstream of RPA and ATR, demonstrating how activation of the DDR can promote resection of DNA leading to repair (Sartori et al., 2007; You et al., 2009; Yuan and Chen, 2009). ATM is suggested to be required for CtIP recruitment to damage, and phosphorylates CtIP at two sites, S664 and S745 (Li et al., 2000). However, mutants of CtIP expressing only the DR (509-557) motif can be recruited independently of phosphorylation (You et al., 2009). It is possible that phosphorylation by ATM causes a conformational change in CtIP, exposing the DR motif that allows for damage recruitment (You et al., 2009). Once recruited to DNA damage, CtIP is suggested to promote resection of DNA ends in concert with the MRN complex (Mimitou and Symington, 2009b; Sartori et al., 2007; You et al., 2009; Yuan and Chen, 2009). Although absence of CtIP shows functional defects in DSB resection (Hartsuiker et al., 2009; Nakamura et al., 2010; Sartori et al., 2007; Yun and Hiom, 2009), an enzymatic role in resection for CtIP has yet to be characterized.

In this chapter, we demonstrate that CtIP promotes *in vitro* concatemerization of the adenovirus genome. To determine the role that CtIP

plays during infection, we characterized the localization of CtIP during infection. Specifically, CtIP localized adjacent to sites of active viral replication and was also inhibitory to *dl*1004 viral replication during infection. As CtIP functions in the DNA damage response, we also characterized the effects of CtIP knockdown on the DNA damage response during *dl*1004 infection. Together, the results in this chapter demonstrate that CtIP inhibits adenovirus infection, most likely due to its role in TP removal from the viral genome. The structural similarity of the TP bound genome during infection and Spo11 bound DNA during meiosis suggest that a role for CtIP in TP removal may have broad implications for the role of CtIP in processing of meiotic breaks.

Results

Xenopus extracts ligate purified adenovirus genome into concatemers

To identify if the formation of concatemers could be studied *in vitro,* we needed to isolate the TP bound adenovirus genome (Ad5-TP) away from the virus capsid and associated proteins. Adenovirus was harvested from infected cells by freeze thawing, and cell debris was separated from virus particles by centrifugation. The virus capsids were isolated by centrifugation over a $CsCl_2$ gradient, and the Ad5-TP was separated from the virus capsids by centrifugation over a guanadinium-CsCl gradient, which denatures the capsids but does not disrupt the covalent bond between the genome and the TP (**Fig. 4-2A**)(Dunsworth-Browne et al., 1980). To verify that the TP was not

Figure 4-2. Purification of Ad5-TP and concatemer formation in *Xenopus* extracts. (A) Diagram of Ad5-TP purification. Ad5 virus is propagated and virus particles are purified over a $CsCl_2$ gradient; the capsid is separated from the genome by denaturation and centrifugation on a guanidinum-CsCl gradient. Fractions were tested for DNA and pooled for the Ad5-TP. (B) The presence of the TP on the genome can be determined by increased mobility of the genome ends on a gel. Ad5-TP was digested with SmaI. Proteinase K (Pro-K) was added ((-) absent (+) present) for 30 min and the digestion products were analyzed on a 0.8% agarose / 0.5XTBE gel. The genome ends are labeled as 5' and 3'. (C) *Xenopus* extracts support formation of Ad5-TP concatemers. Ad5-TP was added to *Xenopus* extracts in concentrations from 10-60 nM. The entire reaction was separated by PFGE. As a control, HCT116 cells were infected with *dl*1004, harvested after 48 hpi, and separated by PFGE (*dl*1004).

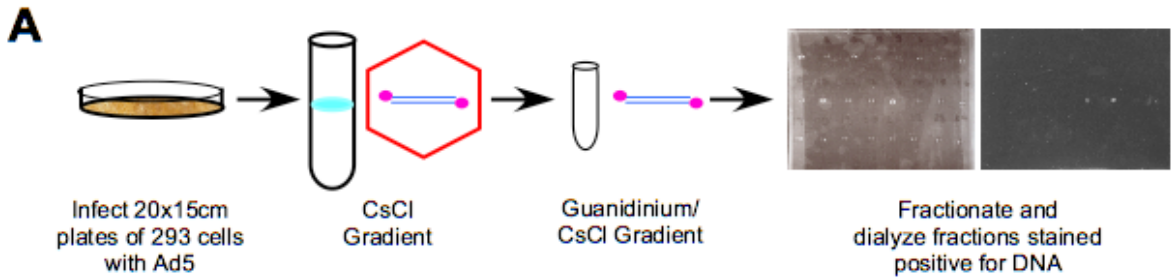
A
Infect 20x15cm plates of 293 cells with Ad5
CsCl Gradient
Guanidinium/ CsCl Gradient
Fractionate and dialyze fractions stained positive for DNA
B
- + Pro-K
5'
3'
C
Ad5 genome (nM)
10 20 30 60 dl1004
Genome monomer

removed from the genome in our purification, we tested for the attachment of the TP (**Fig. 4-2B**). Digestion of the Ad5 genome with SmaI produces multiple DNA fragments, and the fragment sizes of the 5' and 3' ends of the Ad genome are 1009 bp and 582 bp, respectively. The other fragments produced are either below 300 bp or greater than 1300 bp allowing us to resolve specifically the ends of the genome by separation on an agarose gel. If the TP is digested from the genome with Proteinase-K (Pro-K), the bands corresponding to the 5' and 3' ends of the genome are detected at their predicted sizes (**Fig. 4-2B**, Lane 2). However, if the TP is bound to the genome, the genome ends are too large or not negatively charged enough to enter the agarose gel, and bands corresponding to the 5' and 3' ends are absent (**Fig. 4-2B**, Lane 1). From this assay we can demonstrate that the genome preparation is covalently bound to the TP.

To study concatemer formation *in vitro,* we used *Xenopus laevis* cell free extracts produced from unfertilized eggs that are arrested in metaphase of the second meiotic division as described (Smythe and Newport, 1991). The eggs are crushed by centrifugation in the presence of cycloheximide to generate interphase crude extract. The crude extract is fractionated further by ultracentrifugation to generate interphase egg cytosol that will be referred to as *Xenopus* extracts. As mentioned previously, these extracts are useful for studying repair pathways and checkpoint activation (Garner and Costanzo, 2009).

To determine if the *Xenopus* extracts supported concatemer formation *in vitro,* Ad5-TP was added to the extracts at concentrations ranging from 10nM to 60nM, incubated for 2 h at room temperature, and analyzed by Pulse Field Gel Electrophoresis (PFGE) (**Fig. 4-2C**) (Materials and methods). As a control, HCT116 cells infected with *dl*1004 were used to represent the size of concatemers obtained *in vivo* (**Fig. 4-2C**). Titration of the Ad5-TP into the *Xenopus* extracts led to formation of concatemers in a concentration dependent manner (**Fig. 4-2C**). However, while we observed that increasing concentrations of Ad5-TP correlated with increased concatemer formation (10-30 nM), a concentration of 60 nM Ad5-TP led to a high percent of monomeric Ad5-TP in our assay (**Fig. 4-2C**). We do not assume this to be a function of saturating the extracts with DNA, but to dilution of the extracts when adding large volumes of Ad5-TP and altering the optimal concentrations for protein function in the extracts. Our experiments demonstrate that *Xenopus* extracts support concatemer formation of the Ad5-TP.

CtIP is required for concatemer formation in *Xenopus* extracts

Results from various groups suggested that CtIP plays a role in supporting 5' DNA end resection in conjunction with the MRN complex (Sartori et al., 2007; You et al., 2009; Yuan and Chen, 2009). Since the MRN complex is required for concatemer formation, we wanted to determine if CtIP was also required by using our *in vitro* system. To determine if concatemers formed in the absence of CtIP, we depleted the extracts of *Xenopus* CtIP (xCtIP) with an

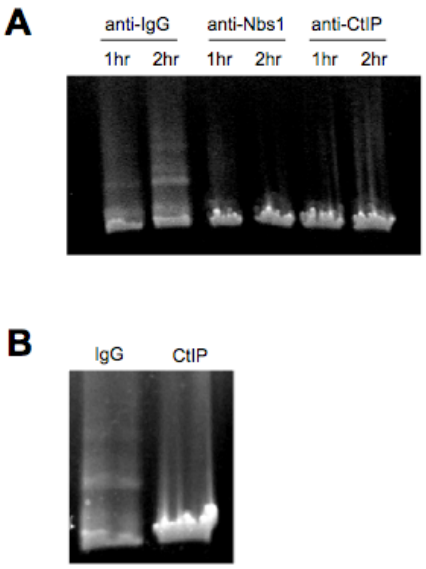

Figure 4-3. Inhibition of xCtIP and xNbs1 prevents concatemerization of Ad5-TP in *Xenopus* extracts. (A) *Xenopus* extracts were pre-incubated with anti-IgG, anti-xNbs1 or anti-xCtIP antibodies for 20 min. Ad5-TP was added at a concentration of 20 nM. The reactions were stopped at either 1 or 2 h with EDTA and the entire reaction was prepared and separated by PFGE. (B) *Xenopus* extracts were immunodepleted with anti-IgG or anti-xCtIP antibodies prior to incubation and analysis on a pulsed field gel.

xCtIP specific antibody, using an antibody to IgG as a control (Materials and methods). The extracts depleted with IgG antibody exhibited Ad5-TP concatemers as expected **(Fig. 4-3B)**. However, extracts depleted with xCtIP antibody did not form concatemers when incubated with Ad5-TP **(Fig. 4-3B)**. Therefore, immunodepletion of xCtIP prevented Ad5-TP concatemerization *in vitro.* To confirm the immunodepletion result, we inhibited CtIP in the extracts by a second method. The *Xenopus* Nbs1 (xNbs1) and xCtIP antibodies have previously been shown to be inhibitory to xNbs1 and xCtIP function when added to *Xenopus* extracts (You et al., 2005; You et al., 2009). Therefore, we pre-incubated the *Xenopus* extracts with antibodies to IgG (control), xNbs1 or xCtIP. After pre-incubation with inhibitory antibodies, Ad5-TP was added to the extracts, incubated for 1 or 2 h and the reactions were prepared for PFGE analysis (**Fig. 4-3A**). Addition of the IgG had no effect on concatemer formation of Ad5-TP, while incubation with the xNbs1 antibody prevented concatemers as expected (**Fig. 4-3A**). The inhibitory effects of xNbs1 demonstrated consistency between our *in vitro* results and our previous results obtained during infection (Stracker et al., 2002). The reactions pre-incubated with the xCtIP antibody were also defective for concatemer formation (**Fig. 4-3A**). Together our results suggest that CtIP function is required to promote Ad5-TP concatemer formation in *Xenopus* extracts.

Incubation of rxCtIP with Ad5-TP promotes mobility of the genome ends

Concatemer formation requires 2 steps: removal of the TP and ligation of genome ends. Our experiments in the *Xenopus* extracts demonstrated that xCtIP is required for concatemer formation *in vitro.* The MRN complex and CtIP are implicated in processing of broken DNA ends (Chen et al., 2008; Nakamura et al., 2010; Sartori et al., 2007; You et al., 2009; Yuan and Chen, 2009; Yun and Hiom, 2009). We asked whether CtIP could promote removal of the TP from the adenovirus genome. In order to determine if CtIP was sufficient for TP removal, we purified fragments of xCtIP protein for use in *in vitro* reactions. We used a bacterial expression system to produce recombinant GST-tagged xCtIP fragments (rxCtIP), which were purified with a glutathione-agarose resin (Materials and methods). The recombinant fragments of xCtIP purified were rxCtIP-479-856 and rxCtIP-621-856 (**Fig. 4-4A**).

In order to test if rxCtIP fragments could remove the TP from the Ad5 genome, we incubated rxCtIP with Ad5-TP (Materials and methods), digested the genome with SmaI, and analyzed the genome on an agarose gel. We assayed for the presence of the Ad5 5' and 3' DNA end fragments at their predicted sizes (**Fig. 4-4B, D**). Exposure of the agarose gel demonstrated equal loading of DNA; however, the 5' and 3' ends were not easily detected in the gel (**Fig. 4-4B**). To increase the sensitivity of our assay, we detected the 5'

Figure 4-4. Incubation of Ad5-TP with rxCtIP increases the mobility of the genome ends after SmaI digestion. (A) Purified GST-CtIP-479-856 and GST-CtIP-621-856 proteins were analyzed via SDS-PAGE and coomassie stained. The arrows mark the predicted sizes of the major bands. (B, D) Ad5-TP was either untreated (-) or incubated with increasing amounts of GFP-CtIP-479-856 or GFP-CtIP-621-856. All reactions were then digested with SmaI, or SmaI followed by ProK (ProK). DNA was visualized by EtBr staining. (C) Probes used for specific detection of the 5' and 3' ends by southern blotting. Probes were created between the ITRs and the most proximal SmaI site. (D) The reaction from (B) was transferred to a membrane and probed for the 5' and 3' ends.

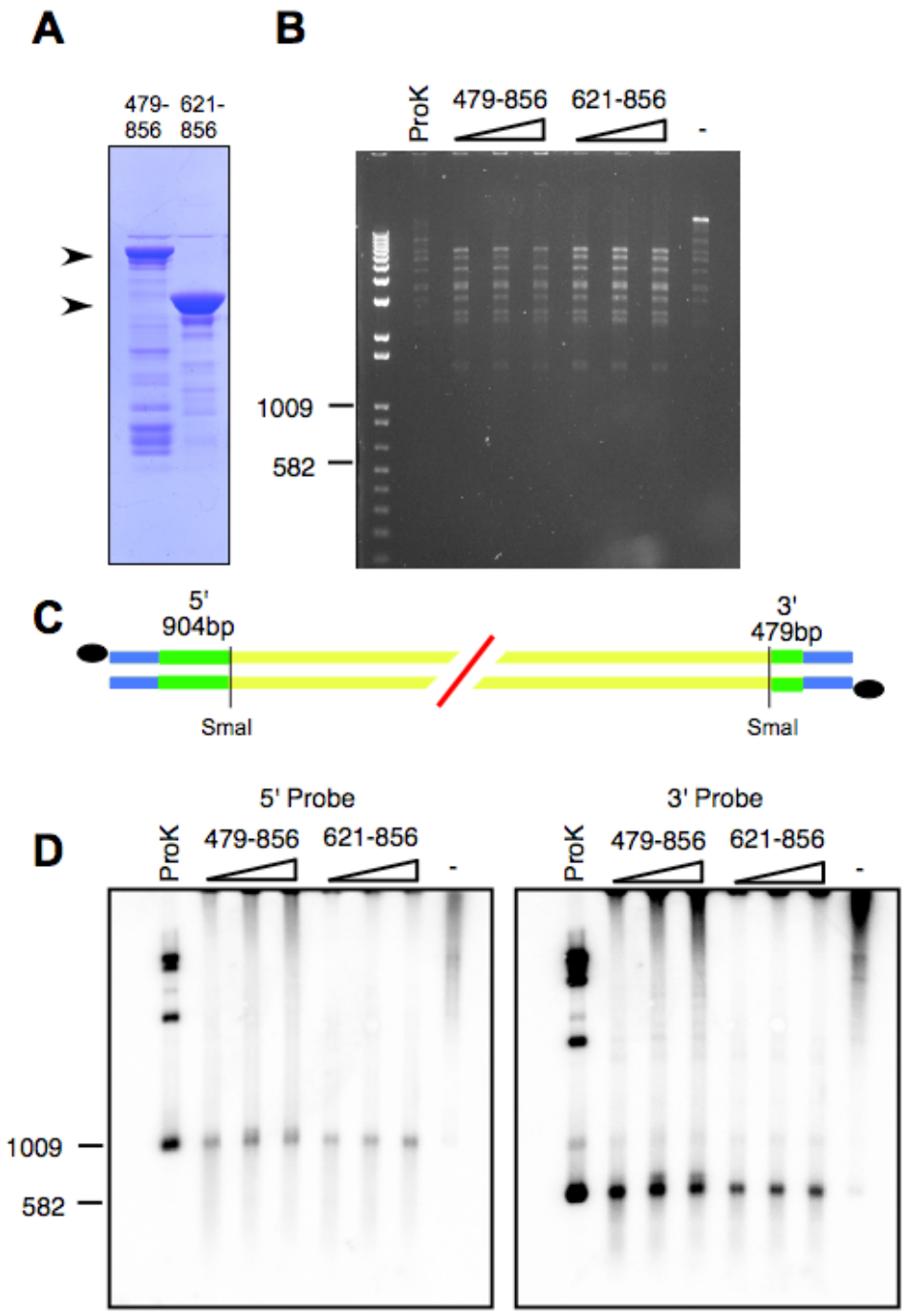
A
479-856
621-856
B
ProK
479-856
621-856
-
1009
582
C
5'
904bp
3'
479bp
SmaI
SmaI
D
5' Probe
3' Probe
ProK
479-856
621-856
-
1009
582

and 3’ ends by Southern blotting (**Fig. 4-4C, D**). We designed specific 5’ and 3’ DNA probes excluding the Inverted Terminal Repeats (ITRs)(**Fig. 4-4C**). In the lane corresponding to the negative control ((-) no Pro-K, no rxCtIP) there were no bands detected at the predicted sizes of 1009 and 582 bp, respectively (**Fig. 4-4D**). In the lane corresponding to the Pro-K treated control, the 5’ and 3’ probes detected a dark band at the predicted sizes (**Fig. 4-4D**). In the reactions with rxCtIP-479-856 and rxCtIP-621-856, we could detect the 5’ and 3’ bands at the predicted sizes (**Fig. 4-4D**). This suggested that incubation with these C-terminal fragments of CtIP was promoting the mobility of the 5’ and 3’ ends of the genome. In the reactions with the rxCtIP-479-856 (but not rxCtIP-621-856) we detected a slightly longer DNA fragment running just above the 5’ and 3’ band. While we cannot explain the appearance of the second band, it does suggest that xCtIP-479-856 has some altered activity when compared to xCtIP-621-856. Our experiments suggest that xCtIP removes TP from the genome ends, allowing the 5’ and 3’ SmaI fragments to enter the gel and run at their predicted sizes.

CtIP localization during adenovirus infection

Our results *in vitro* suggested that CtIP might play an inhibitory role during adenovirus infection. CtIP is reported to interact with the MRN complex (Chen et al., 2008; Sartori et al., 2007; Yuan and Chen, 2009), and the MRN

Figure 4-5. Localization of GFP-CtIP during infection. (A and B) GFP-CtIP was transfected into HeLa cells followed by infection with Ad5 or *dl*1004, or mock infected (Mock). The nuclei are represented by DAPI staining (blue) in the merge panels. (A) GFP-CtIP localizes to sites of replication during Ad infection. RPA staining represents viral centers. (B). Costaining of GFP-CtIP with cellular proteins. Immunofluorescence was performed for DBP, and Nbs1. Immunofluorescence for pTP was in cells that were pre-extracted 20 min prior to fixation as described in Materials and methods.

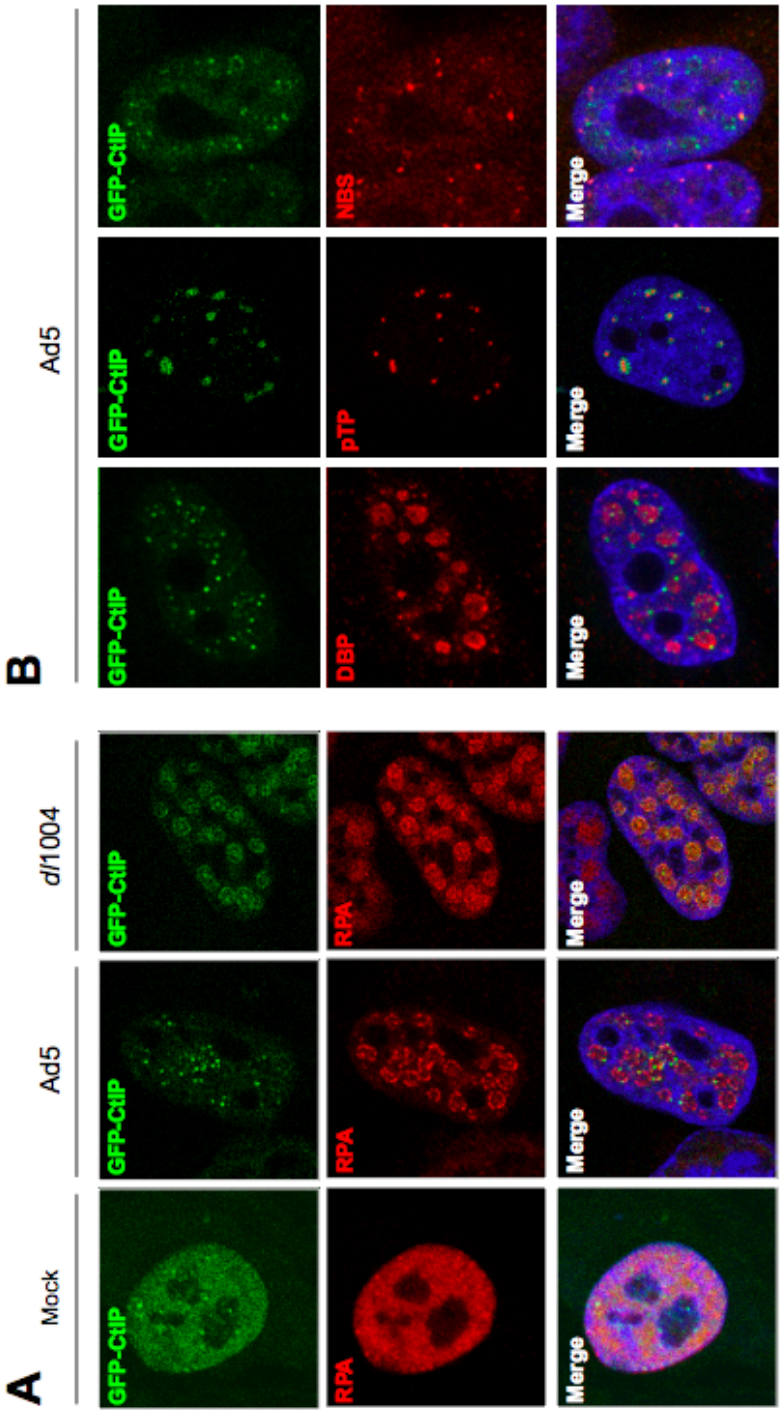
A
Mock
Ad5
dl1004
GFP-CtIP
RPA
Merge
B
Ad5
GFP-CtIP
DBP
pTP
NBS
Merge

complex is detrimental to adenovirus infection (Carson et al., 2003; Evans and Hearing, 2003; Evans and Hearing, 2005; Lakdawala et al., 2008; Mathew and Bridge, 2007; Mathew and Bridge, 2008; Stracker et al., 2002). The MRN complex is mislocalized and then degraded during Ad5 infection, but during *dl*1004 infection MRN localizes to sites of viral replication (Carson et al., 2003; Evans and Hearing, 2003; Evans and Hearing, 2005; Stracker et al., 2002). To examine CtIP localization during infection, HeLa cells were transfected with a vector expressing GFP tagged human CtIP (GFP-CtIP) and subsequently infected with Ad5 or *dl*1004 (**Fig. 4-5A, B**). Cells were fixed 24 hpi and immunofluorescence was performed with an antibody recognizing the cellular ssDNA binding protein RPA, which localizes to viral centers during Ad infection (**Fig. 4-5A**) (Carson et al., 2009; Stracker et al., 2002). In uninfected cells (Mock), GFP-CtIP localized diffusely throughout the nucleus and in small nuclear foci, similar to published data for endogenous CtIP and ectopically expressed GFP-CtIP (**Fig. 4-5A**) (Sartori et al., 2007; You et al., 2009; Yu and Baer, 2000). In Ad5 infected cells, GFP-CtIP localizes to small discrete foci that localize at and around the replication centers (**Fig. 4-5A**). GFP-CtIP fluorescence in *dl*1004-infected cells localizes throughout the replication centers rather than at discrete foci (**Fig. 4-5A**). Our experiment demonstrates that CtIP is being recruited to viral centers in both Ad5 and *dl*1004 infected cells; however, the fluorescence pattern is distinct between the two infections.

To compare the localization of GFP-CtIP to other proteins reported to localize at viral centers, we performed immunofluorescence with antibodies to DBP, pTP and Nbs1 (**Fig. 4-5B**). DBP was used as a control marker for replication centers to confirm the results obtained with RPA (**Fig. 4-5B**, Lane 1). The pTP antibody detects the adenovirus encoded pre-Terminal Protein (TP). During infection, pTP is first detected in foci at early viral centers, and eventually stains in a diffusely nuclear then cytoplasmic pattern (Webster et al., 1997). Cells were pre-extracted prior to fixation limiting detection of pTP to viral centers (Materials and methods). Although pTP localized to viral centers, there was no colocalization between the GFP-CtIP and pTP (**Fig. 4-5B**, Lane 2). Nbs1 is reported to be localized away from viral centers by the adenovirus E4orf3 protein, but is also reported to localize near sites of viral replication during Ad5 infection (Evans and Hearing, 2005; Stracker et al., 2002). When we compared the localization of GFP-CtIP to Nbs1, the proteins were predominantly present in distinct foci. The GFP-CtIP localization corresponded to viral centers and the Nbs1 staining corresponded to E4orf3 tracks (**Fig. 4-5B**, Lane 3). Interestingly, the known interaction of CtIP with MRN does not sequester CtIP to MRN-containing E4orf3 tracks during Ad5 infection (Chen et al., 2008; Sartori et al., 2007; Yuan and Chen, 2009). Thus, the localization of CtIP to foci at Ad5 viral centers may represent a different function of CtIP than when it colocalizes with the MRN complex at *dl*1004 viral centers.

The N- and C-termini of CtIP display distinct localization phenotypes during Ad5 infection

CtIP contains various functional domains that have been described (Chinnadurai, 2006); we wanted to determine which of these domains was required for the localization of GFP-CtIP to viral centers. GFP tagged truncation mutants of CtIP were used for these studies (**Fig. 4-6A** and **Table 4-1**)(You et al., 2009). Various GFP-CtIP mutants were transfected into HeLa cells, which were then infected with Ad5 or *dl*1004 and fixed 24 hpi for analysis by immunofluorescence. The wild-type GFP-CtIP is shown in the left panel and localizes to foci at viral centers (**Fig. 4-6B**). The GFP-CtIP-1-693 mutant localized to the foci at viral centers during Ad5 infection, but the GFP-CtIP-130-693 mutant did not (**Fig. 4-6B**). This suggested that the first 130 amino acids of CtIP are required to form foci at sites of viral centers. The first 130 amino acids of CtIP contain a CXXC zinc hook motif and the majority of the coiled-coil dimerization domain (Dubin et al., 2004) (**Fig. 4-1**). Since there is a second CXXC motif in the C-terminus of CtIP, and the C-terminal mutants did not localize to foci at viral centers (**Table 4-1**), this suggested that the dimerization domain is required for localization at foci at viral centers. The damage recruitment (DR) motif is required for localization of CtIP to sites of damage created by laser microirradiation (You et al., 2009). The DR motif did not localize to foci at viral centers during Ad5 (**Table 4-1**) infection, suggesting that CtIP localization at these foci is not due to DNA damage recognition.

Figure 4-6. Localization of the GFP-CtIP truncation mutants during Ad5 infection. (A) Diagram of mutants used to determine the regions required for the N- terminal and C- terminal localization phenotypes. (B) GFP tagged CtIP mutants were transfected into HeLa cells. Cells were infected with Ad5 for 24 h and fixed for immunofluorescence to DBP. The merged images are stained with DAPI to represent the nuclei.

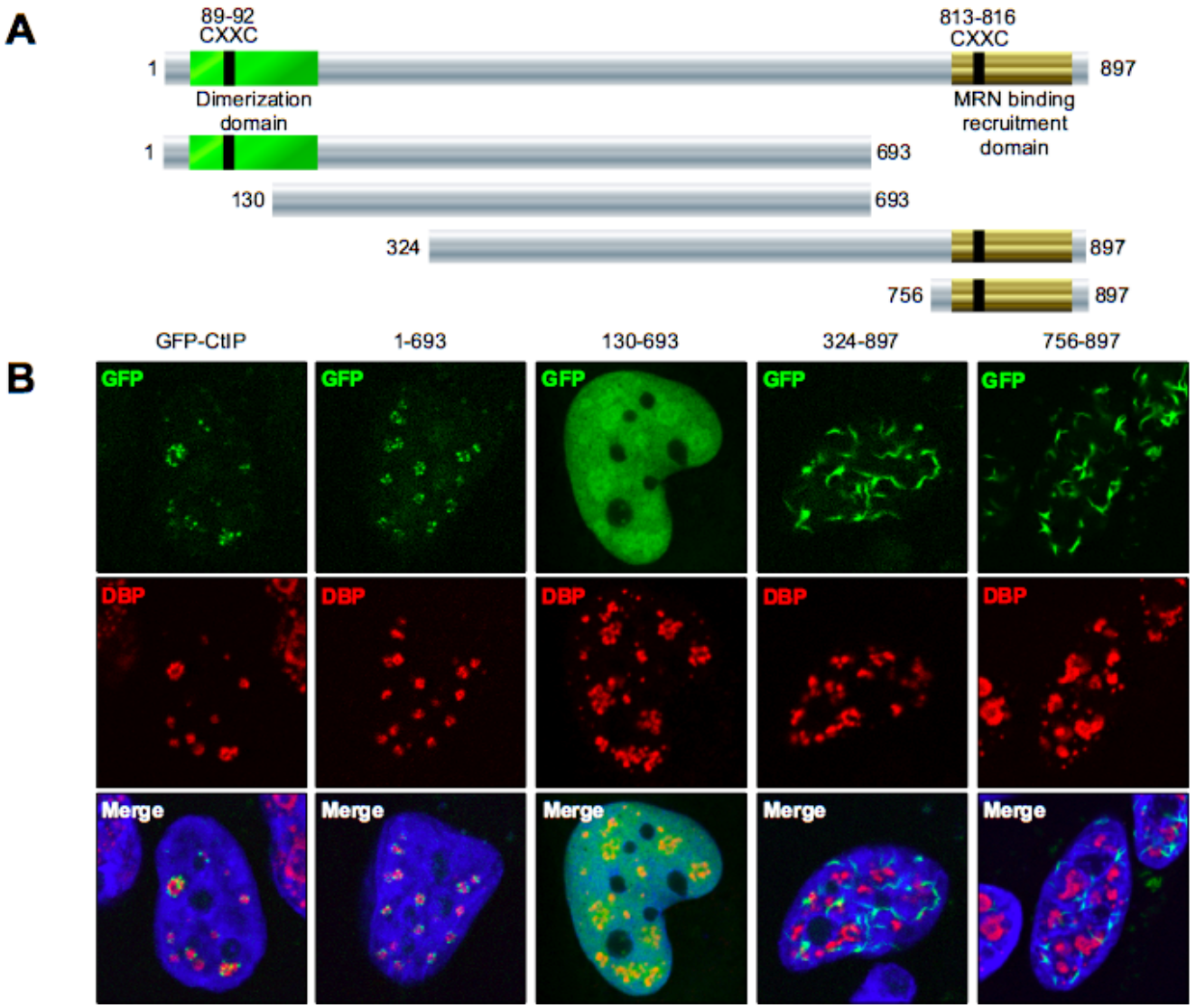
A
89-92
CXXC
813-816
CXXC
1
897
Dimerization
domain
MRN binding
recruitment
domain
1
693
130
693
324
897
756
897
B
GFP-CtIP
1-693
130-693
324-897
756-897
GFP
DBP
Merge

Table 4-1. Localization of GFP-CtIP mutants during infection. GFP-CtIP mutants were transfected into HeLa cells and subsequently infected with Ad5 or *dl*1004. Cells were fixed with 4% PFA or were pre-extracted prior to fixation (Pre-extracted). Description of GFP localization in relation to viral replication centers is as described.

Construct	Mock	Ad5	Ad5 Pre-extracted	*dl*1004	*dl*1004 Pre-extracted
GFP-CtIP	Diffuse and Foci	Foci at viral centers	Foci at viral centers	Throughout viral centers	No stain
1-400	Cytoplsmic and faint nuclear diffuse	Aggresome and cytoplasmic diffuse	Aggresome	Cytoplasmic, faint staining at viral centers	No stain
1-693	Diffuse and speckles	Foci at viral centers/diffuse	Foci at viral centers	Diffuse/brighter speckles at viral centers	No stain
130-693	Nuclear excluded from nucleoli	Diffuse/brighter at viral centers	No stain	Diffuse nuclear brighter at viral centers	No stain
135-500	Nuclear excluded from nucleoli	Diffuse/brighter at viral centers	No stain	Diffuse nuclear barely brighter at viral centers	No stain
324-897	Nuclear excluded from nucleoli	Diffuse/bright tracks away from centers	Tracks	Diffuse nuclear barely brighter at viral centers	No stain
324-897 CC	Nuclear excluded from nucleoli	Diffuse/bright tracks away from centers	Tracks	Diffuse nuclear brighter at viral centers	No stain
462-897	Nuclear excluded from nucleoli	Diffuse/brighter at/around viral centers	Tracks	Diffuse nuclear barely brighter at viral centers	No stain
495-693	Nuclear and faint cytoplasmic	Nuiclear and cytoplasmic	No stain	Diffuse nuclear barely brighter at viral centers	No stain
756-897	Nuclear and nuceloli	Diffuse/bright tracks away from centers	Tracks	Diffuse Nuclear/nuceloli brighter at viral centers	No stain

Although we cannot rule out that the requirement for the dimerization domain is not because this mediates an interaction of GFP-CtIP-1-693 with endogenous CtIP, we do not see recruitment to foci at viral centers in the absence of the dimerization domain.

A second localization pattern of the GFP-CtIP mutants occurred during Ad5 infection. GFP-CtIP mutants expressing the C-terminus of CtIP, but not the dimerization domain, localized to track-like structures away from viral centers (**Fig. 4-6B**). The GFP-CtIP-756-897 construct was the smallest fragment tested that localized to the track structures. All mutants deleted for the dimerization domain that still contained the C-terminal amino acids localized to track structures (**Fig. 4-6B** and **Table 4-1**). Cellular proteins mislocalized by the adenovirus protein E4orf3 are relocated to track-like structures. These proteins include PML (Carvalho et al., 1995; Doucas et al., 1996), the MRN complex (Evans and Hearing, 2003; Stracker et al., 2002) and Tif1α (Yondola and Hearing, 2007). E4orf3 was sufficient for localization of the C-terminus of GFP-CtIP into these structures as demonstrated by colocalization of transfected E4orf3 and GFP-CtIP (**Appendix Fig. 4**). The dominant localization of full length GFP-CtIP during Ad5 infection is at foci at viral centers and is mediated by the N-terminus, but in the absence of the N-terminus, GFP-CtIP localizes with the MRN complex in E4orf3 tracks.

The localization of GFP-CtIP mutants during *dl*1004 infection was more difficult to analyze. All of the mutant constructs located diffusely throughout

the nucleus; however, increased fluorescence was seen at viral centers in all nuclear mutants tested (**Table 4-1**). Cells were pre-extracted prior to fixation to remove the soluble GFP-CtIP from the nucleus to increase detection at the viral centers. In the pre-extracted cells, GFP-CTIP fluorescence was not detected, suggesting that our constructs were not associated with insoluble structures at the viral centers (**Table 4-1**). Therefore, the localization of GFP-CtIP mutants during *dl*1004 infection cannot be analyzed by our detection methods.

GFP-CtIP foci at viral centers are adjacent to sites of active viral replication

The GFP-CtIP foci detected during Ad5 infection resembled foci that were reported to be sites of active viral replication (**Fig. 4-7A**) (Pombo et al., 1994). Active viral replication during adenovirus infection can be visualized by pulsing infected cells with BrdU for 30 min prior to fixation followed by immunofluorescence for BrdU. The BrdU antibody can only detect BrdU incorporated in ssDNA and detects small punctate foci (**Fig. 4-7A**, Panel 1). If fixed cells are treated with HCl to denature the dsDNA the BrdU antibody can access all BrdU incorporated over the 30 min pulse and BrdU detection is throughout viral centers (**Fig. 4-7A**, Panel 2). To identify if GFP-CtIP co-localized with sites of active viral replication, GFP-CtIP was transfected into HeLa cells prior to Ad5 infection, and at 16 hpi the cells were pulsed with BrdU for 30 min. The cells were fixed and immunofluorescence was performed

Figure 4-7. The GFP-CtIP foci at viral centers are adjacent to sites of active viral replication. BrdU staining represents sites of active viral replication. (A) HeLa cells were infected with Ad5, at 16 hpi cells were incubated with BrdU for 30 min and then washed and fixed for immunofluorescence with DBP and BrdU. BrdU foci represent active sites of viral replication. The cells in panel 2 were treated with 0.1M HCl after fixation to denature the dsDNA and represent total incorporated BrdU. The merged image is stained for DAPI to represent nuclei, and the absence of DAPI stain in the +HCl sample demonstrates denaturation of the DNA. In (B), cells were transfected with GFP-CtIP prior to infection with Ad5 and BrdU incubation was similar to (A). Immunofluorescence was performed to BrdU and DBP. The DBP is represented in blue in the merged panel and the nuclear periphery is represented with a white line. The area enclosed in the yellow box in the Merge image in the first panel was represented in panel 2 as a 5X magnification. In (C) the cells were infected with *dl*1004 and BrdU incubation was for 1 h before fixation. BrdU and DBP staining is as described above.

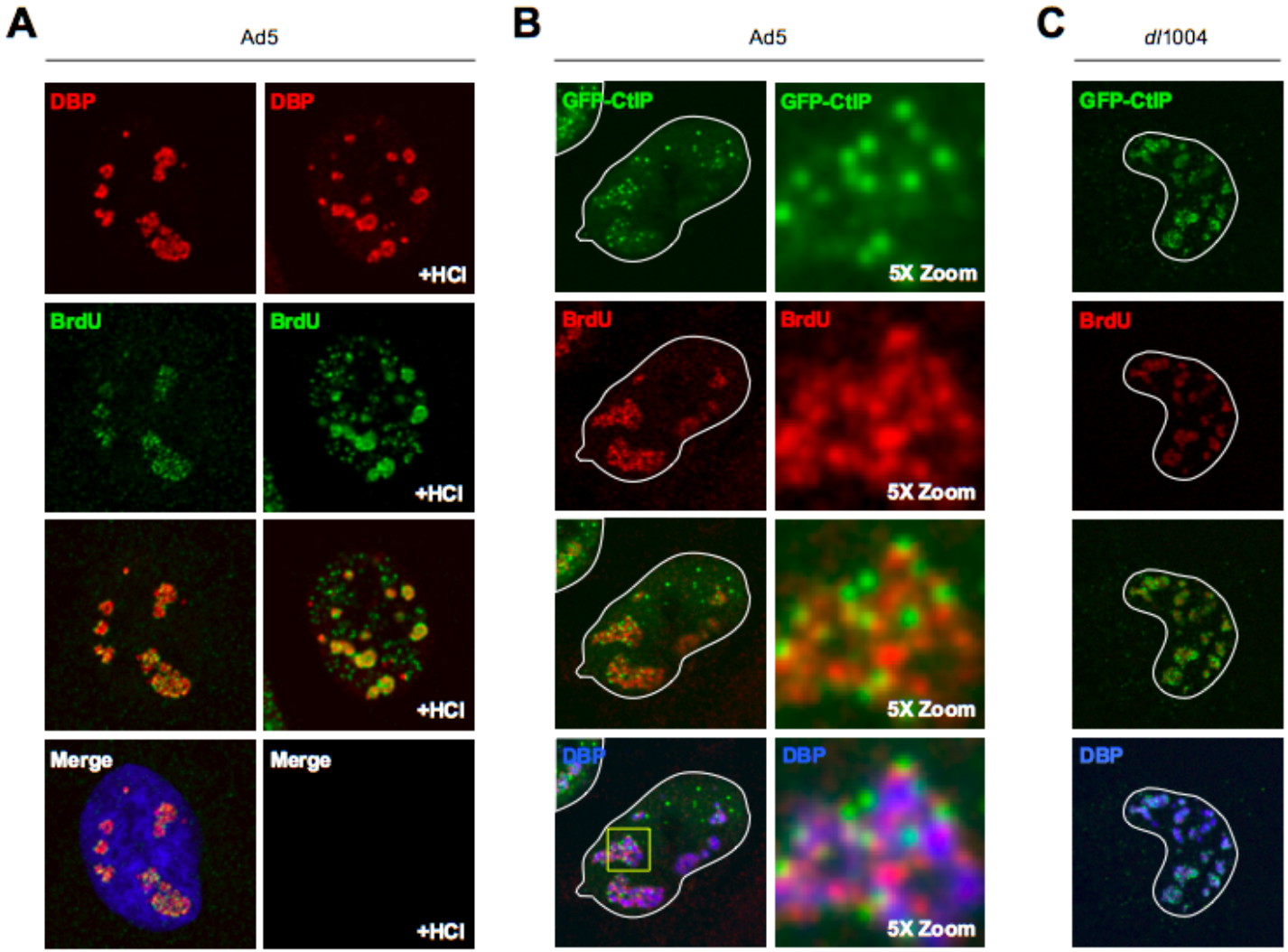
A
Ad5
DBP
DBP
+HCl
BrdU
BrdU
+HCl
+HCl
Merge
Merge
+HCl
B
Ad5
GFP-CtIP
GFP-CtIP
5X Zoom
BrdU
BrdU
5X Zoom
5X Zoom
DBP
DBP
5X Zoom
C
dl1004
GFP-CtIP
BrdU
DBP

using antibodies to BrdU and DBP. The GFP-CtIP foci and the BrdU foci both localized to DBP viral centers; however, the GFP-CtIP foci did not colocalize with the BrdU foci (**Fig. 4-7B**, Panel 1). The separation of GFP-CtIP foci and BrdU foci can be detected more clearly in the 5X image where the foci did not overlap (**Fig. 4-7B**, Panel 2). Therefore, the GFP-CtIP foci are adjacent to but do not overlap with active sites of viral replication.

GFP-CtIP localized throughout the replication centers in *dl*1004-infected cells (**Fig. 4-5A**). We examined whether GFP-CtIP would colocalize with BrdU at sites of active viral replication during *dl*1004 infection (**Fig. 4-7C**). There was no BrdU staining detected after a 30 min pulse, confirming that replication is defective in *dl*1004 infection (Halbert et al., 1985; Weinberg and Ketner, 1986) (Data not shown). However, if we extended BrdU incubation to 60 min in *dl*1004-infected cells, faint BrdU staining was detected at viral centers (**Fig. 4-7C**). GFP-CtIP localization throughout viral centers and delayed incorporation of BrdU in *dl*1004-infected cells suggested that the presence CtIP at viral centers might inhibit *dl*1004 viral replication.

Replication of *dl*1004 is rescued in cells deficient for CtIP

The TP is required for initiation of adenovirus replication (Challberg et al., 1980). Studies from our lab and others have demonstrated that there is a defect in *dl*1004 replication when compared to wild-type Ad5 (Bridge et al., 1993; Evans and Hearing, 2005; Halbert et al., 1985; Lakdawala et al., 2008; Mathew and Bridge, 2008; Weinberg and Ketner, 1986). The *dl*1004 defect

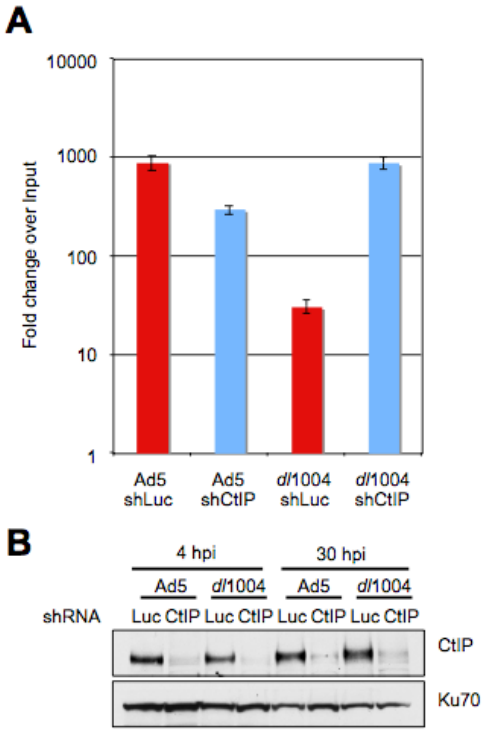

Figure 4-8. The effect of shRNA-mediated CtIP knockdown on Adenovirus replication. (A) HeLa-shLuc cells (red) or HeLa-shCtIP cells (blue) were infected with Ad5 or *dl*1004 in triplicate. Cells were harvested at 4 and 30 hpi. The quantity of viral genomes was measured by qPCR and the data is represented as the fold change of viral genomes at 30 h over that at 4 h. Error bars represent the SEM for each triplicate sample. (B) Cells from each time point were harvested and triplicate samples were pooled. Lysates were analyzed by SDS-PAGE and immunoblotting was performed for the indicated antibodies.

can be overcome if *dl*1004 is infected into cells that are defective for the Mre11 complex (Lakdawala et al., 2008; Mathew and Bridge, 2008). Combined, the reported interaction of CtIP with the MRN complex, the GFP-CtIP localization during infection, and our *in vitro* results suggested that CtIP might inhibit viral replication. To determine the effect of CtIP on viral replication, we created knockdown cell lines by infecting HeLa cells with lentivirus expressing an shRNA to CtIP (HeLa-shCtIP) or luciferase (HeLa-shLuc) (Materials and methods). The HeLa-shLuc and HeLa-shCtIP cells were infected with Ad5 or *dl*1004 virus in triplicate, cells were harvested at 4 and 30 hpi, and viral DNA was quantified by qPCR (Materials and methods). CtIP levels were efficiently reduced in the shCtIP cells as demonstrated by western blot analysis of the samples (**Fig. 4-8B**). Replication was calculated as the fold change of genomes at 30 hpi over the 4 hpi input, and the error bars represent the SEM per triplicate sample (**Fig. 4-8A**). The replication of wild-type Ad5 was decreased in the HeLa-shCtIP compared with the HeLa-shLuc cells (**Fig. 4-8A**, first 2 bars). As expected, in HeLa-shLuc cells, *dl*1004 replication was defective when compared with wild-type Ad5 (**Fig. 4-8A**, red bars). However, in the HeLa-shCtIP cells, *dl*1004 replicated as efficiently as wild-type Ad5 (**Fig. 4-8A**, last 2 bars). Therefore, CtIP is inhibitory to *dl*1004 infection and CtIP knockdown via shRNA rescues the replication defect of *dl*1004.

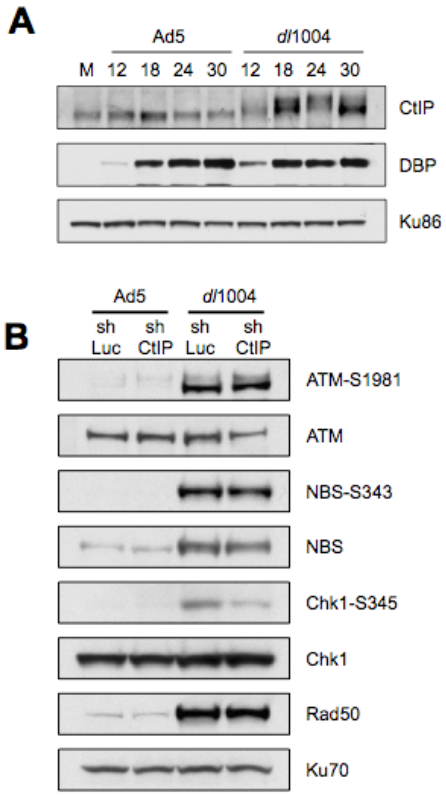

Figure 4-9. Analysis of ATM and ATR damage response activation in the HeLa-shCtIP cells. (A) HeLa cells were uninfected (M) or infected with Ad5 or *dl*1004 from 12-30 h and harvested over regular intervals. (A and B) Lysates were analyzed by SDS-PAGE and immunoblotting was performed with the indicated antibodies. DBP is an indicator of virus infection and Ku86 is used as a loading control. (B) Hela-shLuc (shLuc) or HeLa-shCtIP (shCtIP) cells were infected with Ad5 or *dl*1004 for 24 h. Immunoblotting was performed for antibodies to total protein or using phospho-specific antibodies as indicated.

Dual role of CtIP in ATM and ATR signaling events during infection

CtIP has been implicated in both ATM and ATR dependent DNA damage signaling (Greenberg et al., 2006; Li et al., 2000; Sartori et al., 2007; Yu and Baer, 2000). CtIP is a phosphorylation target of ATM (Li et al., 2000; Yu and Baer, 2000), and has been suggested to be required for ATRdependent phosphorylation of Chk1 by camptothecin treatment or γIR (Sartori et al., 2007; Yu and Chen, 2004; Yuan and Chen, 2009). Since a DNA damage response is activated during *dl*1004 infection, (Carson et al., 2009; Carson et al., 2003), we examined CtIP levels during infection. HeLa cells were uninfected (M) or infected with Ad5 or *dl*1004 virus and cells were harvested in regular intervals from 12-30 hpi. Lysates were prepared for analysis by SDS-PAGE and immunoblotting (**Fig. 4-9A**). Levels of CtIP in the uninfected and Ad5 infected cells were equivalent, suggesting that there is not a decrease in CtIP levels during Ad5 infection (**Fig. 4-9A**). During *dl*1004 infection, the levels of CtIP are increased and there is also a shift in the detected molecular weight (**Fig. 4-9A**). The shift in molecular weight most likely corresponds to the phosphorylation of CtIP by ATM or other downstream kinases (data not shown).

To test the effect of CtIP knockdown on damage signaling during infection, we utilized the HeLa-shLuc and HeLa-shCtIP cell lines. HeLa-shLuc and HeLa-shCtIP cells were infected with Ad5 or *dl*1004 and harvested at 24 or 48 hpi for analysis by SDS-PAGE and immunoblotting (**Fig. 4-9B**). During

infection with Ad5, there was no detectable ATM or ATR activation in the HeLa-shLuc or HeLa-shCtIP cells, confirming our previous results that Ad5 abrogates the ATM and ATR mediated damage responses (**Fig. 4-9B**) (Carson et al., 2009; Carson et al., 2003). We then analyzed the ATM and ATR damage responses during *dl*1004 infection. In the HeLa-shLuc cells infected with *dl*1004 there is activation of ATR and ATM as demonstrated by phosphorylation of ATM-S1981, NBS-S343, Chk1-S3345, Chk2-T68 and RPA32-S4,8 (**Fig. 4-9B** and **Appendix Fig. 2**). In HeLa-shCtIP cells, ATM autophosphorylation at S1981 was unaffected by the absence of CtIP (**Fig. 4-9B**), consistent with reports that ATM activation is upstream of CtIP (Greenberg et al., 2006; Li et al., 2000). Interestingly, Chk2 phosphorylation (Chk2-T68) was increased in the *dl*1004 infected HeLa-shCtIP cells in both mock-infected and *dl*1004-infected cells (**Appendix Fig. 2**). Therefore, ATM activation is either unaffected or hyper activated in the absence of CtIP. In contrast, during *dl*1004 infection, Chk1 phosphorylation (Chk1-S345) was decreased in the HeLa-shCtIP cells when compared to the phosphorylation in HeLa-shLuc cells (**Fig. 4-9B**). The effects of CtIP knockdown on phosphorylation of Chk1 conform to published results demonstrating a similar effect after treatment with camptothecin or γIR (Greenberg et al., 2006; Sartori et al., 2007; Yu and Chen, 2004; Yuan and Chen, 2009). Interestingly, during *dl*1004 infection, hyperphosphorylation of RPA at RPA32-S4,8 in HeLa-shCtIP cells was dramatically increased over that in HeLa-shLuc cells (**Appendix Fig.**

2). This additional increase in RPA phosphorylation may be due to activation of DNA-PKcs and will be discussed in the conclusions. These experiments demonstrate that loss of CtIP leads to an increase in ATM dependent Chk2 phosphorylation and a decrease in ATR dependent Chk1 phosphorylation when cells are infected with *dl*100*4*. Together these results suggest that CtIP plays opposing roles in DNA damage signaling after infection.

CtIP is not required for concatemer formation during infection

The prevention of adenovirus genome concatemers in *Xenopus* extracts by removal of CtIP suggested that CtIP would inhibit concatemer formation during infection. Our biochemical studies also suggested that CtIP promoted removal of the TP from the adenovirus genome thereby allowing NHEJ components to ligate the TP-free genome ends together. In order to test if CtIP was required for concatemer formation *in vivo*, we utilized the stable HeLa-shCtIP and HeLa-shLuc cell lines. The HeLa-shCtIP and HeLa-shLuc cells were infected with *dl*1004, harvested at 48 hpi, and the viral DNA was analyzed by PFGE (**Fig. 4-10**). As expected, infection of the HeLa-shLuc cells with *dl*1004 led to concatemer formation. In the HeLa-shCtIP cells, concatemers also form, thus knockdown of CtIP does not prevent concatemers during infection (**Fig. 4-10**). Our results demonstrate that CtIP is not required for concatemer formation during infection. Therefore, although CtIP is required for concatemers *in vitro* it is not required for concatemer formation *in vivo*.

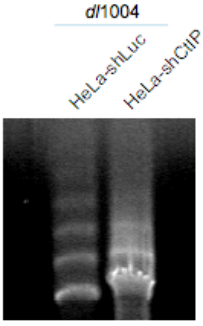

Figure 4-10. The HeLa-shCtIP cells support concatemer formation. HeLa-shLuc and HeLa-shCtIP cells were infected with *dl*1004 for 48 h. Cells were harvested and prepared for analysis on PFGE as described in Materials and methods.

Discussion

In chapter 4, we developed an *in vitro* assay to identify proteins required for concatemer formation. The xCtIP protein was found to be required for concatemer formation in our *in vitro* system. CtIP was most likely promoting removal of the TP, which is required for initiation of viral replication. Confirming this hypothesis, knockdown of CtIP in cells rescued the defective replication of *dl*1004 virus to levels displayed by wild-type Ad5 virus. An ectopically expressed GFP-CtIP protein localized to viral centers during infection. The N- and C-termini of CtIP were required for two distinct localization phenotypes during Ad5 infection, with the N-terminus displaying the dominant phenotype. Our results suggest that CtIP may play an important role during adenovirus infection and our conclusions discuss the role of CtIP in TP removal, in promoting a switch between NHEJ to HR and the dual roles of CtIP itself in transcriptional control and the DDR.

Our combined studies using *Xenopus* extracts, purified protein biochemical reactions, and rescue of *dl*1004 replication with CtIP depletion suggest that CtIP promotes removal of the TP from the Ad genome. Current studies in our lab are pursuing the biochemical mechanism of TP removal, and suggest that it is by an endonucleolytic mechanism (B.J.L., data not shown). The TP bound Ad5 genome is structurally similar to Spo11-bound DNA occuring during meiosis. Spo11 cleaves and covalently binds 5’ ends of the DNA until HR proteins resolve the protein-DNA structure mediating

homologous recombination (Keeney and Kleckner, 1995; McKee and Kleckner, 1997). The *S. cerevisiae* protein Sae2 promotes Spo11 removal and is suggested to be a functional ortholog of CtIP (Sartori et al., 2007). It has yet to be demonstrated whether CtIP possesses the enzymatic activity to process Spo11 bound DNA during meiosis. Therefore, if our studies demonstrate that CtIP functions to remove the TP from the adenovirus genome, it may suggest a more general role for CtIP in removal of Spo11 during meiosis outside the context of viral infection.

Our experiments demonstrated that CtIP is required for concatemer formation *in vitro*, but not during infection. Our conflicting results can be explained by the presence of cell cycle regulation in the cell system and the absence of viral replication in the *Xenopus* system (Garner and Costanzo, 2009). The switch between double strand break repair by NHEJ and HR is cell cycle regulated, even though proteins required for both processes are present throughout the cell cycle (as reviewed by (Branzei and Foiani, 2008)). During G_1, repair by NHEJ predominates, while repair by HR is preferred in S and G_2 (as reviewed by (Branzei and Foiani, 2008)). CtIP is cell cycle regulated, peaking in S/G_2; and the absence of CtIP promotes NHEJ over HR (Yu and Baer, 2000; Yun and Hiom, 2009). We observed DNA-PKcs phosphorylation and increased hyperphosphorylation of RPA at S4, 8 in HeLa-shCtIP cells as compared to HeLa-shLuc cells during *dl*1004 infection (**Appendix Fig. 2**). DNA-PKcs autophosphorylation is required for its

activation (Chan et al., 2002), and phosphorylates RPA32-S4, 8 (Boubnov and Weaver, 1995; Brush et al., 1994; Shao et al., 1999; Zernik-Kobak et al., 1997). In our experiments, levels of CtIP were inversely proportional to RPA-S4,8 phosphorylation during infection (**Appendix Fig. 2**). Therefore, enhanced NHEJ in HeLa-shCtIP cells may overcome the effects of CtIP knockdown in TP removal, resulting in the formation of concatemers during *dl*1004 infection. However, this model suggests that there is another protein required for TP removal during infection that allows NHEJ factors to ligate the DNA ends.

The absence of virus replication in the *Xenopus* extracts allows us to identify proteins required for specific processing of the Ad5-TP substrate. During viral replication a multitude of dsDNA and ssDNA substrates are presented to the cellular machinery (**Fig. 1-3**). Although CtIP may be required for processing the Ad5-TP substrate, it may not be sufficient to process the mass of genome substrates presented during viral replication. It is intriguing that Mre11 is required for concatemer formation and replication inhibition, but CtIP is only required for the inhibition of viral replication. Mre11 has distinct roles in activation of the DDR that are separable from its roles in DNA end-processing (Buis et al., 2008). Interestingly, MRN activation of the ATM and ATR damage responses is not required to inhibit viral replication, but activation of these kinases is required for concatemer formation (Lakdawala et al., 2008). Our combined results leads to a three-step model of concatemer formation: the first step requires removal of the terminal protein, the second step requires

activation of the ATM and/or ATR damage responses, and the third step results in ligation of genomes. Previous studies and the results presented in this chapter suggest that Mre11 and CtIP are involved in the first step of concatemer formation, and may function to activate the second step of concatemer formation. Mre11 has ssDNA endonuclease and 3'-5' exonuclease activity *in vitro* which does not suggest that it can function in TP removal alone (D'Amours and Jackson, 2002). CtIP could be required to promote Mre11 dsDNA endonucleolytic activity, switch the polarity of Mre11 exonuclease activity or may possess endonucleolytic activity itself. However, after removal of the TP, MRN may still be required to recruit factors including ATM or ATR to promote concatemer formation. Similar to the previous model, the caveat with this model is that during infection viral genome concatemers form in the absence of CtIP. Therefore another protein must compensate for CtIP that can collaborate with Mre11 to remove the TP from the genome, or Mre11 possesses functions later during infection that can lead to concatemer formation.

CtIP is a multifaceted protein with several reported functional domains (Chinnadurai, 2006). The N-terminal dimerization domain mediates localization to punctate foci during Ad5 infection. It has been reported that Ad5 replication is slightly defective in the absence of CtIP (Bruton et al., 2007). It was hypothesized that CtIP interaction with E1a promoted expression of adenovirus early proteins, and loss of this interaction resulted in defective Ad5

replication (Bruton et al., 2007). We also observed a minimal decrease in replication of Ad5 in the absence of CtIP. The localization of CtIP at foci during Ad5 infection could be related to the reported function of CtIP in transcriptional control, but association of CtIP with MRN at viral centers during *dl*1004 infection may switch CtIP function towards end processing and activation of a damage response.

Our results have demonstrated that CtIP is inhibitory to *dl*1004 infection. The inhibitory effects of CtIP are most likely due to its function in promoting removal of the TP from the Ad genome. It will be interesting to understand the discrepancy for the role of CtIP in concatemer formation *in vitro* and *in vivo*. Our results also suggested that CtIP has dual functions in either the absence (Ad5) or presence (*dl*1004) of DNA damage. If future studies to determine the biochemical function of CtIP suggest that CtIP can endonucleolytically remove the TP from the Ad genome, our results may translate to a role for CtIP in removal of Spo11 from the cellular genome during meiosis.

Materials and methods

Xenopus extracts. *Xenopus* egg extracts were prepared by Z. You as previously described (Smythe and Newport, 1991). Eggs were obtained from hormonally induced *Xenopus laevis*, and lysed by centrifugation at 16,000g in the presence of cycloheximide. Crude extracts were centrifuged 260,000g to

separate membrane components. Prior to incubation, *Xenopus* extracts were supplemented with ATP regenerating complex (150 mM creatine phosphate, 20 mM ATP, 0.5 mg/mL creatine phosphokinase). To deplete xCtIP from the *Xenopus* extract, 30 μL protein-A agarose beads coupled with 90 μL xCtIP antiserum were incubated with 150 μL extract for 45 min at 4°C. Beads were then removed from the extract by low-speed centrifugation. The extract supernatant was then subjected to two additional rounds of depletion under the same conditions. Unless indicated otherwise, Ad5-TP was incubated at a concentration of 20 nM in 50 μL *Xenopus* extracts for 2 h. The reaction was stopped by addition of 5 μL of 0.5 M EDTA.

Ad5-TP. Ad5 was infected into 4 x 10^8 HEK293 cells for 48 h. Infected cells were harvested and resuspended in 20 mL 10 mM Tris-HCl pH 8. The infected cells were freeze-thawed for 3 cycles of liquid nitrogen / 37ºC incubation to release virus particles from the cells. The cell debris was removed by centrifugation at 3000 rpm. The virus particles were isolated over a $CsCl_2$ gradient by 2 rounds of ultracentrifugation (25,000 rpm). The viral genome was separated from the virus capsid by denaturation and ultracentrifugation over a guanidinium-CsCl gradient. The genome was isolated by fractionation of the gradient, and fractions that contained DNA were combined and dialyzed in TE.

PFGE. The *Xenopus* extract reactions were mixed 1:1 with a solution of 1.25% InCert cell agarose/125 mM Tris-Cl pH 7.5 melted and cooled to 50ºC.

The extract agarose mixture was solidified in a mold for PFGE loading (plug). The plugs were treated with Proteinase-K, washed, and analyzed by PFGE as previously described (Stracker et al., 2002). The PFGE analysis in HeLa-shLuc and HeLa-shCtIP cells was as previously described (Stracker et al., 2002).

Expression and purification of recombinant proteins and probe labeling. The rxCtIP proteins were produced in BL21 (DE3) *E. coli* strains, from the pET41b vector. Induction conditions were 1 mM IPTG for 4 h at 37º, and the bacteria was lysed by emulsification. The proteins were purified using a glutathione-agarose resin, according to the manufacturer's protocol (Sigma, G4510). Southern probes for the 5' and 3' ends were digested from plasmids pCMX-PL2 5' and pCMX-PL2 3' with EcoRI and BamHI. Fragments were gel purified and labeled with α-^{32}PdCTP using the Rediprime II kit (Amersham) and purified with Illustra Probequant G50 columns (Amersham).

Biochemical *in vitro* reactions. Ad5-TP substrate (250 ng) was incubated with 100 nM, 200 nM, or 500 nM of the rxCtIP proteins 479-856 or 621-856 in 25 mM MOPS, 50 mM NaCl, 2mM DTT, and 5mM $MgCl_2$. Reactions were left at 25^{o}C for 1 h and stopped by incubation at 80ºC for 20 min. The reaction was then digested with 10U SmaI for 2 h at 25^{o}C. The Pro-K samples were digested with 1ug Pro-K for 30 min at 37ºC.

Southern Blot. Agarose gels were denatured in 1M NaCl/.5M NaOH and neutralized in 0.5 M Tris-Cl pH7.5/1.5 M NaCl prior to transfer. DNA was

transferred onto a membrane by capillary transfer in SSPE overnight, and the membrane was cross-linked with UV prior to hybridization. Hybridization of denatured 5' and 3' probes in Rapid-Hyb (Amersham) was carried out at 65ºC for 4 h. The membrane was washed in SSC and hybridized.

Plasmids. The GFP-CtIP plasmid and mutant constructs were a gift from Z. You and T. Hunter. The GFP-CtIP-1-400 and GFP-CtIP-130-693 were constructed using the KpnI and SmaI sites in pEGFP-C1. The pET41b plasmids expressing GST-CtIP-479-856-HIS and GST-CtIP 621-856-HIS were from Z. You and T. Hunter. The pCMX-PL2 5' and pCMX-PL2 3' were created by PCR amplification of the Ad5 genome. The 5' probe was amplified from 105-1009 and the 3' probe was from 35357-35836. PCR products were cloned into EcoRI and BamHI sites in pCMX-pL2.

Antibodies. Antibodies were purchased from Santa Cruz (CtIP, Ku70, Ku86, Chk1), Gentex (Rad50), Novus Pharmaceuticals (Nbs1, Nbs1-S343), Cell Signaling (Chk1-S345, Chk2-T68), Epitomics (ATM), Rockland (ATM-S1981), BrdU (Sigma). Anti-pTP was a gift from R. Hay and anti-RPA32 was a gift from T. Melendy. Polyclonal rabbit antisera to DBP was a gift from P. van der Vliet, monoclonal B6 antibody to DBP was from A. Levine, and xCtIP and xNbs1 antibodies were a gift from Z. You. Secondary antibodies were from Invitrogen Molecular Probes (Alexa fluor conjugated) or Jackson Labs (HRP conjugated).

Immunofluorescence and immunoblotting. Cells grown on coverslips were fixed with 4% PFA. Where indicated, cells were pre-extracted for 20 min on

ice by incubation with the solution described in chapter3. Immunoblotting was performed as described in Materials and methods in chapter 2.

Acknowledgments

I would like to thank Zhongsheng You for his guidance, direction and willingness to include me on this project; we collaborated on Figures 4-2C and 4-3. I would also like to thank Z. You and T. Hunter for providing the GFP-CtIP, GFP-CtIP mutant constructs, pET41b CtIP vectors and the vectors used to create the shLuc and shCtIP cell lines. I would also like to thank Brandon Lamarche for helpful discussions relating to this project and for his participation in future studies to understand further the biochemical function of CtIP.

Chapter 5. Discussion

Summary

The cellular DNA damage response (DDR) is a hierarchical response that initiates when DNA damage sensor proteins detect a DNA break, and then activate a signaling cascade that facilitates repair of the DNA break. During infection, the presence of linear dsDNA adenovirus genome in the nucleus results in activation of the DDR. Wild-type adenovirus (Ad5) expresses the E4orf3 and E1b55K/E4orf6 proteins that prevent the detection of the viral genome as cellular DNA breaks. The study of adenovirus infection provides an interesting perspective on the DDR; cells have the DDR and repair pathways to protect the integrity of their genome and the virus counteracts these processes to protect the integrity of its own genome. Our studies have demonstrated that preventing the detection of the viral genome by the DDR machinery is vital to adenovirus, and Ad5 has evolved two mechanisms to prevent the earliest steps of the DDR. The data presented in this thesis demonstrate that proteins involved in the DDR and DNA repair processes impose a barrier to adenovirus infection. Studies to understand the functions of these proteins during adenovirus infection can translate to their function in basic cellular processes.

E4orf3 inhibition of ATR activation

The small viral protein E4orf3 functions redundantly with E1b55K/E4orf6 to inhibit the MRN complex. The fact that the virus has evolved these redundant mechanisms underscores the importance of targeting MRN for the adenovirus lifecycle. While degradation of MRN by E1b55K/E4orf6 inhibits ATM and ATR activation, our results in chapter 2 demonstrate that E4orf3 mislocalization of MRN only prevents ATR activation. E4orf3 can function as efficiently as E1b55K/E4orf6 for rescuing the known defects of an E4-deleted virus (Bridge and Ketner, 1989; Halbert et al., 1985; Stracker et al., 2005). Since E4orf3 inhibits ATR but not ATM activation, inhibiting ATR activation may be more crucial to the adenovirus lifecycle. Consistent with this, we have found that ATR (but not ATM) activation is inhibitory to the accumulation of late proteins during infection (S.S.L. and M.D.W., unpublished) and a recent report demonstrated that adenovirus serotype 12 degrades TopBP1 to inhibit ATR but not ATM signaling (Blackford et al., 2010).

Our studies on E4orf3 raise the question of how mislocalization of MRN inhibits ATR activation. Our experiments demonstrate that MRN is required for ATR activation independently of the activation of ATM during infection. This is distinct from reports suggesting that MRN is only required to activate ATM, and activated ATM subsequently activates ATR after γIR (Jazayeri et al., 2006; Yoo et al., 2009). E4orf3 expression does not prevent recruitment of

ATR/ATRIP/TopBP1/RPA to viral centers, suggesting that the MRN complex activates ATR at a step downstream of recruitment. It has been reported that after γIR, Nbs1 recruits ATM and TopBP1 bringing them in close proximity to promote phosphorylation of TopBP1, which in turn co-activates ATR (Yoo et al., 2009). Our data raise the possibility that physical separation of Nbs1 (in E4orf3 tracks) and TopBP1 (at replication centers) prevents ATM-mediated activation of ATR by phosphorylation of TopBP1. Our results in chapter 2 demonstrate that the nuclease activity of Mre11 is not required for adenovirus-induced activation of ATR. However, in chapter 4 we demonstrate that knockdown of CtIP abrogates ATR during *dl*1004 infection. These two pieces of data have led us to hypothesize that MRN recruitment of CtIP to virus replication centers is required for ATR activation. In an alternate model, the viral ssDNA binding protein DBP could compete with RPA for ssDNA binding at sites of replication. If MRN/CtIP could function to bias RPA coating of ssDNA this would also promote ATR activation. Recently, *S. cerevisiae* RPA was found to promote resection by interactions with the DNA2 nuclease and Sgs1 helicase, suggesting RPA itself may function to promote resection of DNA (Cejka et al., 2010; Niu et al., 2010). While human RPA was not demonstrated to work similarly as the yeast RPA (Niu et al., 2010), this does suggest that proteins not previously characterized for promotion of resection and ATR activation are still being identified. Our results in chapters 2 and 4 suggest that there is more to ATR activation beyond ATRIP/TopBP1/RPA.

Future studies include determining which domain of CtIP is required to promote activation of ATR, if the MRN complex activates ATR by interaction with CtIP, and why recruitment of the reported ATR activators is not sufficient for ATR activation. These studies will provide a greater understanding of ATR activation in the context of cellular damage and adenovirus infection. The evolution of adenovirus proteins to target specific steps of the DDR provides us with a unique system to dissect the activation of ATM and ATR pathways independently of one another.

Cellular requirements for concatemer formation

Over 15 years ago, the observation that E4 deleted adenovirus was ligated into concatemers during infection (Weiden and Ginsberg, 1994), suggested that DNA damage proteins could recognize viral genomes and opened an area of research to determine which cellular proteins were involved. For Adenovirus, we propose that there is a three-step mechanism in concatemer formation: removal of the TP, activation of a damage response, and ligation of the genome ends. The work in this thesis suggests that removal of the TP requires MRN and CtIP, and previous work suggests that NHEJ machinery including DNA-PKcs (Boyer et al., 1999), DNA Ligase IV (Stracker et al., 2002) and XLF (**Appendix Fig. 5**) are required for ligation of viral genomes. The questions that remain are i) what enzymatic functions of CtIP/MRN are required for TP removal and are more proteins involved, and ii)

how does the activation of ATM, ATR and DNA-Pkcs promote the transition from TP removal to end joining.

The *in vitro* assays conducted in *Xenopus* extracts (chapter 4), identified CtIP as being required for *in vitro* concatemer formation, and confirmed the function of Nbs1 in concatemer formation. Since CtIP and Nbs1 also inhibit *dl*1004 replication (chapter 4, and (Lakdawala et al., 2008)), perhaps the initiation of virus replication is hampered by the removal of the TP. The major caveat to these studies is the discrepancy for the requirement of CtIP *in vitro* versus *in vivo*. Studies in the *Xenopus* extracts could be more sensitive as there is a defined amount of substrate and no viral replication. However, in the absence of CtIP, the TP still needs to be removed for concatemer formation to occur during infection. An unidentified protein that removes the TP itself or promotes MRN function in this process could be responsible for this step in concatemer formation. Currently, the same proteins required to inhibit viral replication are also implicated to promote concatemerization *in vitro*. Future studies to determine if other proteins are required for TP removal could be discovered by screening concatemer formation in the *Xenopus* extract system or by assaying the replication of *dl*1004 in cells deficient for candidate proteins. Our system provides a unique way to assay the requirements for removal of proteins bound to DNA ends by using a naturally occurring viral substrate as opposed to an engineered one. Future studies to test if purified CtIP can function endonucleolytically to

remove the TP from the genome would have implications for CtIP in the removal of Spo11 during meiosis.

Another question raised by recent publications and the work presented in this thesis is if MRN/CtIP are required for TP removal, and the NHEJ machinery is required for joining, which proteins are required for the steps in-between? Dual inhibition of the ATM and ATR signaling pathways inhibits concatemer formation (Lakdawala et al., 2008). Our results in chapter 2 demonstrate that E4orf3 can prevent concatemers even though there is robust ATM signaling during *dl*1004 infection. These data suggest that ATM signaling is not sufficient for concatemer formation. E4orf3 also mislocalizes PML (Carvalho et al., 1995; Doucas et al., 1996), but we established that inhibition of concatemers was not due to E4orf3 mislocalization of PML or due to a requirement for PML in E4orf3 track formation (chapter 2 and **Appendix Fig. 8**). Although we cannot rule out that another protein targeted by wild-type E4orf3 but not by the I104R mutation plays a role in concatemer formation, this discussion will focus on the functions of the MRN complex members in concatemer formation. Both the nuclease activity of Mre11, and the presence of the C-terminus of Nbs1 (containing the ATM and Mre11 interaction domains) are required for concatemer formation (Lakdawala et al., 2008; Stracker et al., 2002). We observed that NBS cell lines complemented with an Mre11-NLS that localizes MR to the nucleus did not form concatemers (**Appendix Fig. 9**), demonstrating that Nbs1 has additional requirements

beyond relocalization of Mre11 to the nucleus. Cells deficient for ATM also form concatemers, suggesting that Nbs1 activation of ATM is also not sufficient. Nbs1 interaction with CtIP is not the missing link as concatemers form in the absence of CtIP, and the Nbs1-CtIP interaction is mediated through the N-terminus and not the C-terminus of Nbs1 (Lloyd et al., 2009; Williams et al., 2009a). Based on these reports and on our results from chapter 2 and 4, we can develop two hypotheses for the role of ATR activation in concatemerization based on the status of CtIP. In the presence of CtIP, CtIP/MRN mediated activation of ATM and ATR promotes concatemer formation through a DNA-PK dependent mechanism. In the absence of CtIP, hyper activation of ATM and DNK-PKcs promotes concatemer formation by compensating for the decrease in ATR activation. While these models remain to be tested, they suggest an explanation for the requirement of the PIKKs and for the discrepancies between the roles CtIP plays in concatemer formation. The ability of the adenovirus system to tease apart activation of the ATR and ATM responses and specifically inhibit proteins involved in these pathways may provide information on how this intricate pathway between resection and end joining is regulated.

Localization of cellular damage proteins during wild-type infection

In the context of a wildtype virus infection, we also observed interesting localization phenotypes of several cellular proteins. During Ad5 infection, the foci formed by CtIP, BLM and WRN (**Appendix Fig. 6**), were adjacent to sites

of viral replication. It has also been suggested that CtIP can function in transcriptional regulation (Liu and Lee, 2006; Meloni et al., 1999; Yu et al., 1998), and it is has been reported that knocking down CtIP leads to a slight decrease in wild-type Ad5 viral replication by inhibition of transcription (Bruton et al., 2007). The dual roles of CtIP as a transcriptional repressor and a DNA processing protein have not been clarified by the recent studies on CtIP function in resection. In chapter 3, we show that BLM localizes to foci at viral centers during wild-type Ad5 infection (prior to degradation) and throughout *dl*1004 infection. WRN re-localization to foci at replication centers occurs during wild-type Ad5 infection, but not during *dl*1004 infection (**Appendix Fig. 6**). It is interesting to consider whether WRN could be actively recruited during Ad5 infection for a function beneficial to the viral lifecycle. The recruitment of WRN and CtIP to adenovirus replication centers during wild-type viral replication, suggests that their functions could be beneficial to infection although this has not yet been shown. Study of the recruitment of the proteins during a wild-type adenovirus infection may uncover new roles for CtIP, BLM and WRN that could apply to their role in a non-viral context, separate from their functions in end processing.

Final conclusions

The data presented in this thesis provide new mechanistic insights into the roles of the MRN complex in activation of damage signaling and concatemer formation. Since CtIP and MRN are both implicated in TP

removal, suggesting they can play a role in removal of proteins covalently attached to the 5’ ends of DNA. CtIP and MRN are suggested to play a role in Spo11 removal during meiotic recombination, if we demonstrated that they could enzymatically function to remove the TP, it would strengthen the implication for these proteins functions in meiosis. Perhaps the most interesting observation is the identification of BLM as a novel target for degradation by E1b55K/E4orf6. BLM is implicated in end processing and in suppression of hyper-recombination. It is exciting to imagine that BLM is targeted by adenovirus to promote hyper-recombination between co-infected virus serotypes. Future studies to understand why adenovirus targets BLM for degradation may find a role for BLM in the processing of replication intermediates or in suppression of viral recombination. The idea that DNA processing proteins play a role during adenovirus infection separate from concatemerization may expand the use of adenovirus as a model system to study transcriptional repression, recombination and processing of secondary DNA structures.

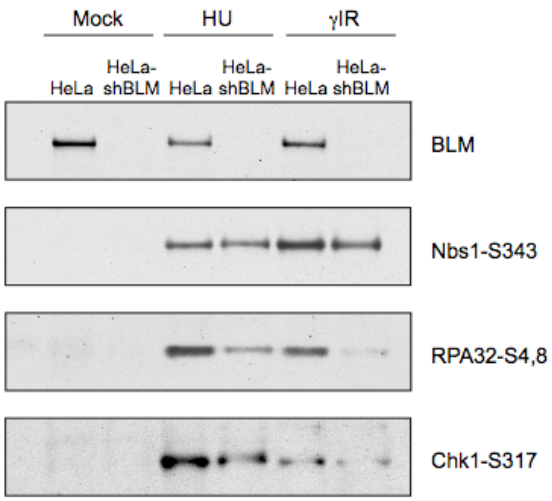

Figure A-1. Knockdown of BLM by shRNA. BLM levels are undetectable after retroviral transformation with shBLM. HeLa cells were transformed with a retrovirus expressing shRNA to BLM. Cells were treated with 2 mM HU for 2 h, or with 10gy γIR and harvested after 2 h. Lysates were analyzed on SDS-PAGE y immunoblotting with the indicated antibodies.

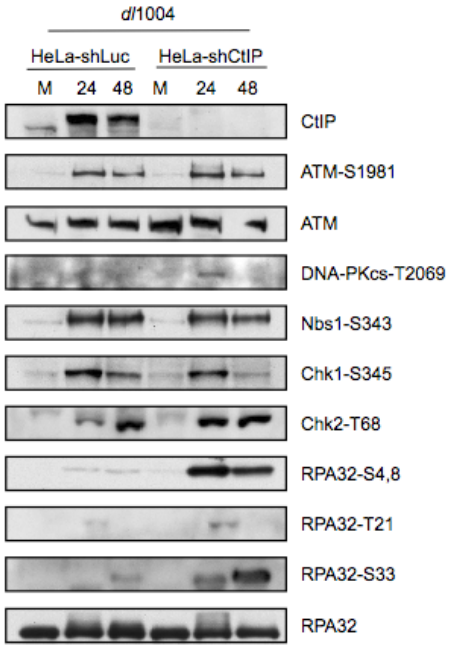

Figure A-2. Knocking down CtIP by shRNA alters phosphorylation of specific PIKK targets. HeLa cells retrovirally transformed to express shRNA against luciferase (control) or CtIP were either uninfected (M) or infected with *dl*1004 and harvested at 24 or 48 hpi. CtIP is knocked down efficiently as levels of CtIP are not detected in the shCtIP lanes. Phospho-specific antibodies detect increase in phosphorylation in the HeLa-shCtIP cells over the control for DNA-PKcs-T2069, Chk2-T68, RPA32-S4,8, and RPA32-S33. Phospho-specific antibodies detect a decrease in Chk1-S345 in the HeLa-shCtIP lanes.

Figure A-3. Expression of GFP-CtIP during infection prevents RPA32-S4,8 phosphorylation at sites of viral replication. (A) HeLa cells were transfected with GFP-CtIP and infected with *dl*1004 (MOI of 25) and harvested at 24 hpi. Immunostaining was performed for RPA32 or RPA32-S4,8. DAPI staining in the merged image represents nuclei. (B) Cells were transfected and infected as above. Immunostaining was performed with RPA32 and three different phospho-specific antibodies. RPA staining is represented in yellow to show sites of replication.

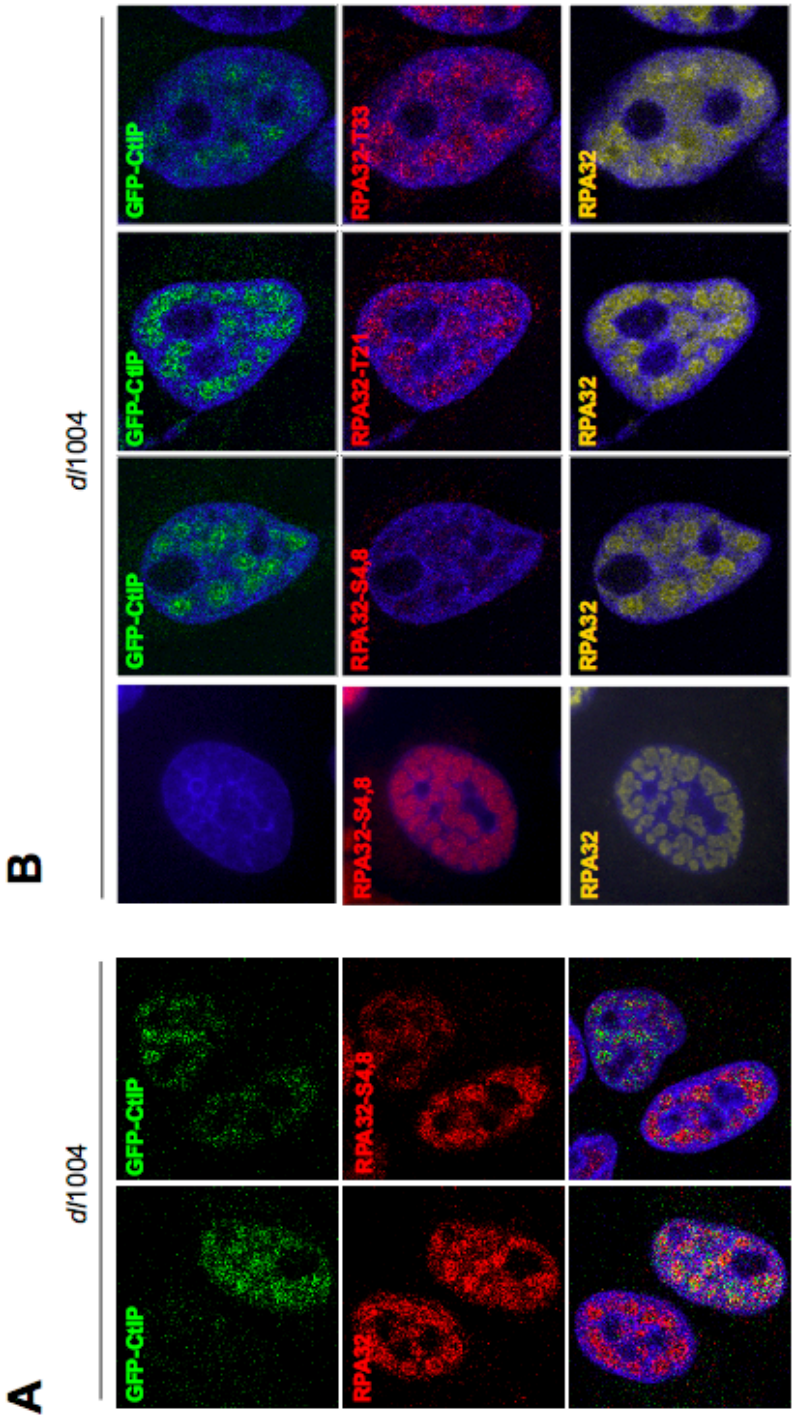
A
dl1004
GFP-CtIP
RPA32
GFP-CtIP
RPA32-S4,8
B
dl1004
GFP-CtIP
RPA32-S4,8
GFP-CtIP
RPA32-T21
GFP-CtIP
RPA32-T33
RPA32
RPA32
RPA32

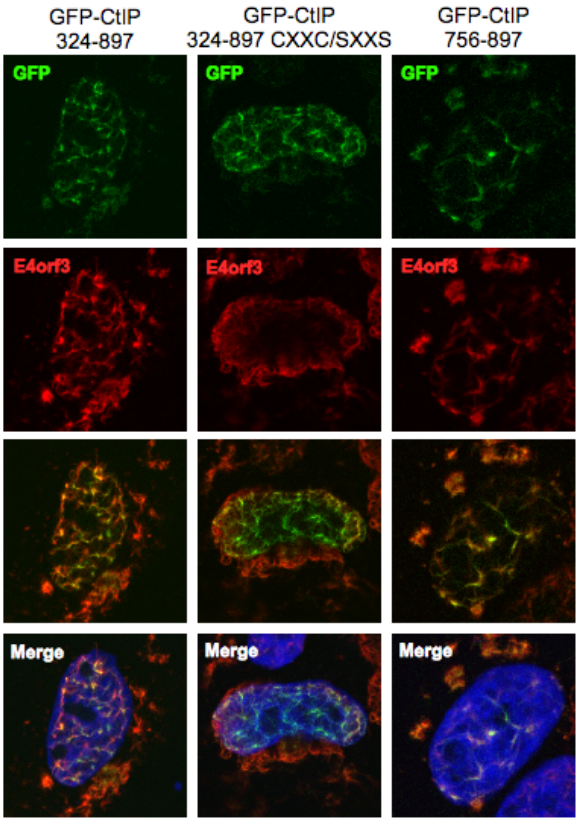

Figure A-4. Localization of GFP-CtIP and E4orf3. HeLa cells were transfected with GPF-CtIP mutants that localized to track like structures during infection (Table 4-1) and a vector expressing Ad5-E4orf3 in a 1:1 ratio. Immunofluorescence was performed for E4orf3. DAPI staining represents the nuclei in the merged images.

Figure A-5. XLF is required for concatemer formation during *dl*1004 infection. HCT116 cells engineered using rAAV gene targeting to reduce expression of XLF or DNA Ligase IV (Fattah et al., 2010; Ruis et al., 2008). HCT116 cells represent the control cell line. Cells were uninfected or infected with Ad5 or *dl*1004. Cells were harvested at 48 hpi and split to determine protein levels by immunoblotting or viral DNA by PFGE. Immunoblotting with the indicated antibodies represents the levels of XLF and DNA Ligase IV.

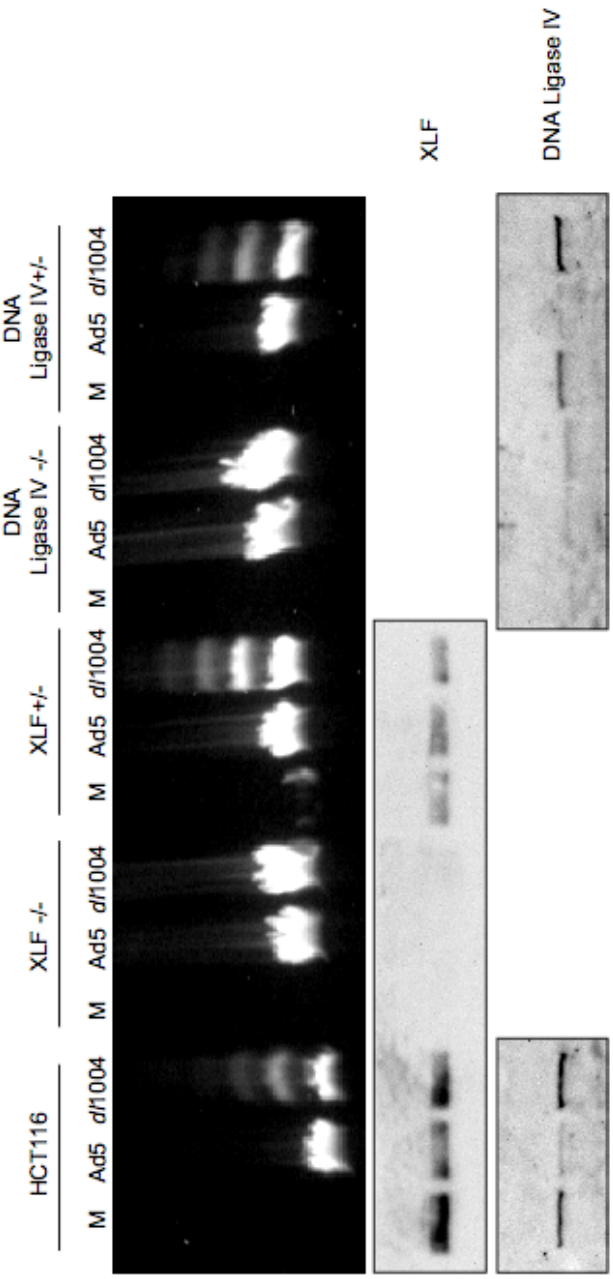
HCT116
XLF -/-
XLF+/-
DNA Ligase IV -/-
DNA Ligase IV+/-
M
Ad5
dl1004
XLF
DNA Ligase IV

Figure A-6. Analysis of WRN levels and localization during infection. (A) Addition of proteasome inhibitors does not increase levels of WRN during Ad5 infection. HeLa cells were uninfected or infected with wild-type Ad5 (MOI of 10) or *dl*1004 (MOI of 25). At 12 hpi epoxomicin and MG132 were added to the cells (+). Cells were harvested 24 hpi. Lysates were analyzed on SDS-PAGE by immunoblotting with the indicated antibodies. Ku86 served as a loading control. (B) HeLa cells were uninfected of infected with Ad5 or *dl*1004. Cells were fixed 24 hpi and immunofluorescence was performed for antibodies to WRN and DBP. WRN is localized to Ad5 replication centers, but not during infection during *di*1004. DAPI staining in the merge images represents the nuclei.

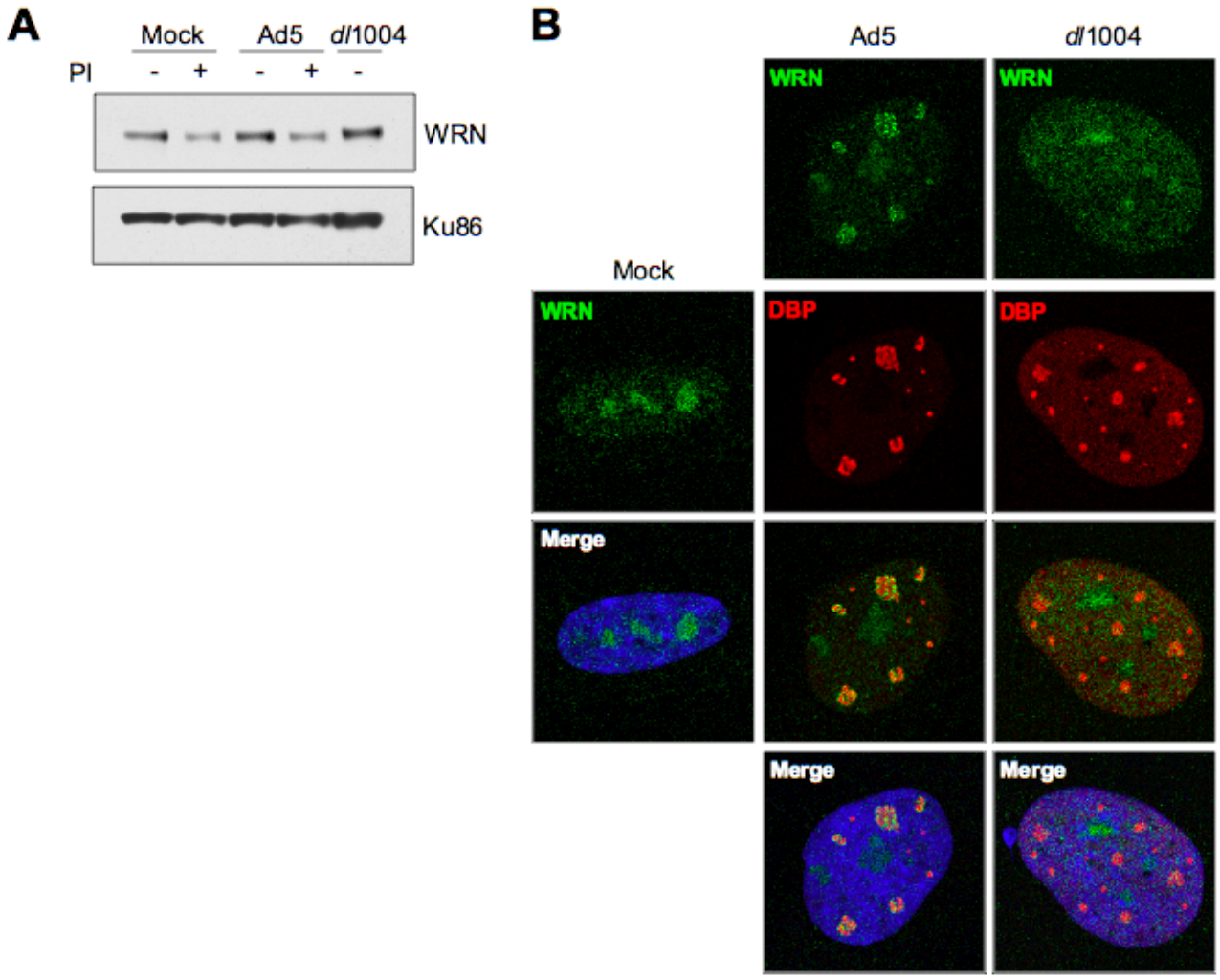
A
Mock
Ad5
dl1004
PI
- + - + -
WRN
Ku86
B
Ad5
dl1004
WRN
WRN
Mock
WRN
DBP
DBP
Merge
Merge
Merge

Figure A-7. BLM localization in primary cell lines during infection. IMR90 cells, cells lines derived from patients with Blooms syndrome (BS) or cells lines derived from patients with Werner syndrome (WS) were infected with Ad5 of *dl*1004 and fixed 48 hpi. Immunofluorescence was performed using antibodies to BLM and DBP. DAPI stain represents the nuclei in the merged images.

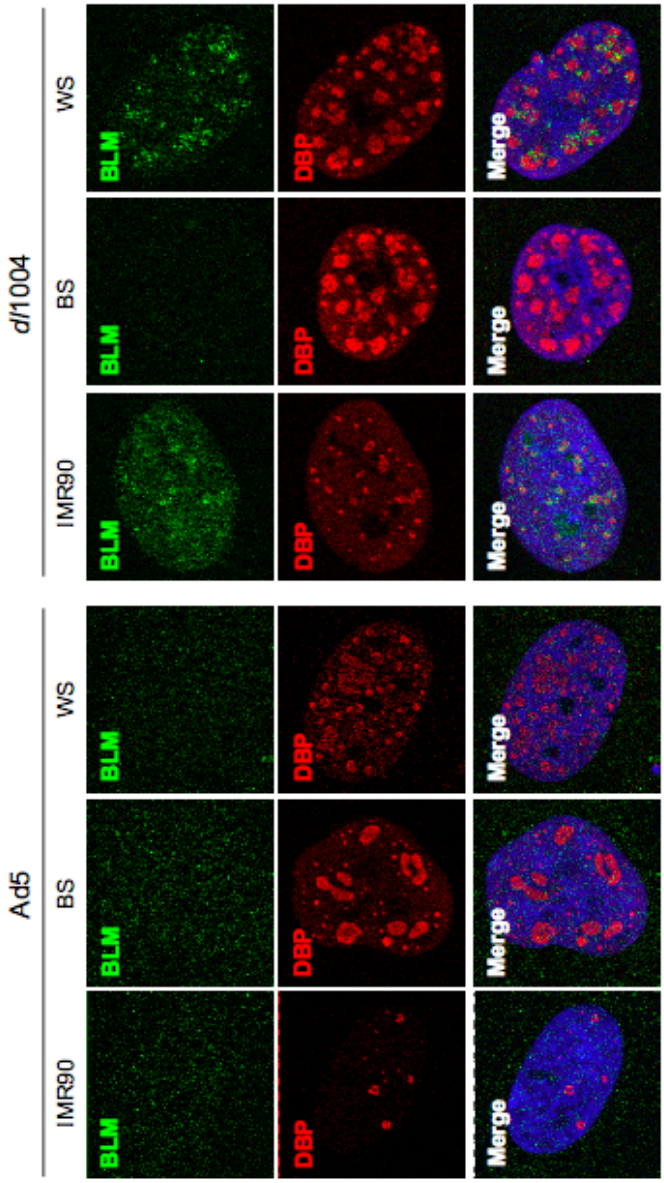
Ad5
d/1004
IMR90
BS
WS
IMR90
BS
WS
BLM
DBP
Merge

Figure A-8. E4orf3 mislocalization of PML is not required for formation of E4orf3 tracks or inhibition of concatemer formation. (A) PML is not required for E4orf3 track formation. HFF cells retrovirally transformed to express an shRNA to Luciferase (control) or PML were infected with *dl*1017 virus. Cells were fixed after 48 hpi and immunofluorescence was performed for PML and E4orf3. DAPI staining in the merged panel represents the nucleus. (B) SUMO1 still localizes to E4orf3 tracks in the absence of PML. HFF-shLuc and HFF shPML cells were infected and fixed as above. Immunofluorescence was performed for an antibody to SUMO1. (C) In the absence of PML, concatemers are still formed during *dl*1004 infection. HFF-shLuc and HFF_shPML cells were infected with Ad5 or *dl*1004 and harvest 96 hpi for analysis by PFGE. Infection with *dl*1004 still produces concatemers in the HFF-shPML cells. (D) Replication of *dl*1004 is increased in the absence of PML. HFF-shLuc and HFF-shPML cells were infected with *dl*1004 and harvested at 4, 48 and 96 hpi. DNA was extracted from cells and viral genomes were quantified by qPCR. The bars represent fold change of the genomes at the indicated times over the input viral genomes.

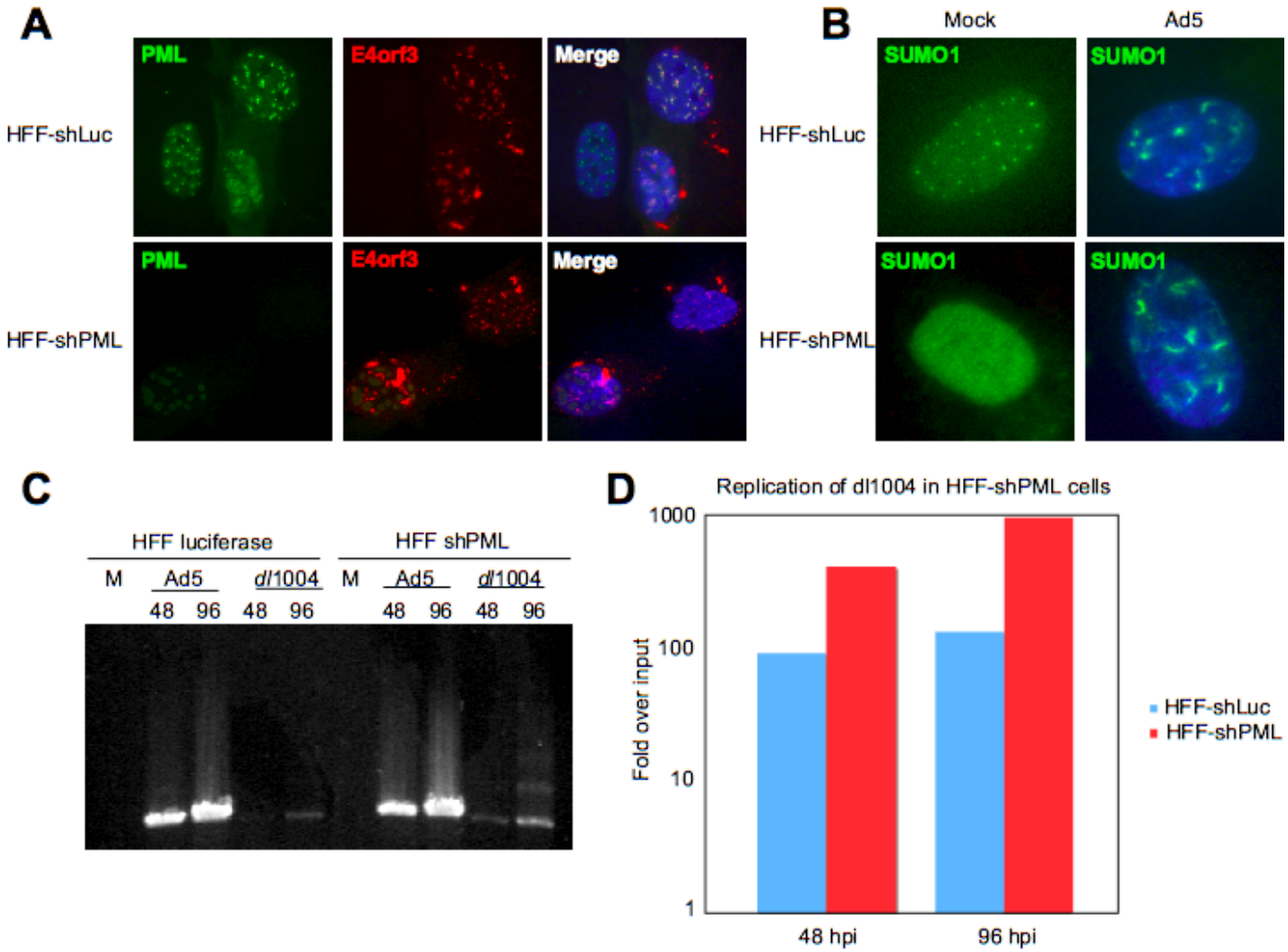
A
PML
E4orf3
Merge
HFF-shLuc
HFF-shPML
B
Mock
Ad5
SUMO1
HFF-shLuc
HFF-shPML
C
HFF luciferase
HFF shPML
M
Ad5
dl1004
48
96
D
Replication of dl1004 in HFF-shPML cells
Fold over input
1000
100
10
1
48 hpi
96 hpi
HFF-shLuc
HFF-shPML

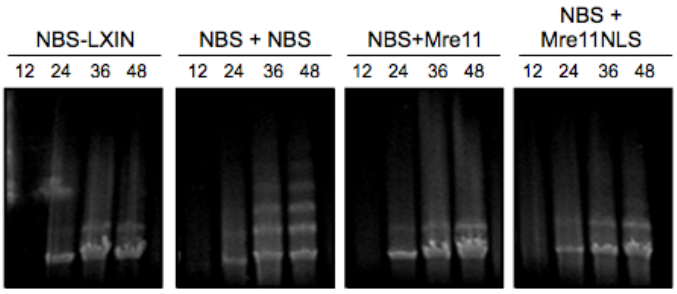

Figure A-9. Re-localization of Mre11 to the nucleus in NBS hypomorphic cells is not sufficient for concatemer formation. NBS hypomorphic complemented with an empty vector (LXIN), wild-type Nbs1 (Nbs1), wild-type Mre11 (Mre11) or an Mre11 engineered to express an NLS (Mre11-NLS) were infected with *dl*1004 and harvested over regular intervals over a 48h time course. Cells were prepared for analysis by PFGE. NBS+Nbs1 cells supported the formation of concatemers, however the Mre11-NLS cells did not.

References

Ababou, M., Dutertre, S., Lécluse, Y., Onclercq, R., Chatton, B., and Amor-Guéret, M. (2000). ATM-dependent phosphorylation and accumulation of endogenous BLM protein in response to ionizing radiation. Oncogene *19*, 5955-5963.

Adams, K. E., Medhurst, A. L., Dart, D. A., and Lakin, N. D. (2006). Recruitment of ATR to sites of ionising radiation-induced DNA damage requires ATM and components of the MRN protein complex. Oncogene *25*, 3894-3904.

Ajimura, M., Leem, S. H., and Ogawa, H. (1993). Identification of new genes required for meiotic recombination in Saccharomyces cerevisiae. Genetics *133*, 51-66.

Alani, E., Padmore, R., and Kleckner, N. (1990). Analysis of wild-type and rad50 mutants of yeast suggests an intimate relationship between meiotic chromosome synapsis and recombination. Cell *61*, 419-436.

Anderson, D. E., Trujillo, K. M., Sung, P., and Erickson, H. P. (2001). Structure of the Rad50 x Mre11 DNA repair complex from Saccharomyces cerevisiae by electron microscopy. J Biol Chem *276*, 37027-37033.

Araujo, F. D., Stracker, T. H., Carson, C. T., Lee, D. V., and Weitzman, M. D. (2005). Adenovirus type 5 E4orf3 protein targets the Mre11 complex to cytoplasmic aggresomes. J Virol *79*, 11382-11391.

Arias, E. E., and Walter, J. C. (2007). Strength in numbers: preventing rereplication via multiple mechanisms in eukaryotic cells. Genes Dev *21*, 497-518.

Babiss, L. E., and Ginsberg, H. S. (1984). Adenovirus type 5 early region 1b gene product is required for efficient shutoff of host protein synthesis. J Virol *50*, 202-212.

Bachenheimer, S., and Darnell, J. E. (1975). Adenovirus-2 mRNA is transcribed as part of a high-molecular-weight precursor RNA. Proc Natl Acad Sci U S A *72*, 4445-4449.

Baker, A., Rohleder, K. J., Hanakahi, L. A., and Ketner, G. (2007). Adenovirus E4 34k and E1b 55k oncoproteins target host DNA ligase IV for proteasomal degradation. J Virol *81*, 7034-7040.

Bakkenist, C. J., and Kastan, M. B. (2003). DNA damage activates ATM through intermolecular autophosphorylation and dimer dissociation. Nature *421*, 499-506.

Barlow, C., Hirotsune, S., Paylor, R., Liyanage, M., Eckhaus, M., Collins, F., Shiloh, Y., Crawley, J. N., Ried, T., Tagle, D., and Wynshaw-Boris, A. (1996). Atm-deficient mice: a paradigm of ataxia telangiectasia. Cell *86*, 159-171.

Bartek, J., and Lukas, J. (2007). DNA damage checkpoints: from initiation to recovery or adaptation. Curr Opin Cell Biol *19*, 238-245.

Beamish, H., Kedar, P., Kaneko, H., Chen, P., Fukao, T., Peng, C., Beresten, S., Gueven, N., Purdie, D., Lees-Miller, S.*, et al.* (2002). Functional link between BLM defective in Bloom's syndrome and the ataxia-telangiectasia-mutated protein, ATM. J Biol Chem *277*, 30515-30523.

Berget, S. M., Moore, C., and Sharp, P. A. (1977). Spliced segments at the 5' terminus of adenovirus 2 late mRNA. Proc Natl Acad Sci U S A *74*, 3171-3175.

Berk, A. J. (2005). Recent lessons in gene expression, cell cycle control, and cell biology from adenovirus. Oncogene *24*, 7673-7685.

Berk, A. J. (2007). Adenoviridae: The Viruses and Their Replication. In Fields Virology, 5th Edition, DM Knipe, PM Howeley *2*, pp. 2355-2394.

Berk, A. J., and Sharp, P. A. (1978). Structure of the adenovirus 2 early mRNAs. Cell *14*, 695-711.

Bhaskara, V., Dupré, A., Lengsfeld, B., Hopkins, B. B., Chan, A., Lee, J.-H., Zhang, X., Gautier, J., Zakian, V., and Paull, T. T. (2007). Rad50 adenylate kinase activity regulates DNA tethering by Mre11/Rad50 complexes. Molecular Cell *25*, 647-661.

Blackford, A. N., Bruton, R. K., Dirlik, O., Stewart, G. S., Taylor, A. M., Dobner, T., Grand, R. J., and Turnell, A. S. (2008). A role for E1B-AP5 in ATR signaling pathways during adenovirus infection. J Virol *82*, 7640-7652.

Blackford, A. N., Patel, R. N., Forrester, N. A., Theil, K., Groitl, P., Stewart, G. S., Taylor, A. M., Morgan, I. M., Dobner, T., Grand, R. J., and Turnell, A. S. (2010). Adenovirus 12 E4orf6 inhibits ATR activation by promoting TOPBP1 degradation. Proc Natl Acad Sci U S A *107*, 12251-12256.

Bohr, V. A. (2008). Rising from the RecQ-age: the role of human RecQ helicases in genome maintenance. Trends Biochem Sci *33*, 609-620.

Boivin, D., Morrison, M. R., Marcellus, R. C., Querido, E., and Branton, P. E. (1999). Analysis of synthesis, stability, phosphorylation, and interacting polypeptides of the 34-kilodalton product of open reading frame 6 of the early region 4 protein of human adenovirus type 5. J Virol *73*, 1245-1253.

Boubnov, N. V., and Weaver, D. T. (1995). scid cells are deficient in Ku and replication protein A phosphorylation by the DNA-dependent protein kinase. Mol Cell Biol *15*, 5700-5706.

Boyer, J., Rohleder, K., and Ketner, G. (1999). Adenovirus E4 34k and E4 11k inhibit double strand break repair and are physically associated with the cellular DNA-dependent protein kinase. Virology *263*, 307-312.

Branzei, D., and Foiani, M. (2008). Regulation of DNA repair throughout the cell cycle. Nat Rev Mol Cell Biol *9*, 297-308.

Bridge, E., and Ketner, G. (1989). Redundant control of adenovirus late gene expression by early region 4. J Virol *63*, 631-638.

Bridge, E., and Ketner, G. (1990). Interaction of adenoviral E4 and E1b products in late gene expression. Virology *174*, 345-353.

Bridge, E., Medghalchi, S., Ubol, S., Leesong, M., and Ketner, G. (1993). Adenovirus early region 4 and viral DNA synthesis. Virology *193*, 794-801.

Brown, E. J., and Baltimore, D. (2000). ATR disruption leads to chromosomal fragmentation and early embryonic lethality. Genes Dev *14*, 397-402.

Brush, G. S., Anderson, C. W., and Kelly, T. J. (1994). The DNA-activated protein kinase is required for the phosphorylation of replication protein A during simian virus 40 DNA replication. Proc Natl Acad Sci U S A *91*, 12520-12524.

Bruton, R. K., Rasti, M., Mapp, K. L., Young, N., Carter, R. Z., Abramowicz, I. A., Sedgwick, G. G., Onion, D. F., Shuen, M., Mymryk, J. S.*, et al.* (2007). C-terminal-binding protein interacting protein binds directly to adenovirus early region 1A through its N-terminal region and conserved region 3. Oncogene *26*, 7467-7479.

Budd, M. E., and Campbell, J. L. (2009). Interplay of Mre11 nuclease with Dna2 plus Sgs1 in Rad51-dependent recombinational repair. PLoS One *4*, e4267.

Buis, J., Wu, Y., Deng, Y., Leddon, J., Westfield, G., Eckersdorff, M., Sekiguchi, J. M., Chang, S., and Ferguson, D. O. (2008). Mre11 nuclease activity has essential roles in DNA repair and genomic stability distinct from ATM activation. Cell *135*, 85-96.

Burgert, H. G., and Blusch, J. H. (2000). Immunomodulatory functions encoded by the E3 transcription unit of adenoviruses. Virus Genes *21*, 13-25.

Cao, L., Alani, E., and Kleckner, N. (1990). A pathway for generation and processing of double-strand breaks during meiotic recombination in S. cerevisiae. Cell *61*, 1089-1101.

Caporossi, D., and Bacchetti, S. (1990). Definition of adenovirus type 5 functions involved in the induction of chromosomal aberrations in human cells. J Gen Virol *71 (Pt 4)*, 801-808.

Carney, J. P., Maser, R. S., Olivares, H., Davis, E. M., Le Beau, M., Yates, J. R., 3rd, Hays, L., Morgan, W. F., and Petrini, J. H. (1998). The hMre11/hRad50 protein complex and Nijmegen breakage syndrome: linkage of double-strand break repair to the cellular DNA damage response. Cell *93*, 477-486.

Carson, C. T., Orazio, N. I., Lee, D. V., Suh, J., Bekker-Jensen, S., Araujo, F. D., Lakdawala, S. S., Lilley, C. E., Bartek, J., Lukas, J., and Weitzman, M. D. (2009). Mislocalization of the MRN complex prevents ATR signaling during adenovirus infection. EMBO J *28*, 652-662.

Carson, C. T., Schwartz, R. A., Stracker, T. H., Lilley, C. E., Lee, D. V., and Weitzman, M. D. (2003). The Mre11 complex is required for ATM activation and the G2/M checkpoint. EMBO J *22*, 6610-6620.

Carvalho, T., Seeler, J. S., Ohman, K., Jordan, P., Pettersson, U., Akusjärvi, G., Carmo-Fonseca, M., and Dejean, A. (1995). Targeting of adenovirus E1A and E4-ORF3 proteins to nuclear matrix-associated PML bodies. J Cell Biol *131*, 45-56.

Cathomen, T., and Weitzman, M. D. (2000). A functional complex of adenovirus proteins E1B-55kDa and E4orf6 is necessary to modulate the expression level of p53 but not its transcriptional activity. J Virol *74*, 11407-11412.

Cejka, P., Cannavo, E., Polaczek, P., Masuda-Sasa, T., Pokharel, S., Campbell, J. L., and Kowalczykowski, S. C. (2010). DNA end resection by Dna2-Sgs1-RPA and its stimulation by Top3-Rmi1 and Mre11-Rad50-Xrs2. Nature *467*, 112-116.

Cerosaletti, K. M., and Concannon, P. (2003). Nibrin forkhead-associated domain and breast cancer C-terminal domain are both required for nuclear focus formation and phosphorylation. J Biol Chem *278*, 21944-21951.

Cerosaletti, K. M., Desai-Mehta, A., Yeo, T. C., Kraakman-Van Der Zwet, M., Zdzienicka, M. Z., and Concannon, P. (2000). Retroviral expression of the NBS1 gene in cultured Nijmegen breakage syndrome cells restores normal radiation sensitivity and nuclear focus formation. Mutagenesis *15*, 281-286.

Chaganti, R. S., Schonberg, S., and German, J. (1974). A manyfold increase in sister chromatid exchanges in Bloom's syndrome lymphocytes. Proc Natl Acad Sci U S A *71*, 4508-4512.

Challberg, M. D., Desiderio, S. V., and Kelly, T. J., Jr. (1980). Adenovirus DNA replication in vitro: characterization of a protein covalently linked to nascent DNA strands. Proc Natl Acad Sci U S A *77*, 5105-5109.

Chan, D. W., Chen, B. P., Prithivirajsingh, S., Kurimasa, A., Story, M. D., Qin, J., and Chen, D. J. (2002). Autophosphorylation of the DNA-dependent protein kinase catalytic subunit is required for rejoining of DNA double-strand breaks. Genes Dev *16*, 2333-2338.

Chan, K. L., North, P. S., and Hickson, I. D. (2007). BLM is required for faithful chromosome segregation and its localization defines a class of ultrafine anaphase bridges. Embo J *26*, 3397-3409.

Chan, K. L., Palmai-Pallag, T., Ying, S., and Hickson, I. D. (2009). Replication stress induces sister-chromatid bridging at fragile site loci in mitosis. Nat Cell Biol *11*, 753-760.

Chen, L., Nievera, C. J., Lee, A. Y.-L., and Wu, X. (2008). Cell cycle-dependent complex formation of BRCA1.CtIP.MRN is important for DNA double-strand break repair. J Biol Chem *283*, 7713-7720.

Chen, M., Mermod, N., and Horwitz, M. S. (1990). Protein-protein interactions between adenovirus DNA polymerase and nuclear factor I mediate formation of the DNA replication preinitiation complex. J Biol Chem *265*, 18634-18642.

Chen, P.-L., Liu, F., Cai, S., Lin, X., Li, A., Chen, Y., Gu, B., Lee, E. Y.-H. P., and Lee, W.-H. (2005). Inactivation of CtIP leads to early embryonic lethality mediated by G1 restraint and to tumorigenesis by haploid insufficiency. Mol Cell Biol *25*, 3535-3542.

Chinnadurai, G. (2006). CtIP, a candidate tumor susceptibility gene is a team player with luminaries. Biochim Biophys Acta *1765*, 67-73.

Chow, L. T., and Broker, T. R. (1978). The spliced structures of adenovirus 2 fiber message and the other late mRNAs. Cell *15*, 497-510.

Chu, W. K., and Hickson, I. D. (2009). RecQ helicases: multifunctional genome caretakers. Nat Rev Cancer *9*, 644-654.

Cortez, D., Guntuku, S., Qin, J., and Elledge, S. J. (2001). ATR and ATRIP: partners in checkpoint signaling. Science *294*, 1713-1716.

Cox, B. S., and Parry, J. M. (1968). The isolation, genetics and survival characteristics of ultraviolet light-sensitive mutants in yeast. Mutat Res *6*, 37-55.

D'Amours, D., and Jackson, S. P. (2002). The Mre11 complex: at the crossroads of dna repair and checkpoint signalling. Nat Rev Mol Cell Biol *3*, 317-327.

Dallaire, F., Blanchette, P., Groitl, P., Dobner, T., and Branton, P. E. (2009). Identification of integrin alpha3 as a new substrate of the adenovirus E4orf6/E1B 55-kilodalton E3 ubiquitin ligase complex. J Virol *83*, 5329-5338.

Davalos, A. R., and Campisi, J. (2003). Bloom syndrome cells undergo p53-dependent apoptosis and delayed assembly of BRCA1 and NBS1 repair complexes at stalled replication forks. J Cell Biol *162*, 1197-1209.

Davies, S. L., North, P. S., Dart, A., Lakin, N. D., and Hickson, I. D. (2004). Phosphorylation of the Bloom's syndrome helicase and its role in recovery from S-phase arrest. Mol Cell Biol *24*, 1279-1291.

de Jong, R. N., Meijer, L. A., and van der Vliet, P. C. (2003). DNA binding properties of the adenovirus DNA replication priming protein pTP. Nucleic Acids Res *31*, 3274-3286.

de Klein, A., Muijtjens, M., van Os, R., Verhoeven, Y., Smit, B., Carr, A. M., Lehmann, A. R., and Hoeijmakers, J. H. (2000). Targeted disruption of the cell-cycle checkpoint gene ATR leads to early embryonic lethality in mice. Curr Biol *10*, 479-482.

Deng, Y., Guo, X., Ferguson, D. O., and Chang, S. (2009). Multiple roles for MRE11 at uncapped telomeres. Nature *460*, 914-918.

Desai-Mehta, A., Cerosaletti, K. M., and Concannon, P. (2001). Distinct functional domains of nibrin mediate Mre11 binding, focus formation, and nuclear localization. Mol Cell Biol *21*, 2184-2191.

Desiderio, S. V., and Kelly, T. J., Jr. (1981). Structure of the linkage between adenovirus DNA and the 55,000 molecular weight terminal protein. J Mol Biol *145*, 319-337.

Dickey, J. S., Redon, C. E., Nakamura, A. J., Baird, B. J., Sedelnikova, O. A., and Bonner, W. M. (2009). H2AX: functional roles and potential applications. Chromosoma *118*, 683-692.

Dinkelmann, M., Spehalski, E., Stoneham, T., Buis, J., Wu, Y., Sekiguchi, J. M., and Ferguson, D. O. (2009). Multiple functions of MRN in end-joining pathways during isotype class switching. Nat Struct Mol Biol *16*, 808-813.

Dobbelstein, M., Roth, J., Kimberly, W. T., Levine, A. J., and Shenk, T. (1997). Nuclear export of the E1B 55-kDa and E4 34-kDa adenoviral oncoproteins mediated by a rev-like signal sequence. Embo J *16*, 4276-4284.

Doucas, V., Ishov, A. M., Romo, A., Juguilon, H., Weitzman, M. D., Evans, R. M., and Maul, G. G. (1996). Adenovirus replication is coupled with the dynamic properties of the PML nuclear structure. Genes Dev *10*, 196-207.

Dubin, M. J., Stokes, P. H., Sum, E. Y. M., Williams, R. S., Valova, V. A., Robinson, P. J., Lindeman, G. J., Glover, J. N. M., Visvader, J. E., and Matthews, J. M. (2004). Dimerization of CtIP, a BRCA1- and CtBP-interacting protein, is mediated by an N-terminal coiled-coil motif. J Biol Chem *279*, 26932-26938.

Dunsworth-Browne, M., Schell, R. E., and Berk, A. J. (1980). Adenovirus terminal protein protects single stranded DNA from digestion by a cellular exonuclease. Nucleic Acids Res *8*, 543-554.

Dupré, A., Boyer-Chatenet, L., and Gautier, J. (2006). Two-step activation of ATM by DNA and the Mre11-Rad50-Nbs1 complex. Nat Struct Mol Biol *13*, 451-457.

Dupré, A., Boyer-Chatenet, L., Sattler, R. M., Modi, A. P., Lee, J.-H., Nicolette, M. L., Kopelovich, L., Jasin, M., Baer, R., Paull, T. T., and Gautier, J. (2008). A forward chemical genetic screen reveals an inhibitor of the Mre11-Rad50-Nbs1 complex. Nat Chem Biol *4*, 119-125.

Durocher, D., Henckel, J., Fersht, A. R., and Jackson, S. P. (1999). The FHA domain is a modular phosphopeptide recognition motif. Mol Cell *4*, 387-394.

Durocher, D., Taylor, I. A., Sarbassova, D., Haire, L. F., Westcott, S. L., Jackson, S. P., Smerdon, S. J., and Yaffe, M. B. (2000). The molecular basis of FHA domain:phosphopeptide binding specificity and implications for phospho-dependent signaling mechanisms. Mol Cell *6*, 1169-1182.

Dutertre, S., Ababou, M., Onclercq, R., Delic, J., Chatton, B., Jaulin, C., and Amor-Guéret, M. (2000). Cell cycle regulation of the endogenous wild type Bloom's syndrome DNA helicase. Oncogene *19*, 2731-2738.

Dynan, W. S., and Yoo, S. (1998). Interaction of Ku protein and DNA-dependent protein kinase catalytic subunit with nucleic acids. Nucleic Acids Res *26*, 1551-1559.

Eladad, S., Ye, T.-Z., Hu, P., Leversha, M., Beresten, S., Matunis, M. J., and Ellis, N. A. (2005). Intra-nuclear trafficking of the BLM helicase to DNA damage-induced foci is regulated by SUMO modification. Hum Mol Genet *14*, 1351-1365.

Evans, J. D., and Hearing, P. (2003). Distinct roles of the Adenovirus E4 ORF3 protein in viral DNA replication and inhibition of genome concatenation. J Virol *77*, 5295-5304.

Evans, J. D., and Hearing, P. (2005). Relocalization of the Mre11-Rad50-Nbs1 complex by the adenovirus E4 ORF3 protein is required for viral replication. J Virol *79*, 6207-6215.

Everett, R. D. (2006). Interactions between DNA viruses, ND10 and the DNA damage response. Cell Microbiol *8*, 365-374.

Falck, J., Coates, J., and Jackson, S. P. (2005). Conserved modes of recruitment of ATM, ATR and DNA-PKcs to sites of DNA damage. Nature *434*, 605-611.

Farah, J. A., Cromie, G. A., and Smith, G. R. (2009). Ctp1 and Exonuclease 1, alternative nucleases regulated by the MRN complex, are required for efficient meiotic recombination. Proc Natl Acad Sci USA *106*, 9356-9361.

Fattah, F., Lee, E. H., Weisensel, N., Wang, Y., Lichter, N., and Hendrickson, E. A. (2010). Ku regulates the non-homologous end joining pathway choice of DNA double-strand break repair in human somatic cells. PLoS Genet *6*, e1000855.

Fleisig, H. B., Orazio, N. I., Liang, H., Tyler, A. F., Adams, H. P., Weitzman, M. D., and Nagarajan, L. (2007). Adenoviral E1B55K oncoprotein sequesters candidate leukemia suppressor sequence-specific single-stranded DNA-binding protein 2 into aggresomes. Oncogene *26*, 4797-4805.

Franchitto, A., and Pichierri, P. (2002). Bloom's syndrome protein is required for correct relocalization of RAD50/MRE11/NBS1 complex after replication fork arrest. J Cell Biol *157*, 19-30.

Fusco, C., Reymond, A., and Zervos, A. S. (1998). Molecular cloning and characterization of a novel retinoblastoma-binding protein. Genomics *51*, 351-358.

Garner, E., and Costanzo, V. (2009). Studying the DNA damage response using in vitro model systems. DNA Repair (Amst) *8*, 1025-1037.

German, J., Archibald, R., and Bloom, D. (1965). Chromosomal Breakage in a Rare and Probably Genetically Determined Syndrome of Man. Science *148*, 506-507.

Goodrum, F. D., Shenk, T., and Ornelles, D. A. (1996). Adenovirus early region 4 34-kilodalton protein directs the nuclear localization of the early region 1B 55-kilodalton protein in primate cells. J Virol *70*, 6323-6335.

Graham, F. L., Smiley, J., Russell, W. C., and Nairn, R. (1977). Characteristics of a human cell line transformed by DNA from human adenovirus type 5. J Gen Virol *36*, 59-74.

Graham, F. L., van der Eb, A. J., and Heijneker, H. L. (1974). Size and location of the transforming region in human adenovirus type 5 DNA. Nature *251*, 687-691.

Grand, R. J., Grant, M. L., and Gallimore, P. H. (1994). Enhanced expression of p53 in human cells infected with mutant adenoviruses. Virology *203*, 229-240.

Gravel, S., Chapman, J. R., Magill, C., and Jackson, S. P. (2008). DNA helicases Sgs1 and BLM promote DNA double-strand break resection. Genes Dev *22*, 2767-2772.

Greenberg, R. A., Sobhian, B., Pathania, S., Cantor, S. B., Nakatani, Y., and Livingston, D. M. (2006). Multifactorial contributions to an acute DNA damage response by BRCA1/BARD1-containing complexes. Genes Dev *20*, 34-46.

Halbert, D. N., Cutt, J. R., and Shenk, T. (1985). Adenovirus early region 4 encodes functions required for efficient DNA replication, late gene expression, and host cell shutoff. J Virol *56*, 250-257.

Harada, J. N., Shevchenko, A., Shevchenko, A., Pallas, D. C., and Berk, A. J. (2002). Analysis of the adenovirus E1B-55K-anchored proteome reveals its link to ubiquitination machinery. J Virol *76*, 9194-9206.

Harper, J. W., and Elledge, S. J. (2007). The DNA damage response: ten years after. Mol Cell *28*, 739-745.

Hartsuiker, E., Neale, M. J., and Carr, A. M. (2009). Distinct requirements for the Rad32(Mre11) nuclease and Ctp1(CtIP) in the removal of covalently bound topoisomerase I and II from DNA. Molecular Cell *33*, 117-123.

Hopfner, K. P., Craig, L., Moncalian, G., Zinkel, R. A., Usui, T., Owen, B. A., Karcher, A., Henderson, B., Bodmer, J. L., McMurray, C. T.*, et al.* (2002). The Rad50 zinc-hook is a structure joining Mre11 complexes in DNA recombination and repair. Nature *418*, 562-566.

Hopfner, K. P., Karcher, A., Shin, D. S., Craig, L., Arthur, L. M., Carney, J. P., and Tainer, J. A. (2000). Structural biology of Rad50 ATPase: ATP-driven conformational control in DNA double-strand break repair and the ABC-ATPase superfamily. Cell *101*, 789-800.

Huertas, P., Cortés-Ledesma, F., Sartori, A. A., Aguilera, A., and Jackson, S. P. (2008). CDK targets Sae2 to control DNA-end resection and homologous recombination. Nature *455*, 689-692.

Hurley, P. J., Wilsker, D., and Bunz, F. (2007). Human cancer cells require ATR for cell cycle progression following exposure to ionizing radiation. Oncogene *26*, 2535-2542.

Ishov, A. M., Sotnikov, A. G., Negorev, D., Vladimirova, O. V., Neff, N., Kamitani, T., Yeh, E. T., Strauss, J. F., 3rd, and Maul, G. G. (1999). PML is critical for ND10 formation and recruits the PML-interacting protein daxx to this nuclear structure when modified by SUMO-1. J Cell Biol *147*, 221-234.

Jazayeri, A., Balestrini, A., Garner, E., Haber, J. E., and Costanzo, V. (2008). Mre11-Rad50-Nbs1-dependent processing of DNA breaks generates oligonucleotides that stimulate ATM activity. EMBO J *27*, 1953-1962.

Jazayeri, A., Falck, J., Lukas, C., Bartek, J., Smith, G. C. M., Lukas, J., and Jackson, S. P. (2006). ATM- and cell cycle-dependent regulation of ATR in response to DNA double-strand breaks. Nat Cell Biol *8*, 37-45.

Johnson, F. B., Lombard, D. B., Neff, N. F., Mastrangelo, M. A., Dewolf, W., Ellis, N. A., Marciniak, R. A., Yin, Y., Jaenisch, R., and Guarente, L. (2000). Association of the Bloom syndrome protein with topoisomerase IIIalpha in somatic and meiotic cells. Cancer Res *60*, 1162-1167.

Keeney, S., Giroux, C. N., and Kleckner, N. (1997). Meiosis-specific DNA double-strand breaks are catalyzed by Spo11, a member of a widely conserved protein family. Cell *88*, 375-384.

Keeney, S., and Kleckner, N. (1995). Covalent protein-DNA complexes at the 5' strand termini of meiosis-specific double-strand breaks in yeast. Proc Natl Acad Sci U S A *92*, 11274-11278.

Konig, C., Roth, J., and Dobbelstein, M. (1999). Adenovirus type 5 E4orf3 protein relieves p53 inhibition by E1B-55-kilodalton protein. J Virol *73*, 2253-2262.

Kudoh, A., Fujita, M., Zhang, L., Shirata, N., Daikoku, T., Sugaya, Y., Isomura, H., Nishiyama, Y., and Tsurumi, T. (2005). Epstein-Barr virus lytic replication elicits ATM checkpoint signal transduction while providing an S-phase-like cellular environment. J Biol Chem *280*, 8156-8163.

Kudoh, A., Iwahori, S., Sato, Y., Nakayama, S., Isomura, H., Murata, T., and Tsurumi, T. (2009). Homologous recombinational repair factors are recruited and loaded onto the viral DNA genome in Epstein-Barr virus replication compartments. J Virol *83*, 6641-6651.

Kumagai, A., Lee, J., Yoo, H. Y., and Dunphy, W. G. (2006). TopBP1 activates the ATR-ATRIP complex. Cell *124*, 943-955.

Kusano, K., Berres, M. E., and Engels, W. R. (1999). Evolution of the RECQ family of helicases: A drosophila homolog, Dmblm, is similar to the human bloom syndrome gene. Genetics *151*, 1027-1039.

Lakdawala, S. S., Schwartz, R. A., Ferenchak, K., Carson, C. T., McSharry, B. P., Wilkinson, G. W., and Weitzman, M. D. (2008). Differential requirements of the C terminus of Nbs1 in suppressing adenovirus DNA replication and promoting concatemer formation. J Virol *82*, 8362-8372.

Lavia, P., Mileo, A. M., Giordano, A., and Paggi, M. G. (2003). Emerging roles of DNA tumor viruses in cell proliferation: new insights into genomic instability. Oncogene *22*, 6508-6516.

Lechner, R. L., and Kelly, T. J. (1977). The structure of replicating adenovirus 2 DNA molecules. Cell *12*, 1007-1020.

Lee, A. Y., Liu, E., and Wu, X. (2007). The Mre11/Rad50/Nbs1 complex plays an important role in the prevention of DNA rereplication in mammalian cells. J Biol Chem *282*, 32243-32255.

Lee, J. H., and Paull, T. T. (2004). Direct activation of the ATM protein kinase by the Mre11/Rad50/Nbs1 complex. Science *304*, 93-96.

Lengsfeld, B. M., Rattray, A. J., Bhaskara, V., Ghirlando, R., and Paull, T. T. (2007). Sae2 is an endonuclease that processes hairpin DNA cooperatively with the Mre11/Rad50/Xrs2 complex. Molecular Cell *28*, 638-651.

Li, S., Ting, N. S., Zheng, L., Chen, P. L., Ziv, Y., Shiloh, Y., Lee, E. Y., and Lee, W. H. (2000). Functional link of BRCA1 and ataxia telangiectasia gene product in DNA damage response. Nature *406*, 210-215.

Lieber, M. R. (2008). The mechanism of human nonhomologous DNA end joining. J Biol Chem *283*, 1-5.

Lilley, C. E., Schwartz, R. A., and Weitzman, M. D. (2007). Using or abusing: viruses and the cellular DNA damage response. Trends Microbiol *15*, 119-126.

Limbo, O., Chahwan, C., Yamada, Y., de Bruin, R. A. M., Wittenberg, C., and Russell, P. (2007). Ctp1 is a cell-cycle-regulated protein that functions with Mre11 complex to control double-strand break repair by homologous recombination. Molecular Cell *28*, 134-146.

Lisby, M., Barlow, J. H., Burgess, R. C., and Rothstein, R. (2004). Choreography of the DNA damage response: spatiotemporal relationships among checkpoint and repair proteins. Cell *118*, 699-713.

Liu, F., and Lee, W.-H. (2006). CtIP activates its own and cyclin D1 promoters via the E2F/RB pathway during G1/S progression. Mol Cell Biol *26*, 3124-3134.

Liu, Q., Guntuku, S., Cui, X. S., Matsuoka, S., Cortez, D., Tamai, K., Luo, G., Carattini-Rivera, S., DeMayo, F., Bradley, A.*, et al.* (2000). Chk1 is an essential kinase that is regulated by Atr and required for the G(2)/M DNA damage checkpoint. Genes Dev *14*, 1448-1459.

Liu, Y., Shevchenko, A., Shevchenko, A., and Berk, A. J. (2005). Adenovirus exploits the cellular aggresome response to accelerate inactivation of the MRN complex. J Virol *79*, 14004-14016.

Lloyd, J., Chapman, J. R., Clapperton, J. A., Haire, L. F., Hartsuiker, E., Li, J., Carr, A. M., Jackson, S. P., and Smerdon, S. J. (2009). A supramodular FHA/BRCT-repeat architecture mediates Nbs1 adaptor function in response to DNA damage. Cell *139*, 100-111.

Lukas, C., Falck, J., Bartkova, J., Bartek, J., and Lukas, J. (2003). Distinct spatiotemporal dynamics of mammalian checkpoint regulators induced by DNA damage. Nat Cell Biol *5*, 255-260.

Lukas, C., Melander, F., Stucki, M., Falck, J., Bekker-Jensen, S., Goldberg, M., Lerenthal, Y., Jackson, S. P., Bartek, J., and Lukas, J. (2004). Mdc1 couples DNA double-strand break recognition by Nbs1 with its H2AX-dependent chromatin retention. The EMBO Journal *23*, 2674-2683.

Luo, G., Yao, M. S., Bender, C. F., Mills, M., Bladl, A. R., Bradley, A., and Petrini, J. H. (1999). Disruption of mRad50 causes embryonic stem cell lethality, abnormal embryonic development, and sensitivity to ionizing radiation. Proc Natl Acad Sci U S A *96*, 7376-7381.

Luo, M. H., Rosenke, K., Czornak, K., and Fortunato, E. A. (2007). Human cytomegalovirus disrupts both ataxia telangiectasia mutated protein (ATM)-and ATM-Rad3-related kinase-mediated DNA damage responses during lytic infection. J Virol *81*, 1934-1950.

MacDougall, C. A., Byun, T. S., Van, C., Yee, M. C., and Cimprich, K. A. (2007). The structural determinants of checkpoint activation. Genes Dev *21*, 898-903.

Manfrini, N., Guerini, I., Citterio, A., Lucchini, G., and Longhese, M. P. (2010) Processing of meiotic DNA double strand breaks requires cyclin-dependent kinase and multiple nucleases. J Biol Chem *285*, 11628-11637.

Manthey, K. C., Opiyo, S., Glanzer, J. G., Dimitrova, D., Elliott, J., and Oakley, G. G. (2007). NBS1 mediates ATR-dependent RPA hyperphosphorylation following replication-fork stall and collapse. J Cell Sci *120*, 4221-4229.

Maser, R. S., Monsen, K. J., Nelms, B. E., and Petrini, J. H. (1997). hMre11 and hRad50 nuclear foci are induced during the normal cellular response to DNA double-strand breaks. Mol Cell Biol *17*, 6087-6096.

Mathew, S. S., and Bridge, E. (2007). The cellular Mre11 protein interferes with adenovirus E4 mutant DNA replication. Virology *365*, 346-355.

Mathew, S. S., and Bridge, E. (2008). Nbs1-dependent binding of Mre11 to adenovirus E4 mutant viral DNA is important for inhibiting DNA replication. Virology *374*, 11-22.

Matsuoka, S., Ballif, B. A., Smogorzewska, A., McDonald, E. R., 3rd, Hurov, K. E., Luo, J., Bakalarski, C. E., Zhao, Z., Solimini, N., Lerenthal, Y.*, et al.* (2007). ATM and ATR substrate analysis reveals extensive protein networks responsive to DNA damage. Science *316*, 1160-1166.

Matsuoka, S., Huang, M., and Elledge, S. J. (1998). Linkage of ATM to cell cycle regulation by the Chk2 protein kinase. Science *282*, 1893-1897.

Matsuoka, S., Rotman, G., Ogawa, A., Shiloh, Y., Tamai, K., and Elledge, S. J. (2000). Ataxia telangiectasia-mutated phosphorylates Chk2 in vivo and in vitro. Proc Natl Acad Sci U S A *97*, 10389-10394.

McKee, A. H., and Kleckner, N. (1997). A general method for identifying recessive diploid-specific mutations in Saccharomyces cerevisiae, its

application to the isolation of mutants blocked at intermediate stages of meiotic prophase and characterization of a new gene SAE2. Genetics *146*, 797-816.

Meloni, A. R., Smith, E. J., and Nevins, J. R. (1999). A mechanism for Rb/p130-mediated transcription repression involving recruitment of the CtBP corepressor. Proc Natl Acad Sci U S A *96*, 9574-9579.

Mimitou, E. P., and Symington, L. S. (2008). Sae2, Exo1 and Sgs1 collaborate in DNA double-strand break processing. Nature *455*, 770-774.

Mimitou, E. P., and Symington, L. S. (2009a). DNA end resection: many nucleases make light work. DNA Repair *8*, 983-995.

Mirzoeva, O. K., and Petrini, J. H. (2001). DNA damage-dependent nuclear dynamics of the Mre11 complex. Mol Cell Biol *21*, 281-288.

Moore, M., Horikoshi, N., and Shenk, T. (1996). Oncogenic potential of the adenovirus E4orf6 protein. Proc Natl Acad Sci U S A *93*, 11295-11301.

Mordes, D. A., Glick, G. G., Zhao, R., and Cortez, D. (2008). TopBP1 activates ATR through ATRIP and a PIKK regulatory domain. Genes & Development *22*, 1478-1489.

Myers, J. S., and Cortez, D. (2006). Rapid activation of ATR by ionizing radiation requires ATM and Mre11. J Biol Chem *281*, 9346-9350.

Naim, V., and Rosselli, F. (2009). The FANC pathway and BLM collaborate during mitosis to prevent micro-nucleation and chromosome abnormalities. Nat Cell Biol *11*, 761-768.

Nakamura, K., Kogame, T., Oshiumi, H., Shinohara, A., Sumitomo, Y., Agama, K., Pommier, Y., Tsutsui, K. M., Tsutsui, K., Hartsuiker, E.*, et al.* (2010). Collaborative action of Brca1 and CtIP in elimination of covalent modifications from double-strand breaks to facilitate subsequent break repair. PLoS Genet *6*, e1000828.

Namiki, Y., and Zou, L. (2006). ATRIP associates with replication protein A-coated ssDNA through multiple interactions. Proc Natl Acad Sci U S A *103*, 580-585.

Neale, M. J., Pan, J., and Keeney, S. (2005). Endonucleolytic processing of covalent protein-linked DNA double-strand breaks. Nature *436*, 1053-1057.

Neff, N. F., Ellis, N. A., Ye, T. Z., Noonan, J., Huang, K., Sanz, M., and Proytcheva, M. (1999). The DNA helicase activity of BLM is necessary for the correction of the genomic instability of bloom syndrome cells. Mol Biol Cell *10*, 665-676.

Nimonkar, A. V., Ozsoy, A. Z., Genschel, J., Modrich, P., and Kowalczykowski, S. C. (2008). Human exonuclease 1 and BLM helicase interact to resect DNA and initiate DNA repair. Proc Natl Acad Sci U S A *105*, 16906-16911.

Niu, H., Chung, W.-H., Zhu, Z., Kwon, Y., Zhao, W., Chi, P., Prakash, R., Seong, C., Liu, D., Lu, L.*, et al.* (2010). Mechanism of the ATP-dependent DNA end-resection machinery from Saccharomyces cerevisiae. Nature *467*, 108-111.

O'Driscoll, M. (2009). Mouse models for ATR deficiency. DNA Repair (Amst) *8*, 1333-1337.

O'Driscoll, M., Ruiz-Perez, V. L., Woods, C. G., Jeggo, P. A., and Goodship, J. A. (2003). A splicing mutation affecting expression of ataxia-telangiectasia and Rad3-related protein (ATR) results in Seckel syndrome. Nat Genet *33*, 497-501.

Olson, E., Nievera, C. J., Lee, A. Y.-L., Chen, L., and Wu, X. (2007a). The Mre11-Rad50-Nbs1 complex acts both upstream and downstream of ataxia telangiectasia mutated and Rad3-related protein (ATR) to regulate the S-phase checkpoint following UV treatment. J Biol Chem *282*, 22939-22952.

Olson, E., Nievera, C. J., Liu, E., Lee, A. Y.-L., Chen, L., and Wu, X. (2007b). The Mre11 complex mediates the S-phase checkpoint through an interaction with replication protein A. Mol Cell Biol *27*, 6053-6067.

Orlando, J. S., and Ornelles, D. A. (1999). An arginine-faced amphipathic alpha helix is required for adenovirus type 5 e4orf6 protein function. J Virol *73*, 4600-4610.

Ouyang, K. J., Woo, L. L., Zhu, J., Huo, D., Matunis, M. J., and Ellis, N. A. (2009). SUMO modification regulates BLM and RAD51 interaction at damaged replication forks. Plos Biol *7*, e1000252.

Paull, T. T., and Gellert, M. (1998a). The 3' to 5' exonuclease activity of Mre 11 facilitates repair of DNA double-strand breaks. Molecular Cell *1*, 969-979.

Paull, T. T., and Gellert, M. (1998b). The 3' to 5' exonuclease activity of Mre 11 facilitates repair of DNA double-strand breaks. Mol Cell *1*, 969-979.

Paull, T. T., and Gellert, M. (1999a). Nbs1 potentiates ATP-driven DNA unwinding and endonuclease cleavage by the Mre11/Rad50 complex. Genes Dev *13*, 1276-1288.

Paull, T. T., and Gellert, M. (1999b). Nbs1 potentiates ATP-driven DNA unwinding and endonuclease cleavage by the Mre11/Rad50 complex. Genes & Development *13*, 1276-1288.

Paull, T. T., Rogakou, E. P., Yamazaki, V., Kirchgessner, C. U., Gellert, M., and Bonner, W. M. (2000). A critical role for histone H2AX in recruitment of repair factors to nuclear foci after DNA damage. Curr Biol *10*, 886-895.

Pellegrini, M., Celeste, A., Difilippantonio, S., Guo, R., Wang, W., Feigenbaum, L., and Nussenzweig, A. (2006). Autophosphorylation at serine 1987 is dispensable for murine Atm activation in vivo. Nature *443*, 222-225.

Pichierri, P., and Rosselli, F. (2004). The DNA crosslink-induced S-phase checkpoint depends on ATR-CHK1 and ATR-NBS1-FANCD2 pathways. Embo J *23*, 1178-1187.

Pombo, A., Ferreira, J., Bridge, E., and Carmo-Fonseca, M. (1994). Adenovirus replication and transcription sites are spatially separated in the nucleus of infected cells. Embo J *13*, 5075-5085.

Querido, E., Blanchette, P., Yan, Q., Kamura, T., Morrison, M., Boivin, D., Kaelin, W. G., Conaway, R. C., Conaway, J. W., and Branton, P. E. (2001a). Degradation of p53 by adenovirus E4orf6 and E1B55K proteins occurs via a novel mechanism involving a Cullin-containing complex. Genes Dev *15*, 3104-3117.

Querido, E., Morrison, M. R., Chu-Pham-Dang, H., Thirlwell, S. W., Boivin, D., and Branton, P. E. (2001b). Identification of three functions of the adenovirus e4orf6 protein that mediate p53 degradation by the E4orf6-E1B55K complex. J Virol *75*, 699-709.

Rao, V. A., Fan, A. M., Meng, L., Doe, C. F., North, P. S., Hickson, I. D., and Pommier, Y. (2005). Phosphorylation of BLM, dissociation from topoisomerase IIIalpha, and colocalization with gamma-H2AX after topoisomerase I-induced replication damage. Mol Cell Biol *25*, 8925-8937.

Rass, E., Grabarz, A., Plo, I., Gautier, J., Bertrand, P., and Lopez, B. S. (2009). Role of Mre11 in chromosomal nonhomologous end joining in mammalian cells. Nat Struct Mol Biol *16*, 819-824.

Reinhardt, H. C., and Yaffe, M. B. (2009). Kinases that control the cell cycle in response to DNA damage: Chk1, Chk2, and MK2. Curr Opin Cell Biol *21*, 245-255.

Rekosh, D. M., Russell, W. C., Bellet, A. J., and Robinson, A. J. (1977). Identification of a protein linked to the ends of adenovirus DNA. Cell *11*, 283-295.

Robison, J. G., Elliott, J., Dixon, K., and Oakley, G. G. (2004). Replication protein A and the Mre11.Rad50.Nbs1 complex co-localize and interact at sites of stalled replication forks. J Biol Chem *279*, 34802-34810.

Rogakou, E. P., Pilch, D. R., Orr, A. H., Ivanova, V. S., and Bonner, W. M. (1998). DNA double-stranded breaks induce histone H2AX phosphorylation on serine 139. J Biol Chem *273*, 5858-5868.

Rosin, M. P., and German, J. (1985). Evidence for chromosome instability in vivo in Bloom syndrome: increased numbers of micronuclei in exfoliated cells. Hum Genet *71*, 187-191.

Roth, J., Konig, C., Wienzek, S., Weigel, S., Ristea, S., and Dobbelstein, M. (1998). Inactivation of p53 but not p73 by adenovirus type 5 E1B 55-kilodalton and E4 34-kilodalton oncoproteins. J Virol *72*, 8510-8516.

Ruis, B. L., Fattah, K. R., and Hendrickson, E. A. (2008). The catalytic subunit of DNA-dependent protein kinase regulates proliferation, telomere length, and genomic stability in human somatic cells. Mol Cell Biol *28*, 6182-6195.

Sartori, A. A., Lukas, C., Coates, J., Mistrik, M., Fu, S., Bartek, J., Baer, R., Lukas, J., and Jackson, S. P. (2007). Human CtIP promotes DNA end resection. Nature *450*, 509-514.

Sasaki, M., Lange, J., and Keeney, S. (2010). Genome destabilization by homologous recombination in the germ line. Nat Rev Mol Cell Biol *11*, 182-195.

Schaeper, U., Subramanian, T., Lim, L., Boyd, J. M., and Chinnadurai, G. (1998). Interaction between a cellular protein that binds to the C-terminal region of adenovirus E1A (CtBP) and a novel cellular protein is disrupted by E1A through a conserved PLDLS motif. J Biol Chem *273*, 8549-8552.

Schreiner, S., Wimmer, P., Sirma, H., Everett, R. D., Blanchette, P., Groitl, P., and Dobner, T. (2010) Proteasome-dependent degradation of Daxx by the viral E1B-55K protein in human adenovirus-infected cells. J Virol *84*, 7029-7038.

Schwartz, R. A., Lakdawala, S. S., Eshleman, H. D., Russell, M. R., Carson, C. T., and Weitzman, M. D. (2008). Distinct requirements of adenovirus E1b55K protein for degradation of cellular substrates. J Virol *82*, 9043-9055.

Sengupta, S., Robles, A. I., Linke, S. P., Sinogeeva, N. I., Zhang, R., Pedeux, R., Ward, I. M., Celeste, A., Nussenzweig, A., Chen, J.*, et al.* (2004). Functional interaction between BLM helicase and 53BP1 in a Chk1-mediated pathway during S-phase arrest. J Cell Biol *166*, 801-813.

Shao, R. G., Cao, C. X., Zhang, H., Kohn, K. W., Wold, M. S., and Pommier, Y. (1999). Replication-mediated DNA damage by camptothecin induces phosphorylation of RPA by DNA-dependent protein kinase and dissociates RPA:DNA-PK complexes. Embo J *18*, 1397-1406.

Shechter, D., Costanzo, V., and Gautier, J. (2004). Regulation of DNA replication by ATR: signaling in response to DNA intermediates. DNA Repair (Amst) *3*, 901-908.

Shen, Y., Kitzes, G., Nye, J. A., Fattaey, A., and Hermiston, T. (2001). Analyses of single-amino-acid substitution mutants of adenovirus type 5 E1B-55K protein. J Virol *75*, 4297-4307.

Skalka, A. M., and Katz, R. A. (2005). Retroviral DNA integration and the DNA damage response. Cell Death Differ *12 Suppl 1*, 971-978.

Smythe, C., and Newport, J. W. (1991). Systems for the study of nuclear assembly, DNA replication, and nuclear breakdown in Xenopus laevis egg extracts. Methods Cell Biol *35*, 449-468.

Steegenga, W. T., Riteco, N., Jochemsen, A. G., Fallaux, F. J., and Bos, J. L. (1998). The large E1B protein together with the E4orf6 protein target p53 for active degradation in adenovirus infected cells. Oncogene *16*, 349-357.

Stewart, E., Chapman, C. R., Al-Khodairy, F., Carr, A. M., and Enoch, T. (1997). rqh1+, a fission yeast gene related to the Bloom's and Werner's syndrome genes, is required for reversible S phase arrest. The EMBO Journal *16*, 2682-2692.

Stewart, G. S., Maser, R. S., Stankovic, T., Bressan, D. A., Kaplan, M. I., Jaspers, N. G., Raams, A., Byrd, P. J., Petrini, J. H., and Taylor, A. M. (1999). The DNA double-strand break repair gene hMRE11 is mutated in individuals with an ataxia-telangiectasia-like disorder. Cell *99*, 577-587.

Stiff, T., Reis, C., Alderton, G. K., Woodbine, L., O'Driscoll, M., and Jeggo, P. A. (2005). Nbs1 is required for ATR-dependent phosphorylation events. Embo J *24*, 199-208.

Stiff, T., Walker, S. A., Cerosaletti, K., Goodarzi, A. A., Petermann, E., Concannon, P., O'Driscoll, M., and Jeggo, P. A. (2006). ATR-dependent phosphorylation and activation of ATM in response to UV treatment or replication fork stalling. EMBO J *25*, 5775-5782.

Stracker, T. H., Carson, C. T., and Weitzman, M. D. (2002). Adenovirus oncoproteins inactivate the Mre11-Rad50-NBS1 DNA repair complex. Nature *418*, 348-352.

Stracker, T. H., Lee, D. V., Carson, C. T., Araujo, F. D., Ornelles, D. A., and Weitzman, M. D. (2005). Serotype-specific reorganization of the Mre11 complex by adenoviral E4orf3 proteins. J Virol *79*, 6664-6673.

Suslova, N. G., and Zakharov, I. A. (1974). A study of the rate of spontaneous mutation in roentgen-sensitive mutants of Saccharomyces cerevisiae. Sov Genet *7*, 1446-1451.

Takeda, S., Nakamura, K., Taniguchi, Y., and Paull, T. T. (2007). Ctp1/CtIP and the MRN complex collaborate in the initial steps of homologous recombination. Mol Cell *28*, 351-352.

Taylor, T. J., and Knipe, D. M. (2004). Proteomics of herpes simplex virus replication compartments: association of cellular DNA replication, repair, recombination, and chromatin remodeling proteins with ICP8. J Virol *78*, 5856-5866.

Terasawa, M., Ogawa, T., Tsukamoto, Y., and Ogawa, H. (2008). Sae2p phosphorylation is crucial for cooperation with Mre11p for resection of DNA double-strand break ends during meiotic recombination in Saccharomyces cerevisiae. Genes Genet Syst *83*, 209-217.

Trujillo, K. M., Yuan, S. S., Lee, E. Y., and Sung, P. (1998). Nuclease activities in a complex of human recombination and DNA repair factors Rad50, Mre11, and p95. J Biol Chem *273*, 21447-21450.

Usui, T., Ogawa, H., and Petrini, J. H. (2001). A DNA damage response pathway controlled by Tel1 and the Mre11 complex. Molecular Cell *7*, 1255-1266.

Uziel, T., Lerenthal, Y., Moyal, L., Andegeko, Y., Mittelman, L., and Shiloh, Y. (2003). Requirement of the MRN complex for ATM activation by DNA damage. The EMBO Journal *22*, 5612-5621.

Varon, R., Vissinga, C., Platzer, M., Cerosaletti, K. M., Chrzanowska, K. H., Saar, K., Beckmann, G., Seemanova, E., Cooper, P. R., Nowak, N. J.*, et al.* (1998). Nibrin, a novel DNA double-strand break repair protein, is mutated in Nijmegen breakage syndrome. Cell *93*, 467-476.

Vo, A. T., Zhu, F., Wu, X., Yuan, F., Gao, Y., Gu, L., Li, G. M., Lee, T. H., and Her, C. (2005). hMRE11 deficiency leads to microsatellite instability and defective DNA mismatch repair. EMBO Rep *6*, 438-444.

Wang, Y., Cortez, D., Yazdi, P., Neff, N., Elledge, S. J., and Qin, J. (2000). BASC, a super complex of BRCA1-associated proteins involved in the recognition and repair of aberrant DNA structures. Genes Dev *14*, 927-939.

Watt, P. M., Hickson, I. D., Borts, R. H., and Louis, E. J. (1996). SGS1, a homologue of the Bloom's and Werner's syndrome genes, is required for maintenance of genome stability in Saccharomyces cerevisiae. Genetics *144*, 935-945.

Weber, J. M. (1995). Adenovirus endopeptidase and its role in virus infection. Curr Top Microbiol Immunol *199 (Pt 1)*, 227-235.

Webster, A., Leith, I. R., Nicholson, J., Hounsell, J., and Hay, R. T. (1997). Role of preterminal protein processing in adenovirus replication. J Virol *71*, 6381-6389.

Weiden, M. D., and Ginsberg, H. S. (1994). Deletion of the E4 region of the genome produces adenovirus DNA concatemers. Proc Natl Acad Sci U S A *91*, 153-157.

Weinberg, D. H., and Ketner, G. (1983). A cell line that supports the growth of a defective early region 4 deletion mutant of human adenovirus type 2. Proc Natl Acad Sci U S A *80*, 5383-5386.

Weinberg, D. H., and Ketner, G. (1986). Adenoviral early region 4 is required for efficient viral DNA replication and for late gene expression. J Virol *57*, 833-838.

Wienzek, S., Roth, J., and Dobbelstein, M. (2000). E1B 55-kilodalton oncoproteins of adenovirus types 5 and 12 inactivate and relocalize p53, but not p51 or p73, and cooperate with E4orf6 proteins to destabilize p53. J Virol *74*, 193-202.

Wilkinson, D. E., and Weller, S. K. (2004). Recruitment of cellular recombination and repair proteins to sites of herpes simplex virus type 1 DNA replication is dependent on the composition of viral proteins within prereplicative sites and correlates with the induction of the DNA damage response. J Virol *78*, 4783-4796.

Williams, R. S., Dodson, G. E., Limbo, O., Yamada, Y., Williams, J. S., Guenther, G., Classen, S., Glover, J. N., Iwasaki, H., Russell, P., and Tainer, J. A. (2009a). Nbs1 flexibly tethers Ctp1 and Mre11-Rad50 to coordinate DNA double-strand break processing and repair. Cell *139*, 87-99.

Williams, R. S., Dodson, G. E., Limbo, O., Yamada, Y., Williams, J. S., Guenther, G., Classen, S., Glover, J. N. M., Iwasaki, H., Russell, P., and Tainer, J. A. (2009b). Nbs1 flexibly tethers Ctp1 and Mre11-Rad50 to coordinate DNA double-strand break processing and repair. Cell *139*, 87-99.

Williams, R. S., Moncalian, G., Williams, J. S., Yamada, Y., Limbo, O., Shin, D. S., Groocock, L. M., Cahill, D., Hitomi, C., Guenther, G.*, et al.* (2008). Mre11 dimers coordinate DNA end bridging and nuclease processing in double-strand-break repair. Cell *135*, 97-109.

Wong, A. K., Ormonde, P. A., Pero, R., Chen, Y., Lian, L., Salada, G., Berry, S., Lawrence, Q., Dayananth, P., Ha, P.*, et al.* (1998). Characterization of a carboxy-terminal BRCA1 interacting protein. Oncogene *17*, 2279-2285.

Woo, J. L., and Berk, A. J. (2007). Adenovirus ubiquitin-protein ligase stimulates viral late mRNA nuclear export. J Virol *81*, 575-587.

Wu, L., Davies, S. L., North, P. S., Goulaouic, H., Riou, J. F., Turley, H., Gatter, K. C., and Hickson, I. D. (2000). The Bloom's syndrome gene product interacts with topoisomerase III. J Biol Chem *275*, 9636-9644.

Wu, X., Avni, D., Chiba, T., Yan, F., Zhao, Q., Lin, Y., Heng, H., and Livingston, D. (2004). SV40 T antigen interacts with Nbs1 to disrupt DNA replication control. Genes Dev *18*, 1305-1316.

Xiao, Y., and Weaver, D. T. (1997). Conditional gene targeted deletion by Cre recombinase demonstrates the requirement for the double-strand break repair Mre11 protein in murine embryonic stem cells. Nucleic Acids Res *25*, 2985-2991.

Xie, A., Kwok, A., and Scully, R. (2009). Role of mammalian Mre11 in classical and alternative nonhomologous end joining. Nat Struct Mol Biol *16*, 814-818.

Xu, Y., Ashley, T., Brainerd, E. E., Bronson, R. T., Meyn, M. S., and Baltimore, D. (1996). Targeted disruption of ATM leads to growth retardation, chromosomal fragmentation during meiosis, immune defects, and thymic lymphoma. Genes Dev *10*, 2411-2422.

Xu, Y., and Baltimore, D. (1996). Dual roles of ATM in the cellular response to radiation and in cell growth control. Genes Dev *10*, 2401-2410.

Yankiwski, V., Marciniak, R. A., Guarente, L., and Neff, N. F. (2000). Nuclear structure in normal and Bloom syndrome cells. Proc Natl Acad Sci U S A *97*, 5214-5219.

Yondola, M. A., and Hearing, P. (2007). The adenovirus E4 ORF3 protein binds and reorganizes the TRIM family member transcriptional intermediary factor 1 alpha. J Virol *81*, 4264-4271.

Yoo, H. Y., Kumagai, A., Shevchenko, A., Shevchenko, A., and Dunphy, W. G. (2009). The Mre11-Rad50-Nbs1 complex mediates activation of TopBP1 by ATM. Mol Biol Cell *20*, 2351-2360.

You, Z., and Bailis, J. M. (2010). DNA damage and decisions: CtIP coordinates DNA repair and cell cycle checkpoints. Trends Cell Biol *20*, 402-409.

You, Z., Chahwan, C., Bailis, J., Hunter, T., and Russell, P. (2005). ATM activation and its recruitment to damaged DNA require binding to the C terminus of Nbs1. Mol Cell Biol *25*, 5363-5379.

You, Z., Shi, L. Z., Zhu, Q., Wu, P., Zhang, Y.-W., Basilio, A., Tonnu, N., Verma, I. M., Berns, M. W., and Hunter, T. (2009). CtIP links DNA double-strand break sensing to resection. Molecular Cell *36*, 954-969.

Yu, X., and Baer, R. (2000). Nuclear localization and cell cycle-specific expression of CtIP, a protein that associates with the BRCA1 tumor suppressor. J Biol Chem *275*, 18541-18549.

Yu, X., and Chen, J. (2004). DNA damage-induced cell cycle checkpoint control requires CtIP, a phosphorylation-dependent binding partner of BRCA1 C-terminal domains. Mol Cell Biol *24*, 9478-9486.

Yu, X., Wu, L. C., Bowcock, A. M., Aronheim, A., and Baer, R. (1998). The C-terminal (BRCT) domains of BRCA1 interact in vivo with CtIP, a protein implicated in the CtBP pathway of transcriptional repression. J Biol Chem *273*, 25388-25392.

Yuan, J., and Chen, J. (2009). N terminus of CtIP is critical for homologous recombination mediated double-strand break repair. J Biol Chem.

Yun, M. H., and Hiom, K. (2009). CtIP-BRCA1 modulates the choice of DNA double-strand-break repair pathway throughout the cell cycle. Nature *459*, 460-463.

Zernik-Kobak, M., Vasunia, K., Connelly, M., Anderson, C. W., and Dixon, K. (1997). Sites of UV-induced phosphorylation of the p34 subunit of replication protein A from HeLa cells. J Biol Chem *272*, 23896-23904.

Zhao, X., Madden-Fuentes, R. J., Lou, B. X., Pipas, J. M., Gerhardt, J., Rigell, C. J., and Fanning, E. (2008). Ataxia telangiectasia-mutated damage-signaling kinase- and proteasome-dependent destruction of Mre11-Rad50-Nbs1 subunits in Simian virus 40-infected primate cells. J Virol *82*, 5316-5328.

Zhong, H., Bryson, A., Eckersdorff, M., and Ferguson, D. O. (2005). Rad50 depletion impacts upon ATR-dependent DNA damage responses. Hum Mol Genet *14*, 2685-2693.

Zhong, S., Hu, P., Ye, T. Z., Stan, R., Ellis, N. A., and Pandolfi, P. P. (1999). A role for PML and the nuclear body in genomic stability. Oncogene *18*, 7941-7947.

Zhu, J., Petersen, S., Tessarollo, L., and Nussenzweig, A. (2001). Targeted disruption of the Nijmegen breakage syndrome gene NBS1 leads to early embryonic lethality in mice. Curr Biol *11*, 105-109.

Zhu, Z., Chung, W.-H., Shim, E. Y., Lee, S. E., and Ira, G. (2008a). Sgs1 helicase and two nucleases Dna2 and Exo1 resect DNA double-strand break ends. Cell *134*, 981-994.

Zhu, Z., Chung, W. H., Shim, E. Y., Lee, S. E., and Ira, G. (2008b). Sgs1 helicase and two nucleases Dna2 and Exo1 resect DNA double-strand break ends. Cell *134*, 981-994.

Zou, L. (2007). Single- and double-stranded DNA: building a trigger of ATR-mediated DNA damage response. Genes Dev *21*, 879-885.

Zou, L., and Elledge, S. J. (2003). Sensing DNA damage through ATRIP recognition of RPA-ssDNA complexes. Science *300*, 1542-1548.